THE IMPACT OF SALMONELLA POLYSACCHARIDE ANTIGENS STRUCTURE AND CONJUGATION CHEMISTRY ON NTS GLYCOCONJUGATE VACCINES

Giuseppe Stefanetti

Dottorato in Scienze Biotecnologiche – XXVI ciclo
Indirizzo Biotecnologie Molecolari e Industriali
Università di Napoli Federico II

Dottorato in Scienze Biotecnologiche – XXVI ciclo
Indirizzo Biotecnologie Molecolari e Industriali
Università di Napoli Federico II

THE IMPACT OF SALMONELLA POLYSACCHARIDE ANTIGENS STRUCTURE AND CONJUGATION CHEMISTRY ON NTS GLYCOCONJUGATE VACCINES

Giuseppe Stefanetti

Dottorando:	Giuseppe Stefanetti
Relatore:	Prof. Giovanni Sannia
Correlatore:	Dr. Francesca Micoli
Coordinatore:	Prof. Giovanni Sannia

Alla mia famiglia

1. Riassunto

Introduzione

La vaccinazione è considerata lo strumento a breve e medio termine più idoneo, efficace, ed economico per proteggere le popolazioni dalle malattie infettive. Le malattie infettive rappresentano il 23% di tutte le malattie che affliggono l'umanità, ma colpiscono in maniera sproporzionata (98.9%) le popolazioni dei paesi a medio e basso reddito e soprattutto i bambini. In particolare, le infezioni enteriche, causate da batteri come *Salmonella, Shigella, Campylobacter jejuni, ETEC* o da virus, rappresentano la terza causa d'infezione globale e, escludendo le condizioni perinatali, la seconda causa di morte tra i bambini sotto i 5 anni. Le *Salmonelle* non tifoidee (NTS), i cui sierotipi più comuni sono Typhimurium ed Enteritidis, sebbene siano solamente una causa di gastroenterite senza particolari complicanze nei paesi industrializzati, sono invece una delle principali cause di setticemia in Africa, soprattutto tra bambini e i soggetti immunocompromessi nella regione subsahariana. Pur essendo un importante problema di salute pubblica, con un tasso di mortalità che raggiunge il 20-25% nel caso di setticemia, NTS è sorprendentemente una malattia negletta principalmente a causa della sua presentazione clinica complessa, che ne rende difficile la diagnosi, e della mancanza di strumenti diagnostici adeguati. Mentre sono stati prodotti vaccini contro le infezioni da *Salmonella* di tipo tifoideo, non esistono attualmente vaccini contro NTS. Maggiore interesse è sorto negli ultimi anni verso questa malattia, di pari passo con il preoccupante emergere di ceppi antibiotico-resistenti, e diversi tipi di vaccini sono attualmente in sviluppo, come gliconiugati, organismi attenuati, GMMA e vaccini a subunità proteica.
Un vaccino glicoconiugato si genera con l'unione tramite legame chimico covalente, o coniugazione, di un saccaride a una proteina immunogenica, avente la funzione di *carrier*. La coniugazione tra saccaride e proteina può avvenire direttamente, o previa attivazione, di una o entrambe le biomolecole, con molecole aventi la funzione di spaziatore. Le cellule di molti agenti patogeni sono infatti ricoperte da un denso strato di carboidrati complessi noto come glicocalice, costituito da glicoproteine, proteoglicani e glicolipidi, la cui esposizione sulla superficie le rende capaci di interagire con le componenti del sistema immunitario, esercitando una funzione protettiva nei confronti della difesa immunitaria dell'ospite e rappresentando quindi un'importante fattore di virulenza del microorganismo. In particolare, batteri incapsulati come *Streptococcus pneumoniae, Haemophilus influenzae, Neisseria meningitidis* e *Salmonella typhi* presentano un guscio polisaccaridico (noto come capsula) che circonda la parete e che è stato utilizzato per la produzione di vaccini polisaccaridici. I vaccini polisaccaridici possiedono tuttavia una grave limitazione: essi non sono capaci di generare memoria immunologica e sono inefficaci nei neonati e nei pazienti immunodepressi. Infatti, i polisaccaridi sono antigeni cellule T-indipendenti, importanti componenti della risposta immunitaria adattiva, e risultano dunque attivi unicamente sulle cellule B. Viceversa, le proteine sono antigeni T-dipendenti e la loro coniugazione chimica a un polisaccaride conferisce a quest'ultimo la capacità di stimolare i linfociti T, migliorando così la risposta immunogenicità e conferendo memoria immunitaria. Sono stati sviluppati per migliorare l'immunogenicità dei vaccini polisaccaridici e, molto probabilmente, in un futuro non remoto, li andranno a sostituire completamente. Non esiste un altro esempio in cui l'introduzione di un nuovo approccio allo sviluppo di vaccini ha avuto un effetto così rapido e positivo nella prevenzione delle infezioni da patogeni umani,

come *Haemophilus influenzae* di tipo b (Hib), *Neisseria meningitidis* e *Streptococcus pneumoniae,* e questo successo ha aperto la strada a nuove applicazioni possibili come i vaccini terapeutici per il cancro e l'Alzheimer e vaccini coniugati per la dipendenza da droghe. L'antigene O (OAg) del lipopolisaccaride è il principale polisaccaride di superficie per le specie NTS. Il lipopolisaccaride è un componente della parete cellulare esterna dei batteri Gram-negativi, composto da una porzione glicolipidica, il lipide A; un porzione oligosaccaridica, definita *Core*; e dall'OAg, una catena polisaccaridica immunodominante la cui composizione conferisce specificità sierologica all'organismo.
La coniugazione dell'OAg a proteine *carrier* ha permesso lo sviluppo di vaccini glicoconiugati efficaci nel produrre anticorpi e in grado di proteggere da infezioni letali di *Salmonella* in modelli animali. Non esistono dati clinici su vaccini glicoconiugati contro NTS, ma un vaccino glicoconiugato basato sull'OAg di *S*. Paratyphi A si è dimostrato immunogenico ed efficace in studi clinici in fase 1 e 2 su adulti e bambini vietnamiti, dimostrando la bontà di questo tipo di approccio.
Diverse variabili possono influenzare l'immunogenicità di un vaccino glicoconiugato. Parametri come la lunghezza della catena saccaridica, il rapporto saccaride/proteina, il tipo di coniugazione chimica, la proteina carrier usata conferiscono ai glicoconiugati diverse caratteristiche chimico-fisiche che possono determinare diverse proprietà immunologiche. Una comprensione razionale degli effetti di questi parametri differenti sull'immunogenicità potrebbe portare a un disegno più razionale dei vaccini glicoconiugati, con conseguente maggiore efficacia e protezione a lungo termine. Tuttavia, questo non è semplice per diverse ragioni. In primo luogo, la risposta immunitaria è altamente antigene dipendente, e perciò risultati contrastanti possono essere ottenuti lavorando con diversi polisaccaridi. Inoltre, studi effettuati finora hanno confrontato l'immunogenicità di vaccini che differiscono per più parametri contemporaneamente, rendendo quindi difficile assegnare l'importanza relativa di una singola variabile sull'immunogenicità. Infine, parametri come la lunghezza della catena saccaridica, il rapporto saccaride/proteina e il tipo di chimica di coniugazione sono fortemente interconnessi. A causa di questa complessità, l'importanza relativa di ogni variabile dovrebbe essere indagata per ciascun antigene polisaccaridico, ogni volta che un vaccino glicoconiugato è in fase di sviluppo.

Il progetto vaccini glicoconiugati contro NTS a NVGH

NVGH sta lavorando allo sviluppo di un vaccino bivalente glicoconiugato che protegga contro le infezioni da S. Typhimurium e S. Enteritidis. L'approccio prevede l'estrazione e purificazione dell'OAg dai rispettivi ceppi e la coniugazione con la proteina carrier $CRM_{197,}$ una variante non tossica della tossina difterica che è già stata ampiamente utilizzata con successo nello sviluppo di altri vaccini gliconiugati ((*Hib*, pneumococco (7 e 13 valente), meningococco tetravalente (ACWY)).
NVGH ha sviluppato un metodo semplice, rapido e a basso impatto ambientale per l'estrazione e la purificazione dell'OAg. Sulla crescita batterica, viene effettuata un'idrolisi acida che rompendo il legame tra il KDO e il lipide A, permette il rilascio dell'OAg direttamente nel sopranatante. Una serie di processi successivi, per lo più precipitazioni e filtrazioni, permette la purificazione dell'OAg da altre impurità presenti, come proteine o acidi nucleici. La chimica di coniugazione in precedenza sviluppata da NVGH per un vaccino glicoconiugato contro *S*. Paratyphi A, è stata applicata al progetto NTS. Questo metodo utilizza l'unità terminale KDO della catena dell'OAg per la coniugazione con la proteina, senza modificare le unità ripetitive della

catena polisaccaridica. Studi preliminari su topi hanno mostrato che il coniugato ottenuto con questa chimica produce alti titoli anti-OAg con attività battericida.

Obiettivi del progetto di dottorato

All'interno del progetto vaccini glicoconiugati contro NTS, Il mio lavoro di dottorato si è interessato di tre aspetti correlati:

1. Caratterizzazione strutturale degli antigeni polisaccaridici di *S*. Typhimurium e *S*. Enteritidis purificati da diversi ceppi.
2. Disegno, sintesi e valutazione immunologica di un pannello di vaccini glicoconiugati contro NTS, che differiscono per alcuni parametri noti influenzare la risposta immunologica: il ceppo di derivazione dell'OAg (e quindi caratteristiche strutturali come glucosilazione e l'O-acetilazione), la chimica di coniugazione, il rapporto OAg/proteina.
3. Progettazione e sviluppo di efficaci metodologie di coniugazione, che permettano la sintesi di glicoconiugati altamente specifici e selettivi, la semplificazione del processo di purificazione e il riciclo dell'OAg, consentendo così una riduzione globale dei costi di processo.

Impatto della struttura dell'OAg sull'immunogenicità di vaccini glicoconiugati contro NTS

L'OAg è stato estratto e purificato da sei ceppi *S*. Typhimurium (un isolato umano, tre animali e due ceppi di laboratorio) e 4 ceppi *S*. Enteritidis (un isolato umano e tre animali). L'utilizzo di metodi analitici, come NMR, HPAEC-PAD, GLC-MS e HPLC–SEC, ha permesso la caratterizzazione strutturale delle unità ripetitive della catena polisaccaridica dei diversi OAg. Gli OAg di Typhimurium testati sono risultati simili in termini di distribuzione di pesi molecolari, ma diversi per quanto riguarda posizione e grado di glucosilazione e O-acetilazione. In particolare, l'OAg D2380, estratto da un isolato clinico del Malawi, ha presentato non solo gruppi O-acetile sul C-2 dell'Abequosio, ma anche sul C-2 e C-3 del Ramnosio. Il glucosio, a seconda del ceppo di origine, è risultato legato 1 → 4 o 1 → 6 al galattosio in percentuali diverse. Gli OAg estratti sono strutturalmente più omogenei e tutti caratterizzati da bassi livelli di glucosilazione e O-acetilazione. Tutti gli OAg sono stati utilizzati per la sintesi dei rispettivi vaccini glicoconiugati, usando CRM_{197} come proteina carrier. L'OAg è stato legato alla proteina attraverso lo zucchero terminale KDO, senza alterare la struttura saccaridica della catena polisaccaridica e consentendo quindi la generazione di un gruppo di coniugati strutturalmente definiti, che differiscono unicamente per le caratteristiche strutturali delle unità ripetitive dell'OAg. Tutti i glicoconiugati testati sono stati immunogenici nei topi, e in grado di produrre anticorpi con attività battericida. L'eterogeneità strutturale dell'OAg si è mostrata essere un parametro in grado di influenzare l'immunogenicità dei vaccini glicoconiugati. In particolare, la produzione di anticorpi anti-OAg ceppo-specifici per il D23580 *S*. Typhimurium è verosimilmente legata alla presenza di gruppi O-acetile sul Ramnosio, caratteristica strutturale non presente negli altri ceppi *S*. Typhimurium testati. Le differenze nei livelli e nelle posizioni di glucosilazione e O-acetilazione sembrano avere un impatto sull'attività battericida degli anticorpi prodotti. Questo lavoro pone l'accento sull'importanza del processo di selezione del ceppo fonte di OAg per la produzione di vaccini glicoconiugati. L'analisi di un maggior numero di ceppi sarà necessaria per evidenziare in maniera più chiara la relazione tra le caratteristiche strutturali dell'OAg e la risposta immunologica dei corrispondenti vaccini glicoconiugati contro NTS.

Impatto della chimica di coniugazione sull'immunogenicità di vaccini glicoconiugati contro *S.* Typhimurium

La chimica di coniugazione usata nella sintesi del vaccino glicoconiugato può influenzare la risposta immunologica. In questo studio, diversi glicoconiugati sono stati sintetizzati e testati nei topi, utilizzando CRM_{197} come proteina carrier e il ceppo 2192 come fonte di OAg. Due diverse strategie sono state considerate: la derivatizzazione su molteplici e casuali posizioni lungo la catena dell'OAg, approccio "*random*", seguita da coniugazione; o l'attivazione selettiva dello zucchero terminale KDO con molecole spaziatori previa coniugazione con la proteina. In particolare, per l'approccio selettivo sono stati considerati due spaziatori di lunghezza diversa, NH_2-SIDEA e ADH-SIDEA, mentre per l'approccio casuale sono state considerate due chimiche di ossidazione, TEMPO e $NaIO_4$, che differiscono notevolmente per il tipo di modifica strutturale e conformazionale che causano allo zucchero.
Tutti i coniugati testati hanno prodotto un alto e simile titolo di anticorpi anti OAg-IgG. Tuttavia, una correlazione inversa è stata verificata tra il grado di modifica della catena dell'OAg e la capacità degli anticorpi indotti di proteggere contro l'infezione, indicando che eccessive modifiche strutturali sugli epitopi possono poi inficiare la risposta degli anticorpi in vivo. I coniugati prodotti tramite chimica casuale hanno indotto anticorpi a maggiore attività battericida di quelli selettivi. In accordo con lo studio SBA, le analisi FACS hanno mostrato come i tipo di derivatizzazione casuale investigati non hanno influenzato negativamente sulla capacità dei corrispondenti coniugati di indurre anticorpi capaci di riconoscere epitopi strutturali.
Oltre alle considerazioni immunologiche, nello sviluppo di un vaccino è anche importante valutare la resa del prodotto, il numero totale di reazioni coinvolte, e le problematiche legate alla purificazione e caratterizzazione dei materiali di partenza, degli intermedi e del vaccino finale. La chimica casuale offre vantaggi anche sotto quest'aspetto: numero minore di reazioni coinvolte e maggiore resa di coniugazione, anche se la complessa e casuale struttura del glicoconiugato risultante ne rende più difficile la caratterizzazione chimico-biologica.

Click chemistry: una metodologia efficace per la sintesi di vaccini glicoconiugati

Lo sviluppo di metodi che permettono la coniugazione di precisi punti nel saccaride a determinati aminoacidi nelle proteine, oltre a fornire a fornire vantaggi dal punto di vista di riproducibilità del processo e facilità di caratterizzazione del prodotto finale, può essere anche un elemento chiave nel chiarire le relazioni struttura-attività immunologica dei glicoconiugati. Tuttavia, la sintesi di vaccini gliconiugati strutturalmente definiti è una sfida difficile che richiede una efficace chimica di coniugazione.
Due strategie sono state inizialmente indagate per la coniugazione dell'OAg 2192 di S. Typhimurium al CRM_{197}: la chimica dei tioli e la click chemistry. In entrambi i casi, l'unità terminale KDO dello zucchero è stata selettivamente attivata con uno spaziatore e fatta reagire con la proteina in precedenza attivata coinvolgendo diversi amminoacidi e inserendo un numero variabile di spaziatori. La chimica dei tioli è stata investigata inserendo un gruppo SH sull'unità KDO dell'OAg e facendolo reagire con CRM_{197} in precedenza attivato con gruppi reattivi, quali maleimmide o bromoacetile. Questo tipo di chimica ha permesso la coniugazione solo in presenza di almeno 8 linkers sulla proteina. La metodologia click chemistry per la coniugazione è stata esplorata inserendo una funzionalità alchino sull'unità KDO dell'OAg e facendolo reagire con il CRM_{197} in precedenza attivato con gruppi azide.

Contrariamente a quanto visto per la chimica dei tioli, utilizzando la click chemistry è stato possibile sintetizzare coniugati ad alta resa anche quando poche posizioni sulla proteina sono attivate (mediamente 4, >80% proteina coniugata) o addirittura quando una sola posizione è risultata coinvolta nel legame (38% proteina coniugata). Un altro vantaggio di questo tipo di chimica è la possibilità di riciclare l'OAg non coniugato dalla miscela di reazione e utilizzarlo per la sintesi di un nuovo lotto di glicoconiugato. Sulla base di questo importante risultato, è stato sviluppato un metodo di coniugazione in fase solida in cui l'OAg coniuga con la proteina carrier immmobilizzata per interazione ionica in una matrice solida. Lo zucchero non reagito può essere facilmente rimosso dalla resina tramite lavaggi, permettendo così la successiva eluizione di coniugato "puro", che non necessità di altre purificazioni. Questo processo può avere un grande impatto sulla riduzione dei costi associati allo sviluppo di un vaccino glicoconiugato, tramite il recupero dello zucchero non coniugato e il suo riutilizzo per coniugazioni successive e la semplificazione dell'intero processo di purificazione.

Conclusioni

Lo sviluppo di un vaccino glicoconiugato contro NTS basato sull'OAg deve prevedere un'attenta analisi delle variabili che possono influenzare l'immunogenicità e il processo di produzione. In primo luogo, la selezione del ceppo da cui estrarre l'OAg è importante, dal momento che differenze strutturali nella catena polisaccaridica influiscono sull'immunogenicità. Un ampio pannello di metodi analitici ha permesso la caratterizzazione completa di OAg estratti da ceppi diversi e potrà essere impiegato per la valutazione di altri ceppi.
La chimica di coniugazione è un altro parametro da considerare. Sulla base delle chimiche testate in questo studio, l'approccio "*random",* che prevede l'attivazione di molteplici e casuali posizioni sullo zucchero, sembra essere preferibile rispetto a una chimica che coniuga selettivamente una posizione dell'OAg alla proteina, sia da un punto di vista immunologico che considerando le rese globali di processo. D'altra parte, un approccio selettivo può avere dei vantaggi da un punto di vista di riproducibilità del processo e facilità di caratterizzazione del prodotto ottenuto. Inoltre, lo sviluppo di metodi che permettono la coniugazione di precisi punti del saccaride a determinati aminoacidi della proteina può essere un elemento chiave nel chiarire le relazioni struttura-attività immunologica dei glicoconiugati. Recenti lavori hanno dimostrato come il sito di coniugazione e il numero di connessioni tra il saccaride e la proteina possono essere parametri cruciali nel determinare l'immunogenicità dei vaccini glicoconiugati. La click chemistry è un metodo di coniugazione altamente efficace nel consentire il legame selettivo tra punti specifici della proteina e lo zucchero. La metodologia di coniugazione sviluppata consente anche il riciclo dello zucchero non coniugato ed è stata applicata con successo alla sintesi di coniugati in fase solida. Utilizzando la coniugazione click, abbiamo intenzione di coniugare l'OAg di *S*. Typhimurium a diversi amminoacidi del CRM_{197}, per introdurre un numero controllato e diverso di unita saccaridiche per proteina. L'immunogenicità dei corrispondenti glicoconiugati sarà testata nei topi. Questi coniugati rappresenteranno il primo esempio di vaccini glicoconiugati a struttura altamente definita contro NTS. Oltre alla rilevanza per lo sviluppo di vaccini contro NTS, questo studio potrebbe aggiungere informazioni utili sui fattori che influenzano la presentazione dell'antigene, l'elaborazione e la cooperazione tra le cellule B e T, aggiungendo quindi importanti informazioni per la progettazione razionale dei vaccini coniugati di nuova generazione.

2. Introduction

2.1 The global burden of infectious diseases

Infectious diseases are caused by pathogenic microorganisms: bacteria, viruses, parasites or fungi. In humans and animals these pathogens enter the host at different sites and produce disease symptoms by a variety of mechanisms. The diseases can be spread, directly or indirectly, from one individual to another.

The Global Burden of Diseases (GBD) concept, first published in 1996, constitutes a comprehensive and consistent set of estimates of mortality and morbidity (*1*), and GBD estimates are revised at intervals by the World Health Organization (WHO) at regional and global level for a set of more than 135 causes of disease and injury (*2*), with the aim to quantify the burden of premature mortality and disability for major diseases or disease groups. The DALY (Disability-Adjusted Life Year) is used as a summary measure of population health, to combine estimates of the years of life lost and years lived with disabilities.

Infectious diseases (including parasitic infections) are the leading cause of DALY and the second leading cause of death worldwide (*2*). According to the published data in 2012, they were responsible for the death of more than 8.7 million people worldwide in 2008 (*3*). Morbidity and mortality caused by infectious diseases disproportionately affect the poorest populations of the world, and contributed to their misery (*2*) (*4*)**.** Data published in 2008 reported that 98.9 % of DALYs and 96.9 % of deaths due to infectious diseases occur in the middle and low income countries (*5*) (Figure 2.1). In addition, infectious diseases disproportionately affect the youngest populations and 54% of DALYS and 43% of deaths from infectious disease are in < 5 year old children. This is 10.8 fold as many DALYs per 1000 population and 16.4 fold as many deaths per 1000 population compared to > 5 year old subjects (*6*). Interestingly, this excess of morbidity and mortality in poor and young populations is not seen for non-infectious diseases (*6*). According to 2010 estimates by WHO, approximately 7.6 million children die each year before reaching the age of five (*7*)**.**

While, in the long term, access to clean water, better hygiene, adequate nutrition, and improvement of sanitary measures would have the greatest impact on infectious diseases, immunization against specific diseases is the best strategy for the short- and mid-term (*8*)**.**

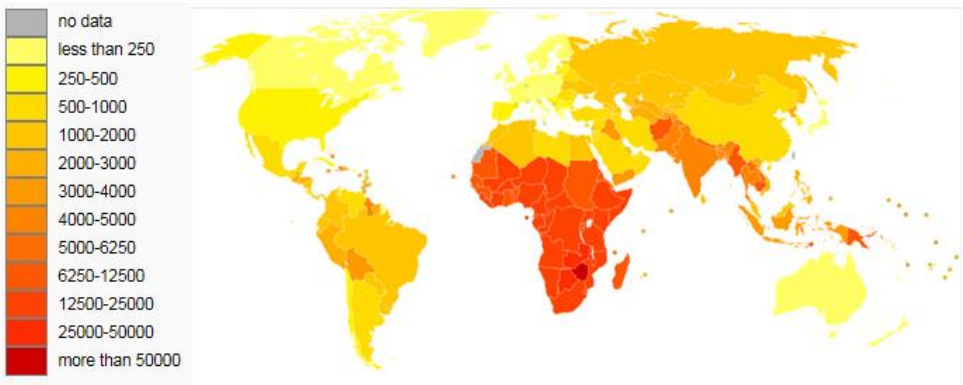

Figure 2.1 DALYs (Disability-adjusted life years) for infectious diseases by country (per 100,000 inhabitants). (Figure reproduced from (*2*)).

2.2 Vaccines

2.2.1 Mechanism of function

Disease control or elimination requires the induction of protective immunity in a sufficient proportion of the population. This is best achieved by immunization programs capable of inducing long-term protection, a hallmark of adaptive immunity that contrasts to the brisk but short-lasting innate immune responses.

Long-term immunity is conferred by the maintenance of antigen-specific immune effectors and/or by the induction of immune memory cells that may be sufficiently efficient and rapidly reactivated in case of subsequent encounters with the same pathogen (*9*).

Vaccination is the deliberate induction of adaptive immunity to a pathogen by injecting a killed or attenuated (nonpathogenic) live form of the pathogen or its antigens (subunit vaccine) (*10*). Vaccines are prophylactic in the sense that they are administered to healthy individuals to prevent a disease. Nevertheless, there is a growing trend to use vaccines to alleviate the suffering of those already with disease. Prophylactic vaccines represent the possibility to prevent global epidemics of infectious diseases.

Vaccine-induced immune effectors are essentially antibodies, produced by B lymphocytes, and capable of binding specifically to a toxin or a pathogen (*11*). They prevent or reduce infections by extra- and intracellular agents and clear extracellular pathogens. Other potential effectors are cytotoxic $CD8^+$T cells, which reduce, control and clear intracellular pathogen by recognizing and killing infected cells or secreting specific antiviral cytokines; and $CD4^+$T cells which participate to the reduction, control and clearance of extra- and intracellular agents by producing IFN-γ, TNF-α/-β, IL-2 and IL-3 and supporting activation and differentiation of B cells, $CD8^+$T cells and macrophages (Th1cells) or by producing IL-4, IL-5, IL-13, IL-6 and IL-10 and supporting B cell activation and differentiation (Th2 cells). These effectors are partly controlled by regulatory T cells (Treg) that are involved in maintaining immune tolerance(*12*). The nature of the vaccine has a direct influence on the type of immune effectors that are predominantly elicited and mediate protective immunity (*9*).

B lymphocytes are cells that originate in the bone marrow, mature in secondary lymphoid tissues, become activated in the spleen/nodes when their surface immunoglobulins bind to an antigen and differentiate either into antibody secreting cells (plasma cells) or in memory B cells. T lymphocytes are cells that originate in the bone marrow, migrate to the thymus, mature in the periphery, become activated in the spleen/nodes if 1) their T cell receptor bind to an antigen presented by an MHC molecule and 2) they receive additional costimulation signals driving them to acquire killing (mainly CD8+ T cells) or supporting (mainly CD4+ T cells) functions. The induction of antigen-specific B and T cell responses requires their activation by specific antigen presenting cells (APC), essentially dendritic cells (DC) that are recruited into the immune reaction. Immature DCs patrol throughout the body. When exposed to pathogens, they undergo a brisk maturation, modulate specific surface receptors and migrate towards secondary lymph nodes, where the induction of T and B cell responses occurs. The central role for mature DCs in the induction of vaccine responses reflects their unique capacity to provide both antigen-specific and costimulation signals required to activate naïve T cells (*13*). The very first requirement to elicit vaccine responses is therefore to provide sufficient danger signals through vaccine antigens and/or adjuvants, to trigger an inflammatory reaction that is mediated by cells of the innate immune system (*14*) (Figure 2.2).

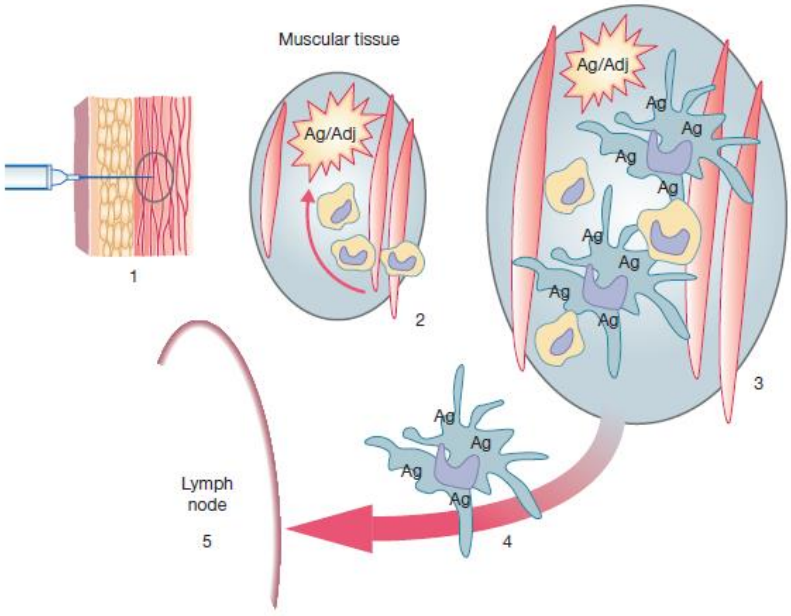

Figure 2.2 Initiation of a vaccine response: following injections (*11*), the pathogen-associated molecular patterns (PAMPS) contained in a vaccine attracts dendritic cells, monocytes and neutrophils that patrol throughout the body (*12*). If vaccine antigens/adjuvants elicit sufficient "danger signals", this activates monocytes and dendritic cells (*15*) which changes their surface receptors and induces their migration along lymphatic vessels (*16*) to the draining lymph nodes (*17*) where the activation of T and B lymphocytes will take place (Figure reproduced from (*9*)). .

2.2.2 A brief history of vaccination

Origin of vaccination is usually attributed to Edward Jenner, who observed, in the late 18th century, that the relatively mild disease of cowpox, or vaccinia, seemed to confer protection, by the inoculation with pus from infected lesions, against the often fatal disease of smallpox. He called the procedure vaccination from *vacca*, Latin for cow, and Pasteur, in his honor, extended the term to the stimulation of protection against other infectious agents. This term is still used to describe the inoculation of healthy individuals with weakened or attenuated strains of disease-causing agents to provide protection from disease. Louis Pasteur in 1885 developed the first rabies human vaccine based on attenuated viruses. He brought a breakthrough in the prevention of infectious diseases by establishing the basis of vaccinology, meaning the principle of isolation, inactivation, and administration of disease causing pathogens (*18*).
Vaccine development in the early part of the 20th century followed two empirical approaches. The first was the search for attenuated organisms with reduced pathogenicity, which would stimulate protective immunity but not cause disease (e.g., *Bacillus Calmette Guerin* BCG, pertussis, and smallpox). In the second half of 20th century improvements and innovation in mammalian cell culture technology led to the growth of viruses and development of live attenuated "second generation" vaccines such as polio (Sabin oral), measles, rubella, mumps, and varicella. More recently, the use of inactivated polio vaccine (Salk type) together with the oral vaccine has almost eradicated polio from the world thanks to global vaccination (*19*). This approach continues into the present with the design of genetically-attenuated pathogens in

which desirable mutations are introduced into the organism by recombinant DNA technologies. This idea is being applied to important pathogens, such as malaria, for which vaccines are currently unavailable, and may be important in the future for designing vaccines against influenza and HIV/AIDS.
The second approach was the development of vaccines based on killed organisms (diphtheria, tuberculosis and plague) and, subsequently, on purified components of organisms that would be as effective as live whole organisms (i.e. subunit vaccines, such as Hepatitis B or Influenza). Killed vaccines were desirable because any live vaccine, including vaccinia, can cause lethal systemic infection in immunosuppressed people. The last decades have seen the development of polysaccharide and glycoconjugate vaccines and the emergence of a new approach, reverse vaccinology, which has been used to identify candidate protein antigens. Ligands that activate Toll-like receptors (TLR) or other innate sensors have been used as adjuvants to enhance responses to simple antigens.

2.3 Infectious diseases in need for a vaccine

There are still many diseases for which an effective vaccine is lacking (Table 2.1). For many pathogens, natural infection does not necessarily generate protective immunity, and infections can become chronic or recurrent. In many infections of this type, antibodies are insufficient to prevent reinfection and to eliminate the pathogen, and cell-mediated immunity may be more important in controlling the pathogen, but is insufficient to provide full immunity, for example against malaria, tuberculosis, and HIV. It is not the absence of an immune response to the pathogen that is the problem, but rather that this response does not clear the pathogen, eliminate pathogenesis, or prevent reinfection.
Even when a vaccine can be used effectively in developed countries, technical and economic problems can prevent its widespread use in developing countries, where mortality from infectious diseases is still high. Therefore the development of vaccines remains an important goal of immunology, and the latter half of the 20th century saw a shift to a more rational approach based on a detailed molecular understanding of microbial pathogenicity, analysis of the protective host response to pathogenic organisms, and an understanding of the regulation of the immune system to generate effective T- and B-lymphocyte responses (*20*).

Table 2.1 Diseases for which effective vaccines are still needed (*2*) (Table adapted from (*20*))

Disease	Estimated annual mortality
Respiratory infections	4 milion
Diarrheal disease	2.2 milion
HIV/AIDS	2 milion
Tuberculosis	1.5 milion
Malaria	889,000
Schistosomiasis	41,000
Intestinal worm infestation	6,000

A successful vaccine must be safe and able to produce protective immunity in a very high proportion of the people to whom it is given; particularly in poorer countries where it is impracticable to give regular 'booster' vaccinations to dispersed rural populations. In addition a vaccine must generate long-lived immunological memory.

Fourth, vaccines must be very cheap if they are to be administered to large populations. Vaccines are one of the most cost-effective measures in health care, but this benefit is eroded as the cost per dose rises. Another benefit of an effective vaccination program is the 'herd immunity' that it confers: by lowering the number of susceptible members of a population, vaccination decreases the natural reservoir of infected individuals in that population and so reduces the probability of transmission of infection. Thus, even unvaccinated members will be protected because their individual chance of encountering the pathogen is decreased. However, the herd immunity effect is only seen at relatively high levels of vaccination within a population; for mumps it is estimated to be around 80%, and below this level sporadic epidemics can occur (*20*).
In the last century vaccines have been of unquestionable value, saving more than 700 million cases of disease and more than 150 million deaths (*18*). Vaccination prevents an estimated 2.5 million deaths each year (*21*).

2.4 Diarrheal diseases

Enteric infections rank third among all causes of disease burden worldwide, being responsible for about 2.2 milions of deaths per year, mostly in young children and infants in developing countries (*8*). Diarrhea is also the second leading cause of death among children under 5 years of age, excluding perinatal conditions (*22*).
Over the past two decades, treatment and prevention measures including fluid replacement, zinc treatment or promotion of hand washing have been responsible for the decline of mortality from diarrhea from an estimated 5 million to about 1.5 million deaths among young children in 2004 (*23*). However, although the number of deaths is decreasing, the high incidence is still a major issue. Furthermore, long-term consequences on physical and mental development of children have been reported as a result of childhood diarrhea (*24*) (*25*) (*26*). Main infectious agents responsible for human enteric infections include several viruses (enteric adenoviruses, astroviruses, human caliciviruses (HuCV), rotaviruses (RV)) and several bacterial agents, such as *Campylobacter jejuni*, a variety of pathogenic *Escherichia coli* strains including enterotoxigenic *Escherichia coli* (ETEC), several *Shigella* species, various *Salmonella* strains including *S.* Typhi*, S.* Paratyphi, non typhoidal *Salmonellae* and *Vibrio cholera*.
Diarrheal diseases represent a major health problem also for travellers who visit these countries, especially in the tropics (*27*). Up to 80 % of diarrheal episodes in travellers are bacterial in nature, caused principally by ETEC strains, followed by *Shigella*, *Campylobacter* and *Salmonella* spp. (*28*).
The increased frequency of antibacterial drug-resistance among these pathogens is a source of major concern (*29*) (*30*). The development of vaccines against enteric diseases seems a good strategy to reduce diarrheal diseases. However, covering the large number of pathogens and serotypes constitutes a serious challenge.

2.5 *Salmonella* disease

Salmonella belongs to the group of Enterobacteriaceae that are aerobic, gram negative rods and approximately 1–3 μm × 0.5 μm in size (*31*) (*32*)**.** *Salmonella* was first identified in 1880 by Eberth from the mesenteric nodes and spleen of a patient dying from typhoid fever (*33*)**.** In 1884 Gaffky was able to isolate the bacillus and a year later Salmon (the name *Salmonella* was coined in 1900 as a tribute to him) and Smith described a bacillus, now known to be *Salmonella* Choleraesuis, the first

affecting both humans and animals (*34*). Currently there are roughly 2400 species of *Salmonella*. *Salmonellae* are divided into two subspecies: *S. enterica* and *S. bongori*. *S. bongori* contains 8 serovars and *S. enterica* contains the other serovars (*35*).
Antisera against Vi (which forms a polysaccharide (PS) capsule around *S*. Typhi and also *S*. Paratyphi C and *S*. Dublin), O-antigen (OAg) of lipopolysaccharide (LPS) (O somatic antigen) and flagella (H antigens) have long been used for the typing of *Salmonella* serovars according to the Kauffmann-White scheme.
Salmonellae are capable of causing disease in a wide range of species and are essentially intestinal parasites of humans and animals including domestic pets, farm animals, birds, reptiles and rodents. They are found in the environment and have been isolated from rivers, sewage and soil where, under the correct conditions, they can survive for many years. They have been detected in animal feeds as well as food such as fruit and vegetables. The vast majority of salmonellosis cases are a result of consumption of contaminated food (including milk) or water, or by direct faecal-oral spread.
In humans, serovars of *Salmonella enterica* are a cause of diarrhea illness in developed countries, while they are responsible for invasive disease in the developing world. *S. enterica sero*var Typhi (*S.* Typhi) and *S. enterica sero*var Paratyphi A (*S.* Paratyphi A) are causes of enteric fever, with high prevalence in South and Southeast Asia, while non-typhoidal *Salmonella* serotypes (frequently referred to as NTS serotypes) (*36*) are major cause of invasive disease in Africa.
S. Typhi is the commonest pathogen isolated from blood cultures in South Asia (*37*), though in some areas enteric fever caused by *S*. Paratyphi A is more common (*38*). The annual global burden of disease due to typhoid fever was estimated at 21.7 million cases in 2000 with a case-fatality rate of 1% resulting in 217,000 deaths (*39*). The highest burden was reported in pre-school and school-aged children (*40*) (*41*) (*42*). The global burden of disease attributable to *S.* Paratyphi A in 2000 was 5.4 million cases (*39*).
Currently two main vaccines are licensed targeting *S*. Typhi only: the live attenuated vaccine, Ty21a, and the Vi capsular PS vaccine, but neither is licensed for use in children under the age of two years.
The Ty21a vaccine was derived from *S*. Typhi through nonspecific chemical mutagenesis of the wild-type strain Ty2 (*43*). It is distributed as enteric-coated capsules and is not licensed in children below 5 years of age. Protective efficacy has been demonstrated for adults and children above 5 years with a cumulative three-dose efficacy of 51% (*44*). Ty21a is not immunogenic in infants and there are reduced levels of seroconversion in young children compared with adults. However there is evidence that it can induce herd protection and, as a live attenuated vaccine, Ty21a has good potential to induce T cell immunity and cross-protection against non-Typhi serovars (*45*) (*46*) (*47*).
Several manufacturers produce unconjugated Vi PS vaccine. Despite its different mechanism of action (*48*), Vi PS has shown a similar three year efficacy of 55% against typhoid fever to that of Ty21a (*44*), but after only one vaccination dose. However, being a T-independent type 2 antigen, the Vi PS is not immunogenic in infants and consequently is only licensed for children over two years of age (*49*) (*50*). Its effectiveness in children between two and five years is uncertain, since two cluster randomized-controlled trails in this age group gave different results, with protective efficacy only demonstrated in one study (*51*) (*52*). As with other PS vaccines, Vi is not able to induce immunological memory. Both Vi PS and Ty21a suffer from drawbacks that have limited their implementation in developing country vaccination

programs. They are not immunogenic in infants (*53*) and cannot be added into existing EPI programs. Both have issues with thermal stability; Ty21a needs multiple doses and a particular concern with Vi is the phenomenon of hyporesponsiveness after re-vaccination (*54*). For all these limitations, there is interest to develop new generation vaccines, that are immunogenic and safe in infants and more protective in older children and adults. No vaccines is currently available against *S*. Paratyphi A (*55*).
New vaccines against typhoidal diseases are currently under development such as glycoconjugates, new generation live attenuated and protein based vaccines (*56*) (*57*) (*58*). Some groups are aiming at a bivalent vaccine to prevent enteric fever (*59*), by separately conjugating Vi and S. Paratyphi A OAg to CRM_{197} or diphtheria toxoid (DT) as carrier proteins.

2.6 Nontyphoidal *Salmonella*: a disease in need for a vaccine

Nontyphoidal *Salmonellae* (NTS) predominantly cause self-limiting diarrheal illness in developed countries, where bloodstream infection is rare (*60*) and mainly occurs in individuals with specific risk factors (*61*). By contrast, in many parts of Africa, NTS are a leading cause of bacteremia (Figure 2.3) (*62*) (*63*) (*64*) (*65*) (*66*)**.** Incidence of disease caused by different serovars varies depending upon the country, but *S.* Enteritidis and *S.* Typhimurium are responsible for the majority of infections, (*36*) (*67*), although investigators at some sites report contributions from other serotypes, such as *S.* Isangi (*68*)**,** *S.* Concord (*69*) and *S.* Dublin (*70*). Invasive NTS (iNTS) disease was recently estimated at 2.58 million cases per year with a 20-25% case-fatality rate leading to 517,000 deaths (*36*). Young children with malaria, anemia and malnutrition (*71*) (*72*) (*73*) (*74*) (*75*) and HIV infected individuals (*65*) (*76*) are particularly affected. A recent study from Mozambique found an incidence of 388/100,000 in children less than one year and 262/100,000 in those aged one to five years (*62*). There is no distinctive clinical syndrome association with this disease, (*36*) (*77*), making diagnosis and treatment a challenge for health-care workers in low-resource settings. Blood culture and microbiological diagnosis of *Salmonella* requires technical expertise and investment in infrastructure, consumables, and quality control, all of which must be strengthened (*78*). An urgent need exists for the development of rapid, accurate point-of-care diagnostics biology. Targets for a non-typhoidal *Salmonella* rapid multi-plexed PCR diagnostic have been identified (*70*), but low numbers of the bacilli in blood make this process a technical challenge (*79*). Other approaches for rapid screening are promising but need validation and translation to real-world application (*80*) (*36*).
Salmonellae were once susceptible to a broad range of affordable and effective antimicrobial drugs, but multidrug-resistant strains (*63*) (*81*) have emerged in Africa. In a recent study around 90% of invasive NTS isolates in Malawi have been found to be multidrug resistant (*63*), emphasizing the need for development of alternative interventions.

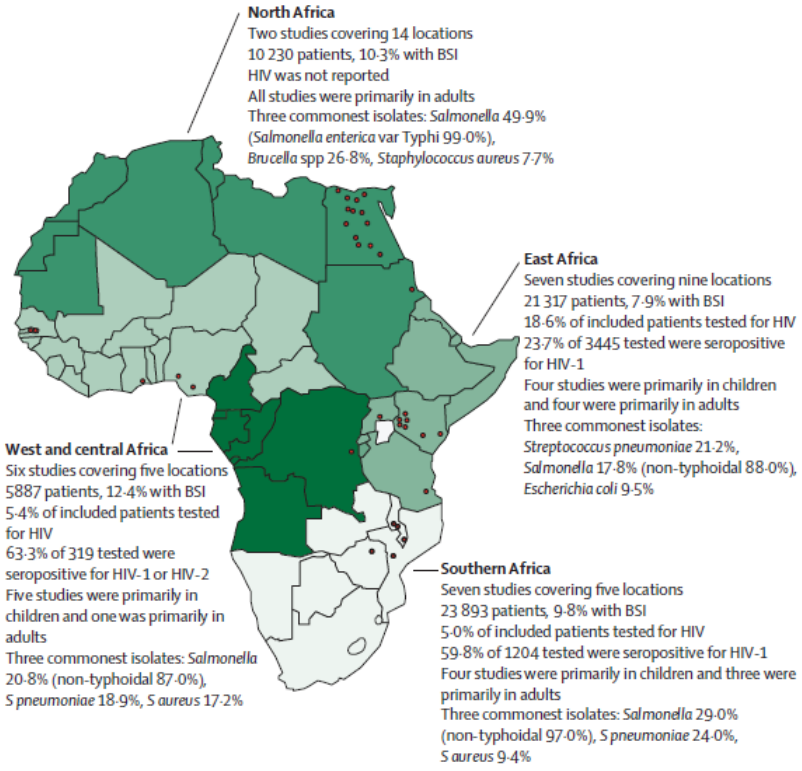

Figure 2.3 Map of Africa showing results of a meta-analysis of studies investigating the cause of bloodstream infection (BSI) in febrile adults and children in Africa (Figure reproduced from (*64*)).

2.6.1 Vaccines in development against nontyphoidal *Salmonella*

While new vaccines against typhoid fever are in advanced stages of development and some glycoconjugate vaccines have been recently licensed in specific countries (*56*) (*57*), the development of vaccines against NTS is a long way behind, despite the comparable burden of disease they cause. This is likely to be attributable to a general lack of appreciation and awareness of the problem of NTS in the global health community (MacLennan and Levine, 2013a). Vaccine development against NTS is also complicated by the immunocompromised nature of susceptible patients (*82*) (*83*), which should be addressed early in clinical development.

However, the enhanced activity in the field of vaccine development against *Salmonella* in the recent years has also increased the attention on NTS and different vaccines are currently in development (Table 2.2).

Table 2.2. Vaccines in development against NTS

Name	Description	Advantage/Disadvantages
O:4,5/O:9-flagellin (*84*) (*85*)	Glycoconjugate	+ High potential efficacy + T-dependent antibody response + Potential for inducing memory + Potential for affinity maturation + Low reactogenicity - Protection only against serovars with same OAg specificity
O:4,5/O:9-CRM_{197} (*86*)		
WT05 (*87*)	Live attenuated	+ Potential to induce *Salmonella*-specific B and T cell immunity + Potential to clear residual infection - Attenuating for optimal balance of immunity and reactogenicity - Breadth of coverage may be limited by insufficient expression of key antigens - Possibility of disease in immunocompromised subjects
CVD 1921 and CVD 1941 (*88*)		
S. Typhimuirum ruvB mutant (*89*)		
Salmonella hfq deletion mutant (*90*)		
SA186 (*91*)		
MT13 (*92*)		
OmpD (*93*)	Outer membrane protein	+ Potential to induce *Salmonella*-specific B and T cell immunity + Potential for pan-specific immunity + Low reactogenicity - Difficulties with purification of integral proteins
NTS GMMA (*50*) (*94*)	GMMA	+ Potential to induce *Salmonella*-specific B and T cell immunity + Potential for pan-specific immunity + Enrichment of membrane antigens + Easy manufacture - Level of reactogenicity uncertain

2.6.2 O-antigen based vaccines against NTS

Previous work has highlighted the potential importance of antibody in African children for complement-dependent cell-free killing of NTS, and opsonization of NTS for uptake by blood phagocytes and killing by oxidative burst (*71*) (*95*), making an antibody-inducing vaccine an attractive goal for prevention of NTS disease in Africa.
While other *Salmonella* species express a capsular PS (for example *S*. Typhi Vi capsule), NTS (with rare exceptions) do not express PS capsules. Their surface PS are the OAg of LPS.
Salmonella LPS is both a virulence factor and a target for protective antibodies. LPS consists of lipid A linked to the 3-deoxy-D-manno-octulosonic acid (KDO) terminus of a conserved core saccharide region (*96*), which is linked to a variable PS chain of repeating units, the OAg chain (Figure 2.4). Lipid A is highly conserved and exerts endotoxic activity, while the OAg chain differs between species and is responsible for the serological specificity of bacteria. This serovar-specific OAg chain is the immunodominant portion of the molecule.
OAg are usually obtained by detoxification of the LPS by acetic acid hydrolysis or by hydrazinolysis (*97*). The first procedure is preferred as it allows the retaining of the OAg O-acetylation level, which can be important for immunogenicity (*97*).
The majority of invasive *Salmonella* isolates from humans fall into *Salmonella* groups A, B, C or D. OAg of *Salmonella* groups A, B and D are similar in overall structure and share a common backbone, but differ in their branching carbohydrate moieties, α-(3,6)-dideoxyhexose-(1,3) linked to D-mannose (Man). With regard to the two most common NTS serovars, the dideoxyhexoses are abequose (Abe), conferring O:4 specificity to *S.* Typhimuirum and tyvelose (Tyv), conferring O:9 specificity to *S.* Enteritidis (Figure 2.5) (*98*). The OAg chain can be partially O-acetylated. O-acetylation at the C-2 position of Abe adds specificity 5 to O:4 (Figure 2.5).
Antibodies directed toward the OAg mediate killing of NTS (*77*) (*99*) and confer protection against NTS infections.
Little is known regarding the immunogenicity of purified *Salmonella* OAg in humans administered parenterally as a PS vaccine, however evidences from studies in mice suggest that *Salmonella* OAg as an isolated PS is a poor immunogen (*100*) (*84*) (*98*). In contrast, conjugation of *Salmonella* OAg to protein carriers results in vaccines that have been effective in generating anti-OAg antibodies in animal models (*100*) (*101*) (*102*) (*84*) (*98*). NTS OAg conjugate vaccines have also demonstrated protection against mortality in the mouse model of lethal *Salmonella* infection. In one study, conjugation of *S.* Typhimurium OAg to the homologous strain porin proteins elicited anti-OAg IgG, protective against challenge with virulent *S.* Typhimurium (*102*). This conjugate in mice, as well as a conjugate with bovine serum albumin (BSA) in rabbits, induced functional opsonophagocytic antibodies that could transfer protection by passive immunization (*101*) (*102*) (*103*). Similar results were seen following immunization of mice with a conjugate of *S.* Typhimurium OAg with tetanus toxoid (TT) (*98*). A conjugate vaccine consisting of *S.* Enteritidis OAg linked to the homologous serovar flagellin elicited LPS-specific IgG and protected mice against lethal challenge with virulent *S.* Enteritidis (*84*).

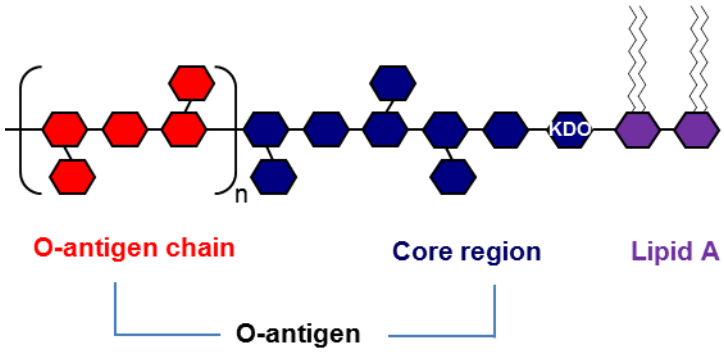

Figure 2.4 Model of *Salmonella* LPS, composed by the polysaccharidic OAg chain and the oligosaccharidic core region, linked to the lipid A by the reducing sugar KDO.

A)

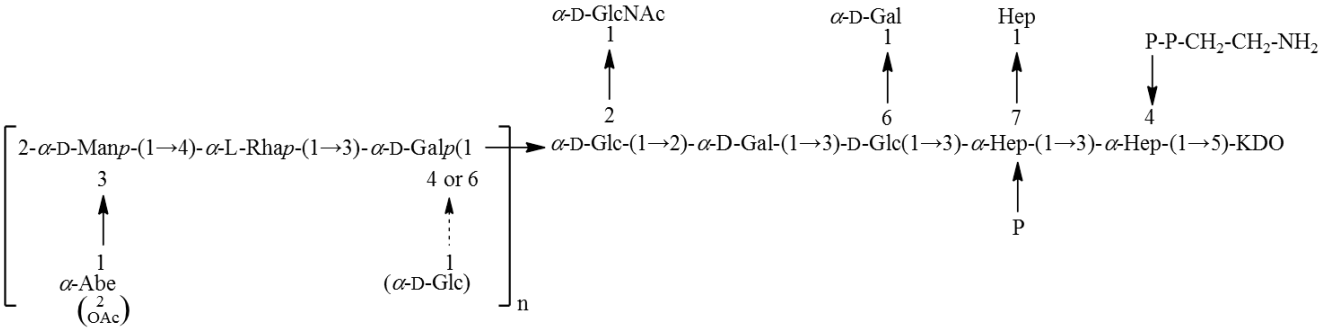

B)

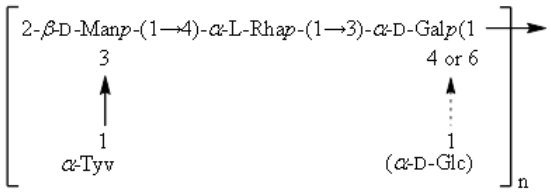

Figure 2.5. A) Structure of the *S.* Typhimurium OAg chain linked to the core region (*96*) after acetic acid hydrolysis. Hydrolysis removes lipid A leaving the OAg chain attached to the core. The core region is common to all *Salmonella* strains. B) Structure of the repeating units of the OAg from *S*. Enteritidis.

2.6.3 Other vaccines under development against NTS

- **Live-attenuated vaccines**

Live-attenuated vaccines have the ability to elicit *Salmonella*-specific T cell responses required for clearance of residual infection, can be given orally and have good capacity to induce mucosal immunity through lymphocyte expression of mucosal homing receptors (*104*). The delivery of multiple *Salmonella* antigens to the immune system increases the possibility of inducing broad protection against different *Salmonella* serovars. The increased ability to introduce targeted mutations and genetic modifications combined with the full availability of the bacterial genomes from whole genome sequencing has improved the capacity to rationally design new live-attenuated vaccines. The major challenge in the development of live-attenuated vaccines is obtaining an optimal level of attenuation without compromising immunogenicity as immunogenicity often decreases together with reactogenicity when *Salmonellae* are attenuated (*105*).
Preclinical studies have been performed with live iNTS vaccines consisting of *S*. Typhimurium and *S*. Enteritidis with deleted *guaBA* and *clpP* genes. These vaccines were able to protect against lethal challenge with the homologous serovars in mice (*88*). A *S*. Typhimurium strain with *aroC* and *ssaV* attenuations is the only live-attenuated iNTS vaccine that has been tested in man to date. This Phase 1 study showed prolonged stool shedding in volunteers for up to 23 days (*87*).

- **Protein-based subunit vaccines**

Surface proteins constitute an other target of protective immunity.
These potentially have the advantage of cross-protection if carefully selected through bioinformatic analysis of whole genome sequences through a reverse vaccinology approach. As proteins, such vaccines can induce both antibody and T cell responses, though the former can be problematic for membrane proteins with multiple membrane-spanning domains.
The proteins that have received most attention to date have been flagellin (*85*) and OmpD porin (*93*). Preclinical studies have demonstrated promise for all of these antigens with immunization resulting in protection against *Salmonella* challenge (*93, 106-108*). Nevertheless, the purification and production processes to make these vaccines are quite complicated. Furthermore it may be crucial to preserve the correct conformation of these antigens to generate protection in mice (*109*).

- **GMMA vaccines**

GMMA (Generalized Modules for Membrane Antigens) are vesicles released from the surface of Gram-negative bacteria, e.g. *Salmonella,* genetically modified in the genes encoding proteins that span the periplasm and maintain the integrity of the inner and outer membranes, such as the *tolR* gene of the Tol-Pal system, to enhance vesicles release (*94*). These particles are 10-300 nm proteoliposomes (*110*) (*111*) and reflect the composition of the bacterial outer membrane, containing LPS, glycerophospholipids, outer membrane proteins in their natural conformation, and enclosing periplasmic components (*112*) (*110*). Further deletions are incorporated to reduce reactogenicity, such as *htrB* and *msbB* (*113*), but unlike live-attenuated vaccines, there is no possibility of infection.
Advantages of GMMA vaccines include simplicity and low cost of production, ability to induce strong immunogenicity and a potential self-adjuvanting effect due to the presence of innate signaling molecules such as TLR ligands. GMMA constitute a

promising platform for the delivery of both surface PS and outer membrane proteins to the immune system in their correct conformation and orientation. GMMA also have good potential to induce *Salmonella*-specific T cell immunity.

2.7 Polysaccharide vaccines

The outermost surfaces of most bacteria are coated with PS (*114*) (*115*). PS expressed in pathogenic bacteria (e.g., *Haemophilus influenzae*, *Streptococcus pneumoniae* and *Neisseria meningitidis*) play major roles in the virulence of these organisms. PS protect bacteria from the immune response and therefore act as virulence factors through numerous mechanisms such as inhibiting complement activation, increasing bacterial attachment to host tissues, preventing phagocytosis and helping bacteria escape immune surveillance by mimicking host-glycans (*116*).
Around the 1930s the protective role of antibodies induced by pneumococcal PS started to be investigated and in 1945 the first vaccine composed of purified PS from selected pneumococcal serotypes was tested in man (*117*) (*118*).
The research for vaccine development was subsequently slowed down by the introduction of antibiotics. However, with the emergence of drug-resistant strains, the development of PS vaccines started again and a number of them were tested in large clinical trials (*119*) (*120*). Polysaccharide vaccines against meningococcus serogroup ACWY, *Streptococcus pneumoniae* and *Haemophilus influenzae* type b (Hib) were licensed between the seventies and eighties. Examples of pure PS vaccines used today include a multi-valent vaccine of PS obtained from 23 different *Streptococcus pneumoniae* serotypes; Vi PS from *S*. Typhi; and PS from serotypes A, C, W135 and Y of *Neisseria meningitidis* (*121*).
Although these vaccines have variable degrees of success in adults, they are poorly protective in high-risk populations such as children below two years and immunocompromised patients (*16*). These characteristics are due to the fact that PS are T-cell independent (TI) antigens. Polysaccharide antigens directly activate PS-specific B cells which differentiate into plasma cells to produce antibodies, but memory B cells are not formed. In addition, the antibody response to bacterial PS is weakly affected by adjuvants, IgM represents the major class of antibodies induced and, since their immune response does not induce memory, it is not boosted by subsequent immunizations.

2.8 Glycoconjugate vaccines

Glycoconjugate vaccines are composed of a weak antigen (hapten), containing only B-cell epitopes, but lacking T-cell epitopes, covalently linked to a protein as a source of T-cell epitopes (carrier) (*122*).
The concept of glycoconjugate vaccine has its origin in 1929, when Avery and Goebel demonstrated that derivatives of non-immunogenic glucose and galactose, when conjugated to proteins, were able to induce specific antibodies in rabbits (*123*).
The first protein-PS conjugate vaccines were developed against *Haemophilus influenzae type b* and licensed between 1987 and 1990. Subsequently, glycoconjugate vaccines have been developed against *Neisseria meningitidis*, *Streptococcus pneumoniae* and *group B streptococcus* (*124*) (*125*) (*126*). Covalent conjugation to an appropriate carrier protein (*121*) provides T cell-dependent immunogenicity against the saccharide hapten. With the involvement of T cells, immunological memory is invoked, and avidity maturation and isotype switching occur. Importantly, glycoconjugate vaccines are effective in young infants.

Today glycoconjugate vaccines are among the safest and most efficacious vaccines developed and are used in the immunization schedules of different countries (Table 2.3).

Table 2.3 Glycoconjugate vaccines licensed or in advanced development in the EU, US and WHO (Table adapted from (*127*)).

Vaccine[a] *Manufacturer*	Target infection	Development stage
PRP–TT *Sanofi-Pasteur* PRP–OMPC *Merck* PRP–CRM197 *Pfizer* Hib–CRM197 *Novartis V&D*	*Haemophilus influenzae* type b	Commercial
PRP–TT *CGEB, Cuba*		
MenC/Hib–TT *GSK*	*Haemophilus influenzae* type b/*Neisseria meningitidis* serogroup C	
MenA–TT *Serum Institute India*	*Neisseria meningitidis* serogroup A	
MenC–CRM197 *Pfizer*	*Neisseria meningitidis* serogroup C	
MenC–CRM197 *Novartis V&D*		
MenC-TT *Baxter*		
MenACWY–DT *Sanofi-Pasteur*	*Neisseria meningitidis* serogroup A, C, W, Y	
MenACWY–CRM197 *Novartis V&D*		
MenACWY-TT *GSK*		
7 valent-CRM197 (4, 6B, 9V, 14, 18C, 19F, 23F) *Pfizer* 13 valent-CRM197 (1, 3, 4, 5, 6A, 6B, 7F, 9V, 14, 18C, 19A, 19F, 23F) *Pfizer* 10 valent-DT/TT Protein D (1, 4, 5, 6B, 7F, 9V, 14, 18C, 19F, 23F) *GSK*	*Streptococcus pneumoniae*	
15 valent-CRM197 (1, 3, 4, 5, 6A, 6B, 7F, 9V, 14, 18C, 19A, 19F, 22F, 23F, 33F) *Merck*		Clinical development (Phase II)
3-valent-CRM197 (Ia, Ib, III) *Novartis V&D*	Group B *Streptococcus*	Clinical development (Phase I)

Many studies have been performed to understand the mechanisms of internalization and processing of the glycoconjugate molecules by the immune system (*128*) (*49*) (*129*) (*130*) (*115*).

According to the classical mechanism proposed, the polysaccharidic component of the vaccine binds to surface immunoglobulin of PS-specific B cells. Following internalization of the vaccine, the protein component is processed and resulting peptide fragments are presented to the T cell receptor of CD4+ peptide-specific T cells in the peptide-binding groove of major histocompatibility complex class II molecules (MHCII). In addition to this cognate interaction, further signals are essential in eliciting CD4+ T cell help for the B cell (*131*) (*132*) (Figure 2.5). When B cells receive T cell help, they proliferate and differentiate, with class switching particularly to IgG, into plasma cells and memory B cells. These can rapidly proliferate and differentiate into plasma cells on subsequent encounter of the specific antigen producing high antibody titers (*133*) (*134*) (*135*) (*136*) (*137*). Antibody avidity is increased through affinity maturation in germinal centers (*138*). Not all PS are strictly T-independent antigens and zwitterionic PS, such as PS A from *Bacteroides fragilis*, containing both positive and negative charges, are able to stimulate T cell help (*115*) (*139*) (*139*) (*140*) (*141*). Recently it has been found that the carbohydrate fragments of the glycopeptides, produced by glycoconjugate vaccine processing, recognizes CD4+ T cells with the peptide portions useful for binding to MHCII molecules (*142*) (*128*).

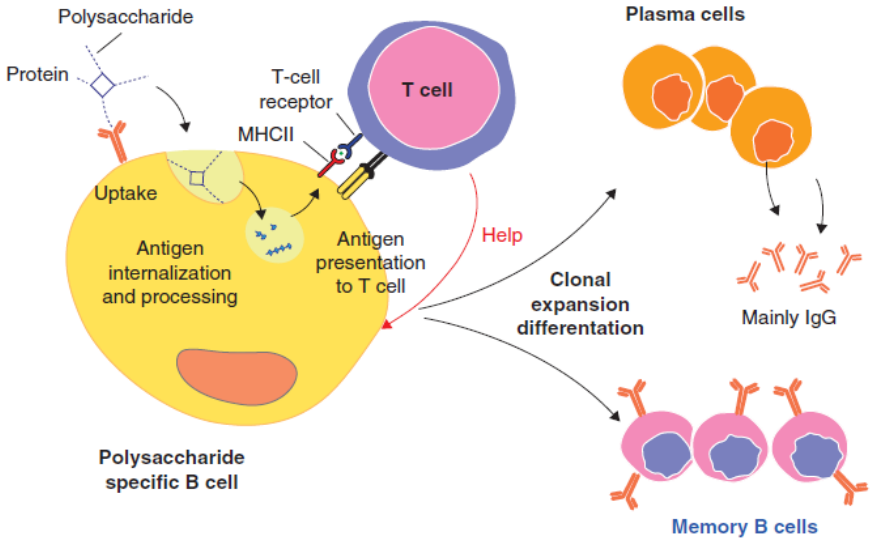

Figure 2.5 Mechanism of action proposed for conjugate vaccines (*122*).

The process of developing T cell mediated immunity by a glycoconjugate vaccine can be influenced by the formulation. The adjuvants can be used for various purposes: (i) to increase the immunogenicity of the antigens; (ii) to reduce the amount of antigens or the number of immunizations needed for protective immunity; (iii) to improve the efficacy of vaccines in newborns, the elderly, or immunocompromised individuals; and (iv) as delivery systems to facilitate the uptake of antigens by the mucosa (*143*). Some of the adjuvants commonly used in clinical and preclinical settings have been recently reviewed (*127*) and can be classified as mineral salts (*144*), carbohydrates (*145*), lipids (*146*), glycolipids (*147*), lipopeptides (*148*), TLR agonists (*149*), saponins and bacterial toxins (*150*). Many of these adjuvants have been successfully used alone or in combination with conjugates of carbohydrate antigens (*151*).

2.8.1. The chemistry of glycoconjugation

Conjugate formation requires the covalent linkage of the PS to the carrier protein. Different conjugation strategies have been used to prepare conjugate vaccines and two main approaches have been developed: one based on random chemical activation along the PS chain, followed by conjugation and the other based on coupling of the protein through activation of the saccharide terminal group (*122*). The random approach often results in complex mixtures of cross-linked glycoproteins with variable saccharide loading and antigen positioning.
The selective approach is often applied to oligosaccharides. Oligosaccharides can also be synthesized starting from suitable monosaccharides. This methodology is increasingly attractive as it provides homogeneous, well-defined and well-characterized molecules with built-in chemical terminal functionalities suitable for conjugation to carrier proteins. (*152*) (*153*) (*154*) (*155*)**.**
Covalent linkage of PS to proteins is generally achieved by targeting the amines of lysines, the carboxylic groups of aspartic/glutamic acids or the sulfhydryls of cysteines on the protein. There are now novel methodologies that enable also the precise glycosylation of proteins and that may be used to improve the consistency and characterization of glycoprotein vaccine candidates**.** The possibility of designing and synthesizing chemically-defined glycoconjugate vaccines with different carbohydrate densities, conformations, and shapes, could potentially lead to the selection of candidates with enhanced efficacy**.**
A new bioconjugation approach, called protein glycan coupling technology (PGCT), is based on glyco-engineering the N-glycosylation pathway in bacteria such as *Escherichia coli*. The PS, encoded by the inserted genes, is produced on a polyisoprenoid carrier and then is transferred to an asparagine residue of the carrier protein which has to contain at least one (native or engineered) N-glycosylation site (*156*) (*157*) (*158*) (*159*). Although this new *in vivo* conjugation technology is currently limited in the variety of glycan or protein substrates it can utilize, it has great potential to generate new-generation vaccines, in which the conjugation reactions are well controlled and conjugation products are homogeneous and structurally defined. Moreover the use of such methodology avoids the need for pathogenic bacteria from which to isolate PS and/or proteins since both glycan and protein synthesis and glycoconjugate assembly occur exclusively in an *E. coli* system (*160*). Recently PGCT has been used to generate novel glycoconjugate vaccines against *Shigella dysenteriae* type 1 *(159)*.

2.8.2. Parameters that affect glycoconjugate immunogenicity

Several parameters can affect the immunogenicity of conjugate vaccines (*122*). Saccharide chain length, saccharide to protein ratio in the purified conjugate, conjugation chemistry, the nature of the linkers used for saccharide and/or protein derivatization and of the protein carrier are key parameters to investigate. Studies performed so far have compared the immunogenicity of vaccines differing for multiple parameters at the same time, making therefore difficult to assign the relative importance of the single variables to immunogenicity. However, it is clear that the influence of conjugation variables varies for different carbohydrate antigens and these variables are strongly interconnected.
Some studies have investigated the impact of these parameters on the immunogenicity of OAg glycoconjugate vaccines.

- **Size of the saccharide moiety**

When tetra-, octa-, and dodecasaccharides from the OAg of *S.* Typhimurium were conjugated through the terminal reducing ends to BSA, anti-LPS antibody titers increased with saccharide size in mice and rabbits (*101*). *S.* Paratyphi A conjugates, with random coupling of OAg to TT using an adipic acid dihydrazide (ADH) linker, elicited high antibody levels with high MW OAg and no detectable antibodies with low MW OAg (average MW 122 and 23.4 kDa respectively) (*161*).
In contrast, *Shigella dysenteriae* type 1 and *Shigella sonnei* conjugates significantly improved with lower MW saccharides compared with full length OAg, bound at their reducing ends to the protein carrier at defined densities. Similarly, a study with synthetic *Shigella dysenteriae* type 1 oligosaccharides coupled to human serum albumin at multiple attachment points, found that conjugates with short oligosaccharides (2, 3 and 4 repeating units respectively) elicited higher antibody levels than a conjugate with full length OAg (approximately 27 repeating units) (*162*). Also *Shigella sonnei* conjugates with low MW OAg fragments (average of 3.5 repeating units) terminally linked to BSA or DT induced significantly higher antibody levels in mice than the full length OAg (approximately 29 repeating units) conjugated to *r*EPA by random chemistry (*163*). For *Shigella flexneri* 6, OAg with an average of seven repeating units and full length OAg induced similar antibody levels (*164*). Phalipon et al. found that a synthetic sequence of three repeating units of the *Shigella flexneri* 2a OAg conjugated to TT had higher immunogenicity and better protective efficacy in mice compared to conjugates with one or two repeating units (*165*). The nature of the OAg seems to influence the effect that saccharide chain length can have on immunogenicity and there is likely to be a minimum chain length required to induce a strong immunological response for each saccharide type (*166*) (*167*).
However, this parameter seems to be affected also by other factors. For example, Phalipon and Pozsgay have reported a strong correlation between saccharide chain length and saccharide loading (*165*) (*162*). Also the conjugation chemistry used can have an impact. Use of low MW saccharide may maximize the T cell help afforded by the carrier protein, but such glycoconjugates can fail to raise anti-PS antibodies if key conformational epitopes on the whole PS are lost (*168*). Probably due to the complexity of the immune response and the high number of variables associated, it is not always possible to see a clear correlation between the variation of MW and the immunological response for a given antigen. However, OAg-based glycoconjugate investigations for *Salmonella* seem to indicate that the immunological response would benefit from the use of higher MW saccharide hapten.

- **Conjugation chemistry and linker**

The choice of conjugation strategy and linker have an important effect on efficiency of conjugation, saccharide to protein ratio and vaccine size, with consequent impact on immunogenicity (Beuvery et al., 1983) (Carmenate et al., 2004).
The linker (or spacer) is a short linear molecule that is generally linked to the sugar chain or to the protein or to both moieties, depending on the coupling chemistry used. Linkers differ in length, flexibility and functional groups involved and facilitate the saccharide-protein coupling by alleviating the steric hindrance factors. The creation of immunogenic neoepitopes as a result of the linker/conjugation chemistry used might drive the antibody response of the conjugate away from targeted epitopes located on the hapten (*122*).

With regard to OAg based vaccines, S. Typhimurium OAg-TT conjugates produced by random activation and ADH linker were more immunogenic in mice than when selective chemistry with the same linker was used. Immunogenicity was also affected by the amount of linker incorporated (*98*). Similarly, *Vibrio cholerae* O1 serotype Inaba deacylated LPS conjugated to cholera toxin (CT) were more immunogenic when obtained by random chemistry with ADH than when produced by single-point attachment, even if a different linker, SPDP, was used for the last approach (*169*). The same antibody levels and protection were obtained by comparing *S*. Enteritidis OAg conjugated directly to flagellin monomers by random activation or with selective chemistry through diaminooxy cysteamine and N-(γ-maleimidobutyloxy)-sulfosuccinimide ester linkers (*106*).
Escherichia hermannii OAg linked directly to BSA gave earlier and more persistent antibody response in mice than when ADH linker was used (*170*). For *Escherichia coli* O111 OAg-TT conjugates, for immunogenicity in mice, ADH was a more effective linker than SPDP (*171*). Other studies did not find an influence of linkers on immunogenicity and for example linkers of three different chain lengths did not impact on the immunogenicity of *Vibrio cholerae* O1, Ogawa serotype hexasaccharide-BSA conjugates tested in mice (*172*).
The choice of conjugation chemistry is also related with the efficiency and consistency of the process: if the sugar MW is too high, it is not trivial to obtain a selective derivatization in a single point while it is much easier to apply random derivatization chemistry. However, a single selective derivatization impacts to a lesser extent on the antigenicity of the saccharide hapten and enables vaccines which are easier to be characterized, and because of that some authors have suggested this as the preferred strategy (*122*).

- **Saccharide to protein ratio**

Considering OAg-based glycoconjugates, reported studies have confirmed an influence of this parameter on conjugate vaccine immunogenicity. For example, Svenson (*101*) found that immunogenicity of *S.* Typhimurium octasaccharide-BSA conjugates in mice was enhanced by increasing the molar ratio of saccharide to protein from 7 to 23 (*101*). For *Shigella flexneri* 2a conjugates with a synthetic pentadecasaccharide, an average molar ratio of two induced no anti-LPS antibodies in mice, and an average ratio of 14 was more immunogenic than eight (*165*). With terminally-linked saccharides, immunogenicity usually increases with increasing molar saccharide to protein ratio (*173*) (*174*) (*165*). This is likely to result from better cross-linking and activation of saccharide-specific B cells with increased sugar loading. However, with high saccharide-to-protein ratios, essential carrier epitopes may be hidden from the immune system, hindering recognition of the conjugate vaccine as a T-dependent antigen. Pozgay, testing the immunogenicity of *Shigella dysenteriae* type 1 conjugates in mice, found that the optimal carbohydrate chain density differed with oligosaccharide length, highlighting the connection between these two parameters (*162*).

- **Carrier protein**

Carrier proteins used for carbohydrate antigen conjugation are preferably proteins that are non-toxic, non-reactogenic and can be obtained in sufficient amount and purity. They should also be stable under standard chemical conditions (concentration, pH, ionic strength) of conjugation procedures. Current proteins used in commercial or under development conjugate vaccines include: DT, nontoxic cross

reactive material of diphtheria toxin (CRM_{197}), TT, keyhole limpet hemocyanin (KLH), the outer membrane protein of *N. meningitidis* (OMPC), *recombinant exoprotein Pseudomonas aeruginosa* (*r*EPA) and, more recently, protein D derived from non-typeable *H. influenzae*. In some cases, bacterial PS have been conjugated to a protein from the same pathogen to combine the effects of the carbohydrate and the protein antigens (*84*) (*127*).
Most animal studies indicate that the choice of the carrier protein has an impact on conjugate vaccine immunogenicity (*122*), but few studies have investigated on the effect of carrier protein on the immunogenicity of OAg-based glycoconjugate vaccines. Vaccination in healthy adults using OAg of *Shigella sonnei* conjugated to native or succinylated *r*EPA or *Corynebacterium diphtheriae* toxin mutant CRM9 by random chemistry and with ADH as linker, gave the same anti-LPS IgG levels (*175*). With *Shigella flexneri* 2a OAg, the *r*EPAsucc conjugate gave instead significantly higher antibody levels (*175*). The opposite result was obtained in mice, with succinylated *Shigella flexneri* 2a-CRM9 being more immunogenic than succinylated *Shigella flexneri* 2a-*r*EPA (*176*). *S.* Enteritidis OAg conjugates were similarly immunogenic in mice when coupled to *S.* Enteritidis flagellin monomers, polymers or CRM_{197} by random conjugation with no linker (*177*).

2.9 NTS glycoconjugate project at NVGH

NVGH is working on the development of a bivalent glycoconjugate vaccine covering both *S.* Typhimurium and *S.* Enteritidis. OAg purified from the two strains will be independently conjugated to CRM_{197} (*178*) as carrier protein.
CRM_{197} is a non-toxic variant of DT that does not require chemical detoxification. Because of that, CRM_{197} has a well-defined physico-chemical profile, consistent from one preparation to another one. It has been successfully used as carrier for many glycoconjugate vaccines against Hib, Pneumococcus (7 and 13 valent) and recently for a tetravalent (ACWY) meningococcal conjugate vaccine which have been proved to be safe and immunogenic for all ages (*179*).
NVGH has developed a simplified method for OAg extraction and purification (*86*). In the adopted strategy, the labile linkage between the KDO of the core and the lipid A is cleaved directly in the bacterial growth medium; the OAg, still linked to the core, is then easily purified from the cells and used for the production of conjugate vaccines. In this way, LPS purification from bacterial membranes, a very time-consuming and often hazardous process, is avoided. The conjugation chemistry developed for *S.* Paratyphi A OAg (*180*) has been applied to NTS OAg. This method uses the terminal KDO unit of the OAg chain for linkage to the protein, without modifying the sugar moiety. Preliminary studies in mice showed that the conjugate obtained by this chemistry with the OAg from *S.* Typhimurium strain D23580 induced high anti-OAg titers with bactericidal activity.

2.10 PhD project aims

In the contest of the NTS glycoconjugate vaccine project, my PhD project has been focused in three related aspects:

1) Structural and biological characterization of NTS polysaccharide purified from different S. Typhimurium and S. Enteritidis strains.

2) Synthesis, characterization and immunological evaluation of a panel of NTS glycoconjugate vaccine variants (OAg source, conjugation chemistry, OAg/protein ratio) to better understand the key factors in glycoconjugate vaccine design required for optimal antibody-mediated immunity.

3) Design of new efficient glycoconjugation methodologies which allow the synthesis of structurally high-defined glycoconjugate vaccines and simplify the conjugation process.

These studies will contribute to design an improved conjugate vaccine against NTS.

3. Impact of OAg structure on the immunogenicity of NTS glycoconjugate vaccines

3.1 Abstract

The influence of parameters like saccharide chain length and O-acetylation level has been investigated for several antigens and can impact on the immunogenicity of their corresponding conjugate vaccines. Here, OAg from 6 different *S.* Typhimurium and 4 different *S.* Enteritidis strains were purified and fully characterized and immunogenicity of corresponding glycoconjugates evaluated in mice.
S. Typhimurium OAg showed a similar bimodal molecular weight distribution, but differed with respect to the amount and position of O-acetylation and glucosylation. For the D23580 strain, O-acetyl groups were found not only on C-2 of abequose (factor 5 specificity), but also on C-2 and C-3 of rhamnose; glucose was found to be linked 1→4 or 1→6 to galactose in different amounts according to the strain of origin. *S.* Enteritidis OAg were not only similar for average chain length but also for sugar composition, all characterized by low O-acetylation and glucosylation levels.
Corresponding conjugates were synthesized using CRM_{197} as carrier protein, without altering the OAg chain, in order to examine the impact of OAg structure on immunogenicity. All the NTS glycoconjugates were immunogenic in mice and able to elicit bactericidal antibodies. OAg fine specificities appeared to influence glycoconjugate immunogenicity. In particular, the presence of additional O-acetyl groups on rhamnose for *S*. Typhimurium D23580 OAg resulted in the production of strain-specific anti-OAg antibodies. O-acetylation and glucosylation appeared to have an impact on the bactericidal activity when antibodies produced in mice were tested against a broad panel of *S.* Typhimurium endemic strains.

3.2 Introduction

Bacterial LPS can demonstrate high levels of heterogeneity, particularly LPS from NTS. OAg can vary in chain length and other modifications, like glucosylation and O-acetylation of the repeating units, which can constitute additional specific OAg factors (*181*).
In particular, with regards to *S.* Typhimurium and *S.* Enteritidis OAg, galactose (Gal) may be α(1→6) or α(1→4) glucosylated, giving the factor 1 or factor 12_2 specificity respectively (*181*) (*182*) (*183*) (*184*). For *S.* Typhimurium, the abequose (Abe) may be 2-O-acetylated, which adds O:5 specificity in the Kauffman-White scheme . Wollin et al. (*185*) reported the O-acetylation of C-2 and C-3 of rhamnose (Rha) as a new, hitherto unknown modification of *S.* Typhimurium OAg chain. In *S.* Enteritidis, instead, some of the glucose (Glc) residues have been found to be O-acetylated at C-2 (*184*).
O-acetylation level of glycoconjugate vaccines has been investigated for several antigens and can have an impact on immunogenicity (*186*) (*97*) (*187*) (*188*) (*189*) (*190*)**,** but few data has been reported for NTS conjugate vaccines (*98*). Wollin et al. showed that O-acetyl groups on Rha did not elicit specific antibodies in rabbits. No data have been reported so far on the influence of glucosylation level and/or position.
Here OAg chains purified from six different *S.* Typhimurium strains and four different *S.* Enteritidis strains have been fully characterized. The results obtained are important for understanding to what extent structural variability of NTS LPS can be

associated with the strain of origin. Corresponding conjugate vaccines have been synthesized by using CRM_{197} as carrier protein without altering the OAg chain structure in order to investigate if this structural variability can have an impact on the immunogenicity of corresponding glycoconjugate vaccines. This in turn is required to verify the importance of the selection of the NTS strain used as OAg source for the development of a candidate conjugate vaccine with broad coverage against NTS.

3.3 Material and methods

Reagents

The following chemicals were used in this study: triethylamine (TEA), adipic acid dihydrazide (ADH), sodium cyanoborohydride ($NaBH_3CN$), sodium acetate (AcONa), dimethyl sulfoxide (DMSO), sodium phosphate monobasic (NaH_2PO_4), sodium chloride (NaCl), hydrochloric acid 37% (HCl) [Sigma]; acetonitrile (CH_3CN) [LC-MS Chromasolv]; adipic acid bis(N-hydroxysuccinimmide) (SIDEA) [PFANSTIEHL Laboratories]; absolute ethanol [Carlo Erba]. CRM_{197} was obtained from Novartis Vaccines and Diagnostics (NV&D).

Origin and growth of S. Typhimurium and S. Enteritidis strains

The clinical isolate D23580 was obtained from the Malawi-Liverpool-Wellcome Trust Clinical Research Programme, Blantyre, Malawi. D23580 is a typical and representative Malawian invasive NTS isolate belonging to the ST313 sequence type and pathovar (*81*). 1418, 2189 and 2192 are animal isolates (*191*) (*192*) and were obtained from the University of Calgary. The laboratory strains NVGH1791 and LT2 (*193*) were obtained from the University of Birmingham, UK, and Novartis Master Culture Collection, respectively. SEN animal strains 502, 618 and IV3456074 were obtained from Quotient Bioresearch Limited, UK, and were isolated by the European Antimicrobial Susceptibility Surveillance in Animals (EASSA), coordinated by the European Animal Health Study Centre, Brussels (CEESA). Those strains belonged to CEESA EASSA collections II and III (de Jong, Intern Journ Antimicrob Agents 2013). SEN D24359 is a human isolate obtained from the Malawi-Liverpool-Wellcome Trust Clinical Research Programme, Blantyre, Malawi.
All *S.* Typhimurium and Enteritidis strains (except for 618) were grown in a chemically defined medium, using glycerol as the carbon source. S. Enteritidis 618 was grown in a complex medium containing: 10 g/L Soytone, 5g/L ultrafiltered yeast extract (Difco), 10 g/L NaCl, 3% glycerol. All strains were fermented in a 7 L bioreactor (EZ-Control, Applikon) as previously described (*86*) (*194*).

OAg purification

S. Typhimurium and *S*. Enteritidis OAg were purified as previously described (*86*). Briefly, acid hydrolysis (2% acetic acid at 100°C for 3 hours) was performed directly on the fermentation culture and the supernatant, containing the released OAg chains linked to the core sugars, was recovered following centrifugation. Lower MW impurities were removed and the supernatant concentrated by tangential flow filtration (TFF), using a Hydrosart 30 kD membrane. Protein and nucleic acid impurities were co-precipitated in citrate buffer 20 mM at pH 3. The protein content was further reduced by ion exchange chromatography. Nucleic acids were further removed by precipitation in 18 mM Na_2HPO_4, 24% EtOH and 200 mM $CaCl_2$, pH > 4.5. OAg was then recovered in water by a second TFF 30 kD step.

OAg characterization

Phenol sulfuric acid assay was used for total sugar quantification (*195*); micro BCA for protein quantification (using bovine serum albumin (BSA) as a reference following the manufacturer's instructions [Thermo Scientific]); UV spectroscopy for nucleic acid content (assuming that a nucleic acid concentration of 50 µg/mL gives an OD 260 = 1) and chromogenic kinetic LAL (Limulus Amoebocyte Lysate) for endotoxin level (Charles River Endosafe-PTS instrument). Size-Exclusion High Pressure Liquid Chromatography (HPLC-SEC) with differential refractive index (dRI) detection was used to estimate the molecular size distribution of OAg populations (*86*). Samples were run on a TSK gel G3000 PWXL column (30 cm x 7.8 mm; particle size 7 µm; cod. 808021) with TSK gel PWXL guard column (4.0 cm x 6.0 mm; particle size 12 µm; cod.808033) (Tosoh Bioscience). The mobile phase was 0.1 M NaCl, 0.1 M NaH_2PO_4, 5% CH_3CN, pH 7.2 at the flow rate of 0.5 mL/min (isocratic method for 30 min). Void and bed volume calibration was performed with λ-DNA (λ-DNA Molecular Weight Marker III 0.12-21.2 Kbp, Roche) and sodium azide (NaN_3, Merck), respectively and dextrans were used as standards. For Kd determination, the following equation was used: Kd = (Te-T0)/(Tt-T0) where: Te = elution time of the analyte, T0 = elution time of the biggest fragment of λ-DNA and Tt = elution time of NaN_3. The sugar monomers constituting the OAg repeating unit and N-acetyl glucosamine (GlcNAc), a unique sugar of the core region, were quantified by use of HPAEC-PAD (*86*). KDO amount was calculated by semicarbazide/HPLC-SEC method (*180*). 1D ^{1}H NMR analysis was recorded on all OAg samples to confirm identity and purity and to calculate the level of O-acetylation (*86*). Sugar composition analysis was also performed by GLC, after hydrolysis of the polysaccharides with 2 M TFA at 125°C for 1 h, and derivatization to alditol acetates (*196*). The sugar linkage positions were determined by GLC-MS after per-methylation of the samples (*197*), hydrolysis with 2 M TFA at 125°C for 1 h, followed by reduction and per-acetylation to obtain the partially methylated alditol acetate (PMAA) derivatives. Peak areas were corrected by using the effective carbon response factors (*198*); for Abe the response factor of 6-deoxy hexose were applied. Determination of the absolute configuration of the sugar residues of OAg samples was performed as previously described (*199*).
In order to determine the position of the O-acetyl groups, the OAg were per-methylated following the method of Prehm (*200*), which leaves the O-acetyl groups in their native positions. Samples were then treated as above to obtain the PMAA derivatives, which were then analyzed by GLC and GLC-MS. Analytical GLC was performed on a Perkin Elmer Autosystem XL gas chromatograph equipped with a flame ionization detector and a SP2330 capillary column (Supelco, 30 m), using He as carrier gas. The following temperature programs were used: for alditol acetates, 200–245 °C at 4 °C/min; for PMAA, 150–250 °C at 4°C/min. Separation of the trimethylsilylated (+)-2-butyl glycosides, for determining the absolute configuration of the sugars, was obtained on a HP1 column (Hewlett–Packard, 50 m), using the following temperature program: 50 °C 1 min, 50-130 °C at 45 °C/min, hold 1 min, 130–240 °C at 1 °C/ min, hold 20 min. GC–MS analyses were carried out on an Agilent Technologies 7890A gas chromatograph coupled to an Agilent Technologies 5975C VL MSD.

Synthesis of OAg-ADH-SIDEA-CRM_{197} conjugates

The following procedure was applied to the OAg purified from all the different strains. OAg was solubilized in 100 mM AcONa pH 4.5 at a concentration of 40 mg/mL. ADH and $NaBH_3CN$ were added as solids, both with a ratio 1.2:1 by weight with respect to the OAg. The solution was mixed at 30°C for 1 h. The reaction mixture was desalted against water on a HiPrep™ 26/10 desalting column 53 mL, prepacked with Sephadex™ G-25 Superfine [GE Healthcare].
For introduction of the second linker, SIDEA, OAg-ADH was dissolved in water/DMSO 1:9 (v/v) at a concentration of 50 mg/mL. When the derivatised OAg was completely solubilized, TEA was added (molar ratio TEA/total NH_2 groups = 5; total NH_2 groups included both phosphoethanolamine groups on the OAg and the hydrazide groups introduced with the linker ADH) and then SIDEA (molar ratio SIDEA/total NH_2 groups = 12). The solution was mixed at RT for 3 h. Purification was performed precipitating OAg-ADH-SIDEA by addition of dioxane (90% volume in the resulting solution) and then washing the pellet with the same organic solvent (ten times with 1/3 of the volume added for the precipitation) to remove residual free SIDEA. Working with the OAg from LT2 and all *S.* Enteritidis strains, the OAg-ADH-SIDEA was purified in a different way. The reaction mixture was added to a volume (equal to two times the reaction mixture volume) of HCl 82.5 ppm and mixed at 4°C for 30 min. Under these conditions, unreacted SIDEA precipitated and was separated by centrifugation. OAg-ADH-SIDEA was recovered from the supernatant by precipitation with EtOH/HCl 55 ppm (80% final). The pellet was washed twice with 100% EtOH (1.5 times the reaction mixture volume) and lyophilised.
For conjugation to CRM_{197}, OAg-ADH-SIDEA was solubilized in NaH_2PO_4 buffer pH 7.2 and CRM_{197} was added to give a protein concentration of 20 mg/mL, final buffer capacity of 100 mM and a molar ratio of OAg active ester groups to CRM_{197} of 30 to 1. The reaction was mixed at RT for 3 h.
Conjugates were purified by hydrophobic interaction chromatography on a Phenyl HP column [GE Healthcare], loading 500 µg of protein for mL of resin in 50 mM NaH_2PO_4 3M NaCl pH 7.2. The purified conjugate was eluted in water at 1 mL/min and the collected fractions were dialysed against 10 mM NaH_2PO_4 pH 7.2.

Characterization of OAg-ADH-SIDEA-CRM_{197} conjugates

Total saccharide was quantified by phenol sulfuric assay (*195*), protein content by micro BCA (using BSA as standard and following manufacturer's instructions [Thermo Scientifics]) and the ratio of saccharide to protein calculated. HPLC-SEC analysis was used to characterize conjugates, in comparison with free OAg and free CRM_{197}. All samples were eluted on a TSK gel 6000PW (30 cm x 7.5 mm) column (particle size 17 µm; Sigma 8-05765) connected in series with a TSK gel 5000PW (30 cm x 7.5 mm) column (particle size 17 µm; Sigma 8-05764) with TSK gel PWH guard column (7.5 mm ID x 7.5 cm L; particle size 13 µm ; Sigma 8-06732) (Tosoh Bioscience). The use of the two columns in series gave better separation of conjugate from free saccharide and protein, allowing the conjugate to enter into the column. The mobile phase was 0.1 M NaCl, 0.1 M NaH_2PO_4, 5% CH_3CN, pH 7.2 at the flow rate of 0.5 mL/min (isocratic method for 60 min). Void and bed volume calibration was performed with λ-DNA (λ-DNA Molecular Weight Marker III 0.12-21.2 Kbp, Roche) and sodium azide (NaN_3, Merck), respectively. OAg peaks were detected by dRI, while UV detection at 214 nm and 280 nm was used for free protein and conjugate detection. Protein and conjugate peaks were also detected using

tryptophan fluorescence (emission spectrum at 336 nm, with excitation wavelength at 280 nm). Kd values were determined using the equation reported before for free OAg characterization. Free protein was estimated by HPLC-SEC, running a calibration curve of the un-conjugated protein in the range 5-50 µg/mL under the same conditions as for the conjugate. The percentage of unconjugated CRM_{197} was calculated by dividing the amount of free protein detected by HPLC-SEC by the total amount of protein quantified in the sample by micro BCA. A method for free saccharide determination is currently under development. O-acetylation level was calculated by ^{1}H NMR in 200 mM NaOD (*180*).
Derivatized OAg intermediates were all characterized by phenol sulfuric assay for sugar content and by HPLC-SEC for verifying aggregation or degradation after modification. Introduction of NH_2 groups was verified by TNBS colorimetric method (*201*) using ADH as standard and subtracting the number of NH_2 groups already present on the un-derivatized OAg sample. Free ADH was detected by RP-HPLC (*180*). Activation on the terminus KDO was calculated as moles of linked ADH/moles of KDO %, indicating the % of OAg chain activated. Total active ester groups introduced with SIDEA were quantified by A260 (Miron and Wilchek 433-35) and free SIDEA was detected by RP-HPLC (Micoli et al. paratyphi). Percentage of derivatization with SIDEA was calculated as molar ratio % of linked active ester groups/total NH_2 groups by TNBS before derivatization, indicating the moles % of NH_2 groups activated by this reaction.

Immunogenicity studies in mice

Groups of 8 mice (C57BL/6, female, 5 weeks old), purchased from Charles River Laboratory and maintained at Novartis Vaccines and Diagnostics, were immunized in a three-dose immunization regimen at 14 days-interval with 1 and 8 µg/dose of OAg with 200 µL/dose.
Mice were bleed before the first immunization (day 0) and on immunization days 14 and 28. Mice were sacrificed and sera collected 2 weeks after the third immunization, on day 42. All animal protocols were approved by the local animal ethical committee (approval N. AEC201018) and by the Italian Minister of Health in accordance with Italian laws.

Serum antibody analysis by ELISA

Serum IgG levels against OAg and CRM_{197} were measured by ELISA as previously described (*86*) (*194*). Unconjugated purified OAg used for making glycoconjugates at either 5 or 15 µg/Ml and CRM_{197} at 2 µg/mL were used for ELISA coating. Mouse sera were diluted 1:200 in PBS containing 0.05% Tween 20 and 0.1% BSA. ELISA units were expressed relative to mouse anti-OAg or anti-CRM_{197} IgG standard serum curves, with best 4 parameter fit determined by modified Hill Plot. One ELISA unit was defined as the reciprocal of the standard serum dilution that gives an absorbance value equal to 1 in this assay. Each mouse serum was run in triplicate. Data are presented as scatter plots of individual mouse ELISA units, and geometric mean of each group.
Statistical analysis of ELISA results was conducted on day 42 samples. Groups were compared using Kruskal-Wallis One-Way ANOVA. Post hoc analysis was performed using Student-Newman-Keuls test for both anti-OAg and anti-CRM_{197} antibody units (using $\alpha = 0.05$).

Serum bactericidal activity (SBA)

Equal volumes of day 42 mouse serum, belonging to the same immunization group, were pooled together for SBA experiments. *S.* Typhimurium D23580 strain was grown in Luria Bertani (LB) medium to log-phase (OD: 0.2), diluted 1:30,000 in SBA buffer (50 mM phosphate; 0.041% $MgCl_2$ $6H_2O$; 33 mg/mL $CaCl_2$; 0.5% BSA) to approximately 3 X 10^3 colony forming units (CFU)/mL and distributed into sterile polystyrene U bottom 96-well microtiter plates (12.5 µL/well). To each well (final volume 50 µL, ~620 CFU/mL), serum samples serially diluted 1:3 (starting from 1:20-1:100 dilution) were added. Sera were heated at 56ºC for 30 min to inactivate endogenous complement. Active Baby Rabbit Complement (BRC, Pel-Freez lot 0405/lot 12521) used at 50% of the final volume was added to each well. BRC source, lot and percentage used in SBA reaction mixture were previously selected by lowest toxicity against *S.* Typhimurium. To evaluate possible nonspecific inhibitory effects of BRC on mouse serum, bacteria were also incubated with: a. the same tested sera plus heat-inactivated BRC (HI-BRC); b. sera alone (no BRC); c. SBA buffer and active BRC. Each sample and control was tested in triplicate. Seven microliter reaction mixture from each well was spotted on LB-agar plates at time zero (T0) to assess initial colony forming units (CFU), and at 1.5 h (T90) after incubation at 37ºC. LB-agar plates were incubated overnight at 37ºC and resulting CFU were counted the following day. Bactericidal activity was determined as percent CFU counted in each pooled serum dilution with active/inactive BRC, compared with CFU of the same sera dilutions with no BRC. SBA graphs show bacterial growth inhibition as a function of anti-OAg ELISA units detected in each tested serum pool.

3.4 Results

Characterization of OAg purified from different S. Typhimurium strains

S. Typhimurium OAg were purified from 6 different strains, and characterized. Independently from the strain of origin, OAg were similar in terms of molecular weight (MW) distribution (Figure 3.1), with two main populations at relatively higher (HMW) and lower MW (LMW) in the range of 80-87 and 28-31 kDa respectively, as determined by HPLC-SEC using dextrans as standards. Only 2192 OAg showed one main peak at average MW of 34.5 kDa. For this more homogeneous sample, average MW was also calculated based on the molar ratio of Rha (OAg chain) to GlcNAc (unique sugar of the core region), equal to 28, and according to the sugar composition analysis by HPAEC-PAD and to the O-acetylation level by ^{1}H NMR, and corresponded to 20.5 kDa.

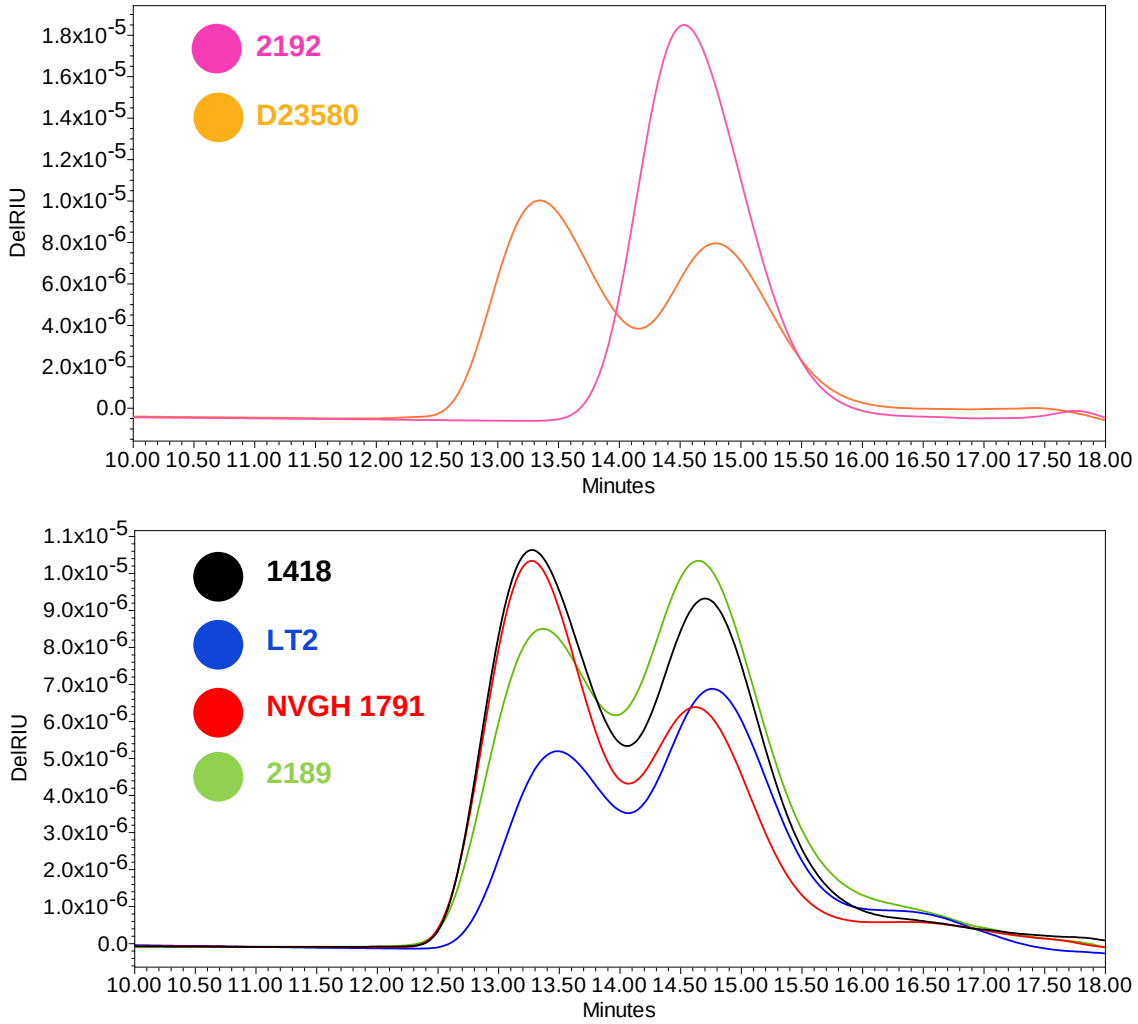

Figure 3.1 HPLC-SEC profiles for *S*. Typhimurium OAg isolated from six different strains. TSKgel 3000 PWXL, 0.5 mL/min, 100 mM NaCl 100 mM NaH_2PO_4 5% CH_3CN pH 7.2; Vtot 23.29 min; V0 11.20 min; dRI detection.

Sugar composition analysis by HPAEC-PAD confirmed the presence of Rha, Gal and Man, the sugars constituting the backbone of the OAg chain, in a ratio 1:1:1 for all the samples examined, while a variable amount of glucosylation was found depending on the strain of origin (Table 3.1). In the absence of a monomer standard, Abe was quantified by ^{1}HNMR analysis which yielded the expected molar ratio of 1:1 with respect to Man for all samples (Fig. 3.2**)**. Analysis by ^{1}H NMR performed after the addition of 200 mM NaOD revealed different O-acetylation levels according to the source of OAg (Table 3.1). In D_2O all samples contained the characteristic signal near 2.13 ppm assigned to OAc on C-2 Abe, with D23580 OAg having additional OAc signals at 2.23 and 2.19 ppm (Figure 3.3). Further structural analysis was performed on all purified OAg, except NVGH 1791 which was similar to the other laboratory strain (LT2) from this preliminary characterization (Table 3.1).

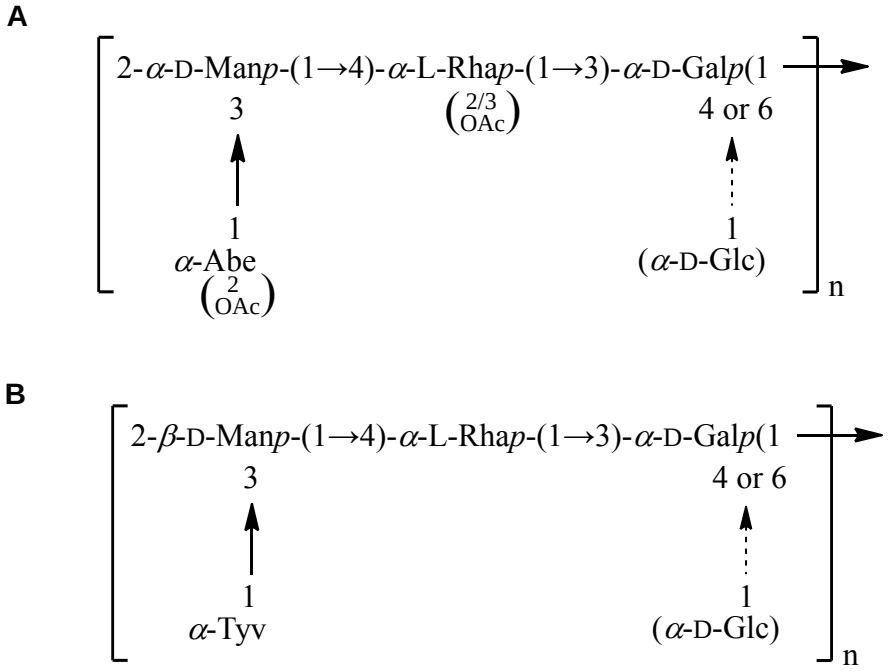

Figure 3.2 OAg chain structure resolved by HPAEC-PAD, GC, GC-MS, and NMR investigation for *S*. Typhimurium (A). OAg chain structure reported in literature for S. Enteritidis (B) and confirmed by HPAEC-PAD and NMR investigations.

Table 3.1 Main differences detected for OAg purified from different *S.* Typhimurium strains.

OAg source	Glc %	Glc linkage	OAc on Rha	% OAc	avMW
1418 (animal isolate)	84	1→4 Gal (8%) 1→6 Gal (92%)	no	73	87.0 and 30.4 kDa
2189 (animal isolate)	51	1→4 Gal (86%) 1→6 Gal (14%)	no	58	80.8 and 31.6 kDa
2192 (animal isolate)	24	1→4 Gal (56%) 1→6 Gal (44%)	no	100	34.5 kDa
D23580 (human isolate)	39	1→4 Gal	yes	200	82.6 and 28.3 kDa
LT2 (laboratory strain)	11	1→4 Gal	no	65	82.6 and 28.3 kDa
NVGH1791 (laboratory strain)	8	nd	no	75	82.6 and 28.3 kDa

Glucosylation level calculated as molar ratio % to Man by HPAEC-PAD analysis. Glc linkage to Gal determined by GLC-MS analysis of PMAA derivatives. O-acetylation level calculated by ^{1}H NMR of de-O-acetylated samples (integral of acetate ion peak compared to Rha-H6 peak). Average molecular weight (avMW) expressed in kDa using dextrans as standards on the TSK gel 3000 PWXL column (flow rate: 0.5 mL/min; eluent: 100 mM NaH_2PO_4 100 mM NaCl 5% CH_3CN pH 7.2). nd: not determined

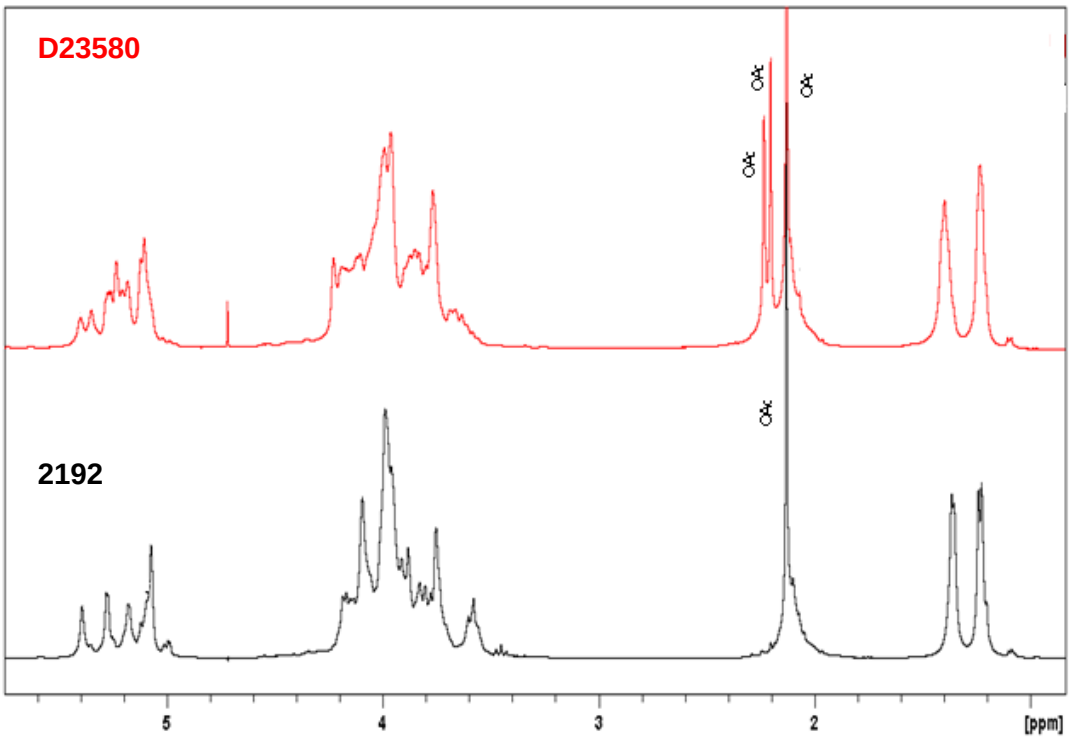

Figure 3.3 ^{1}H NMR comparison of D23580 (red) and 2192 OAg (black), showing the presence of additional OAc groups for D23580 OAg (at 2.23 and 2.19 ppm) with respect to 2192 OAg (at 2.11 ppm).

Composition of the OAg chain found by HPAEC-PAD was confirmed by GLC analysis of the alditol acetates derivatives (Table 3.2). The linkage positions for the constituent sugars of the OAg samples were determined by GLC and GLC–MS of the PMAA derivatives (Table 3.3). As expected (*101*), the OAg chains from all sources contained terminal non-reducing 3,6 dideoxyhexose, identified as Abe by NMR (t-Abe), 4-linked Rha (4-Rha), terminal non-reducing glucose (t-Glc) (its peak overlaps with that of 4-Rha and was not quantified in samples with a low level of glucosylation), 3-linked Gal (3-Gal), 2,3 linked Man (2,3-Man). Glc was found to be linked to Gal in position 4 or 6, in different amounts according to the strain of origin. LT2 and D23580 had Glc linked 1→4 to Gal, as shown by the presence of 3,4-Gal (Table 3.3). For 1418 OAg, Glc was predominantly linked 1→6 to Gal, as shown by the presence of 3,6-Gal rather than 3,4-Gal (Table 3.3), while the opposite was found for 2189 OAg. 2192 sample showed equal amounts of Glc linked 1→4 and 1→6. The amount of t-Glc determined was variable in the different OAg samples (*183*) and the sum of 3,4-Gal and 3,6-Gal for each sample was in agreement with the total amount of Glc determined by GLC analysis of the alditol acetates (Table 3.2). The results are consistent with the structural variations reported for the *S.* Typhimurium OAg (*202*) (*101*), (Figure 3.2.). GLC analysis of the chiral glycosides of all the OAg samples showed that the hexoses were in the D absolute configuration and Rha in the L absolute configuration. As before, the absence of a standard meant that this analysis could not be performed for Abe, and its D configuration was established by NMR glycosylation shifts.

Table 3.2 Sugar composition analysis by HPAEC-PAD for all *S*. Typhimurium O-antigen was confirmed by GLC.

Molar ratio to Man	1418	2189	2192	D23580	LT2
Rha	1.05 (1.34)	0.99 (1.37)	1.01 (1.13)	0.95 (1.18)	0.97 (1.06)
Gal	1.10 (1.02)	1.08 (1.03)	1.07 (1.06)	1.03 (1.01)	0.94 (1.03)
Glc	(0.84) (0.85)	0.51 (0.48)	0.24 (0.23)	0.39 (0.28)	0.11 (0.08)

Sugar composition analysis by GLC is reported in brackets

Table 3.3 Determination of glycosidic linkages in *S*. Typhimurium O-antigen by GLC-MS of PMAA derivatives.

Linkage	RRT[a]	1418	2189	2192	D23580	LT2
t-Abe[b]	0.45	0.16	0.05	0.42	0.07	0.15
4-Rha	0.72	0.87	0.84	1.12	1.00	1.40
t-Glc	0.73	0.63	0.29	nd[c]	nd[c]	nd[c]
3-Gal	0.91	0.22	0.56	0.91	0.76	0.85
2,3-Man	1.00	1.00	1.00	1.00	1.00	1.00
3,4-Gal	1.03	~0.05	0.37	0.10	0.26	~0.04
3,6-Gal	1.14	0.59	0.06	0.08	-	-

[a] Relative retention time; [b] t-Abe = the amount of this derivative is underestimated because it is acid labile. [c] nd = not determined because t-Glc peak overlaps with that of 4-Rha and was not quantified in samples with a low level of glucosylation.

In order to determine the position of the additional O-acetyl groups found for D23580 OAg and to confirm that OAc on Abe was at C-2, the OAg were permethylated following the method of Prehm (*200*), which leaves the O-acetyl groups in their native positions. Analysis of the corresponding PMAA derivatives was performed by GLC and GLC–MS. Figure 3.4 shows the GLC chromatograms of the PMAA derivatives for the D23580 OAg, as an example, obtained without (A) and with (B) retention of the O-acetyl groups. Comparison of the two chromatograms showed that new peaks were present when PMAA derivatives were obtained with retention of O-acetyl position. 2-Abe was a new signal, confirming esterification with O-acetyl on C-2 of the terminal Abe. In addition, the expected 4-Rha, 3,4-Rh and 2,4-Rha were also present, indicating partial esterification of the 4-linked Rha on C-2 or C-3. Separation of the 4-Rha into three derivatives also resulted in the partial separation of the peak assigned to t-Glc from that of 4-Rha. In the chromatogram obtained without retention of O-acetyl groups (Fig. 3.3 A), t-Glc was a shoulder on the side of the 4-Rha peak and therefore its integration was not possible (Table 3.3). This analysis was

performed on all the OAg samples (Table 3.4) and confirmed the results from ^{1}H NMR analysis (Table 3.1): all OAg were variably O-acetylated on C-2 of Abe, whereas only the D23580 sample had additional OAc groups on Rha (Table 3.4). According to the analysis, OAc were on C-2 and C-3 of Rha (Fig. 3.2). This has been confirmed by NMR analysis (*203*).

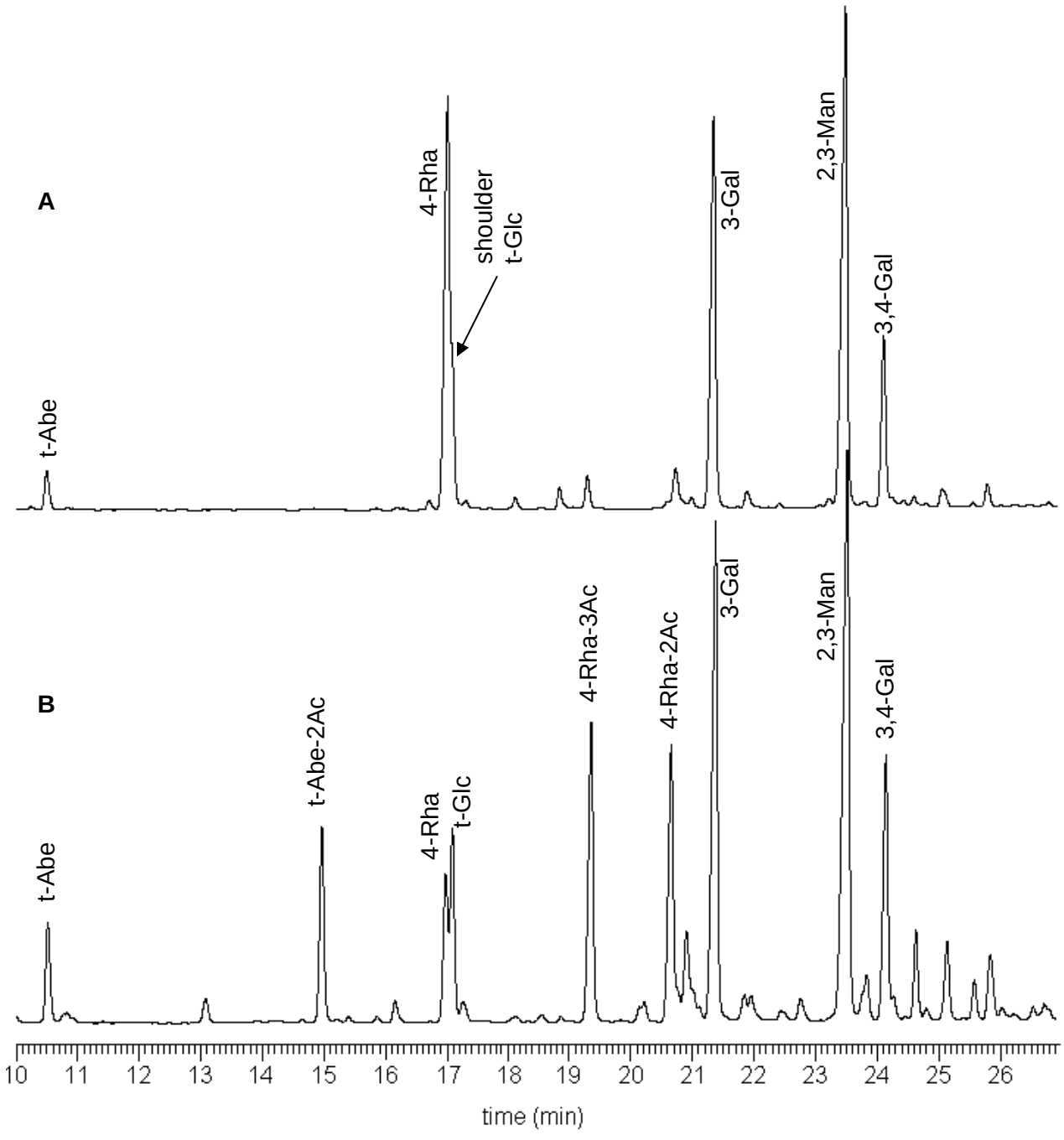

Figure 3.4 GLC chromatograms of the PMAA derivatives from D23580 OAg obtained without (A) and with (B) retention of O-acetyl position. Peak assignments are reported: t-Abe = terminal non-reducing Abe; t-Abe-2Ac = terminal non-reducing Abe acetylated on C-2. The numbers indicate the position of hydroxyl functions engaged in linkages. Similar chromatograms were obtained for the other OAg and the results are summarized in Table 3.4.

Table 3.4 Deduced OAc position and quantification of substitution based on the relative molar ratios of O-antigen PMAA derivatives obtained with and without retention of *O*-acetyl substituents.

Residue	1418	2189	2192	D23580	LT2
t-Abe	48%	63%	20%	37%	37%
t-Abe-2Ac	52%	37%	80%	63%	63%
4-Rha	100%	100%	100%	22%	100%
4-Rha-3Ac	-	-	-	43%	-
4-Rha-2Ac	-	-	-	35%	-

Characterization of OAg purified from different S. Enteritidis strains

OAg from 4 different *S.* Enteritidis strains were purified. Characterization by HPLC-SEC showed that they were similar in terms of MW distribution: all showed a main peak at relatevely lower MW (in the range 29.6-32.6 kDa, as determined using dextrans as standards) with a shoulder, except SA 618, at higher MW (in the range 77-82.6 kDa). For SA 618, average MW was also calculated based on the molar ratio of Rha to GlcNAc, equal to 27, and according to the sugar composition analysis by HPAEC-PAD and to the O-acetylation level by ^{1}H NMR, and corresponded to 18.9 kDa. Analysis by HPAEC-PAD for sugar composition and by ^{1}H NMR for O-acetylation level revealed low heterogeneity: all the OAg were in fact characterized by low glucosylation and O-acetylation level (Table 3.5; Figure1.5). Due to the low variability found for *S.* Enteritidis OAg, no further structural investigations have been perfomed.

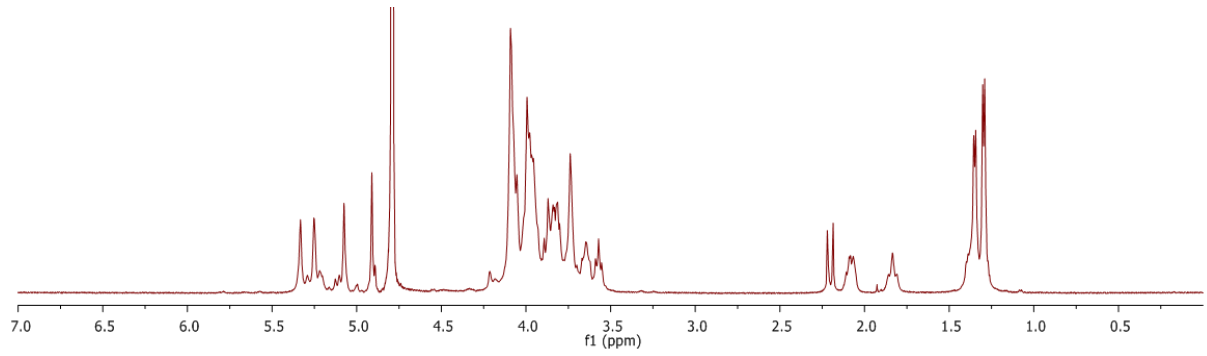

Figure 3.5 ^{1}H NMR spectrum of D24359 OAg, as an example of the *S.* Enteritidis strains analyzed.

Table 3.5 Fine specificities for *S*. Enteritidis OAg.

OAg source	avMW	Glc %	% OAc
D24359 (human isolate)	32.6 (and 82.5) kDa	9	35
SA 502 (animal isolate)	30.5 (and 77) kDa	12	22
IV3453219 (animal isolate)	(30.5 (and 82.6) kDa	11	32
SA 618 (animal isolate)	29.6 kDa	15	10

Glucosylation level calculated as molar ratio % to Man by HPAEC-PAD analysis. O-acetylation level calculated by ^{1}H NMR of de-O-acetylated samples (integral of acetate ion peak compared to Rha-H6 peak). . Average molecular weight (avMW) expressed in kDa using dextrans as standards on the TSK gel 3000 PWXL column (flow rate: 0.5 mL/min; eluent: 100 mM NaH_2PO_4 100 mM NaCl 5% CH_3CN pH 7.2).

Synthesis and characterization of OAg-ADH-SIDEA-CRM_{197} conjugates

Acid hydrolysis, performed for extracting OAg from bacteria, cleaves the labile linkage between the toxic lipid A and the KDO sugar at the proximal end of the core region releasing OAg. The KDO sugar has been used for introducing ADH and then SIDEA linkers, and for binding OAg to the carrier protein, CRM_{197}. The choice of a selective conjugation chemistry was driven by the need of not impacting the OAg chain, since the aim of the study was to evaluate the influence of fine specificities on immunogenicity (Figure 3.6) (*180*).

OAg derivatization with ADH and then SIDEA was characterized by good reproducibility both in terms of sugar recovery and percentage of activation for all the samples. In all cases, sugar recovery was >75%. For the ADH-derivatization step, activations >90% were obtained with free ADH <5% in moles. The reaction with SIDEA resulted in about 70% of NH_2 groups modified in active ester groups and free SIDEA determined to be <10% in moles.

The main characteristics of the conjugates synthesized and then tested in mice are reported in Table 3.6, where also the main differences of the corresponding unconjugated OAg are highlighted. For all the conjugates, kd values were higher than those of free OAg and free protein (kd of CRM_{197} of 0.72), confirming the formation of the conjugate at higher MW. Analysis by HPLC-SEC showed that free CRM_{197} was not detectable. All the conjugates were characterized by a similar weight ratio of saccharide to protein and MW distribution of the OAg (Table 3.6). A saccharide to protein molar ratio of 4.8 and 3.7 was estimated for 2192 and SA 618 OAg respectively, based on the MW of 20.5 and 18.9 kDa calculated for these more homogeneous OAg samples. Analysis of the conjugates by ^{1}H NMR confirmed that O-acetylation levels remained unchanged after conjugation to the protein (*180*).

Table 3.6 Characterization of conjugates tested in mice.

OAg	Strain	OAg/CRM_{197} (w/w)	Kd conjugate	Kd free OAg	O-acetylation % (OAg)	Glucosylation % (OAg)
O:4,5	**D23580**	2.1	0.44	0.58 and 0.68	200 (Abe/Rha)	39
	NVGH 1791	2.1	0.43	0.58 and 0.68	75 (Abe)	7
	LT2	1.9	0.47	0.58 and 0.68	64 (Abe)	11
	2192	1.7	0.49	0.67	100 (Abe)	24
	2189	2.0	0.46	0.57 and 0.68	58 (Abe)	51
	1418	1.7	0.48	0.56 and 0.67	73 (Abe)	84
O:9	**SA 502**	1.7	0.50	0.62 and 0.53	22.4	12
	D24359	1.2	0.52	0.62	35.4	9
	SA 618	1.2	0.55	0.62	10.0	15
	IV3453219	1.8	0.52	0.62 and 0.52	31.6	11

OAg/CRM_{197} ratios were calculated based on OAg concentration by phenol sulphuric assay and protein concentration by micro BCA. Kd values were calculated by HPLC-SEC analysis on TSK gel 6000-5000 PW columns (flow rate: 0.5 mL/min; eluent: 100 mM NaH_2PO_4 100 mM NaCl 5% CH_3CN pH 7.2) using Λ-DNA and NaN_3 for determining void and total volume respectively. O-acetylation and glucosylation level of unconjugated OAg were calculated by ^1H NMR and HPAEC-PAD analysis respectively.

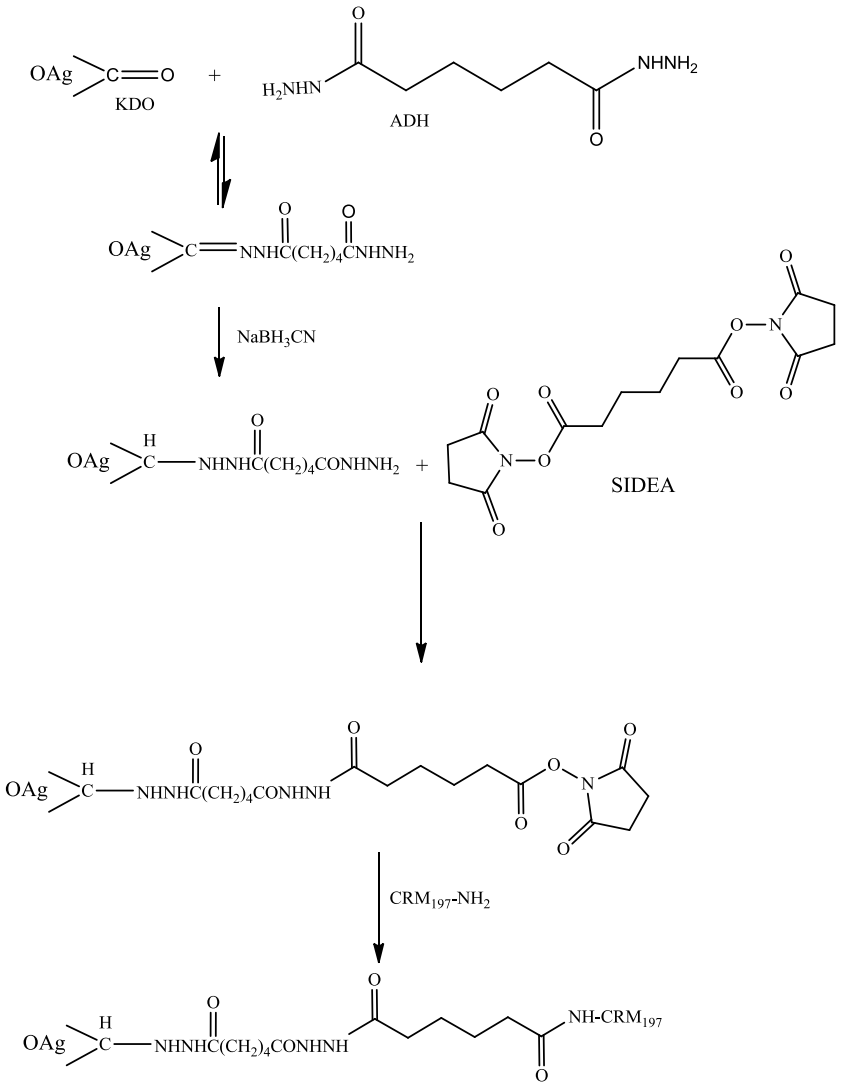

Figure 3.6 OAg-ADH-SIDEA-CRM_{197} conjugation scheme. OAg is derivatized with adipic acid dihydrazide (ADH), then with adipic acid bis(N-hydroxysuccinimmide (SIDEA) and conjugated to CRM_{197}.

Immunogenicity of OAg-ADH-SIDEA-CRM_{197} conjugates in mice

All the conjugates (Table 3.6) were tested in mice, with the objective to determine if OAg structural differences can impact on the immunogenicity of the corresponding glycoconjugate vaccines.
When ELISA was performed using D23580 OAg as coating agent (Figure 3.7), all conjugates (except NVGH1791 and 2192 at 1 µg/dose) elicited anti-OAg IgG after the second immunization significantly higher than CRM_{197} alone used as negative control, and the immunoresponse was boosted after the third immunization. Higher antibody levels were detected at 8 µg/dose for all the conjugates, but for 1418 and 2189, which exhibited similarly high anti-OAg levels at both 1 µg and 8 µg/dose (Figure 3.7). No statistically significant differences were found in anti-OAg IgG levels among all groups at 8 µg/dose. At 1 µg/dose, the only significant difference was found for 2189-conjugate which elicited higher anti-IgG units than LT2 (p=0.04) and NVGH1791 (p=0.04) conjugates.

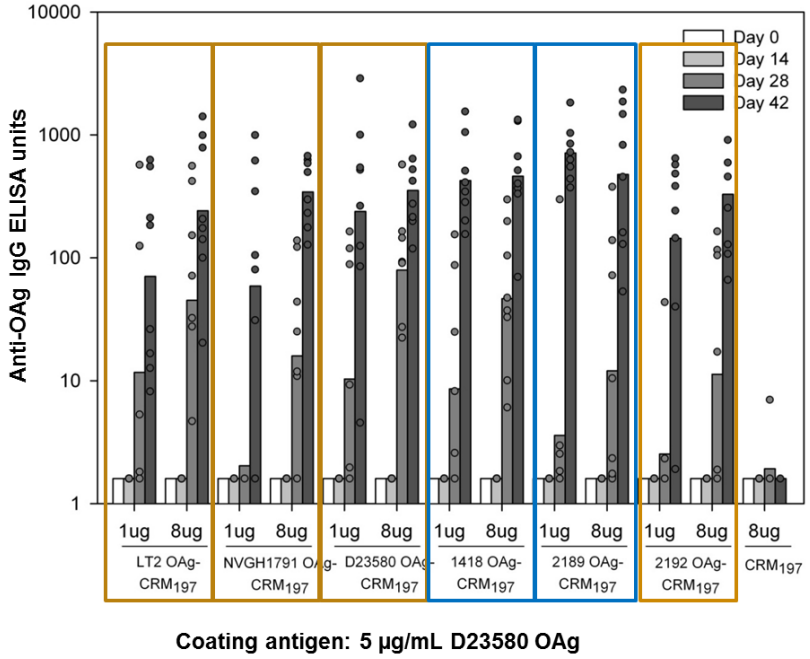

Figure 3.7 Anti-OAg IgG ELISA units using D23580 OAg as coating agent. Individual animals are represented by the scatter plots; horizontal bars represent Geometric Mean Units.

Sera collected at day 42 from groups immunized with 8 µg OAg per dose were tested in ELISA using OAg from all the other strains (LT2, NVGH1791, 1418, 2189 and 2192) as coating agents (Figure 3.8). 2189 and 1418-conjugates elicited significantly higher anti-OAg IgG than D23580 when coating agents were LT2-OAg ($p = 0.06$), NVGH1791-OAg ($p = 0.03$) and 2189-OAg ($p = 0.06$). Similar anti-OAg levels were detected for each immunization group when tested against all other coating agents, except for D23580-conjugate which showed a marked increase when tested against the homologous OAg (Figure 3.8).

When ELISA was performed to detect anti-CRM_{197} IgG levels, as expected higher values were obtained with conjugates at 8 µg/dose, except with 1418 and 2189-conjugates, for which anti-CRM_{197} levels were similar at 1 and 8 µg/dose (Figure 3.9), as found for anti-OAg antibodies. Unconjugated CRM_{197} elicited significantly lower antibodies than LT2, D23580, 1418, 2189-conjugates at 8 µg/dose.

Sera collected at day 42 were also tested for serum bactericidal activity (SBA) against the Malawian human isolate D23580 strain (Figure 3.10). All the conjugates showed strong bactericidal activity, with as little as 0.1 (and less than this) ELISA anti-OAg antibody units. Increased SBA was found when sera from mice immunized with the homologous conjugate to D23580 strain was used, paralleling the strain-specificity found by ELISA (Figure 3.10). When sera of conjugates obtained with OAg from animal isolates were tested against a broader panel of endemic strains, 2189 and 1418 conjugates showed stronger activity that 2192 (data nit shown). This could be related to their higher glucosylation level or to the presence of a population at HMW.

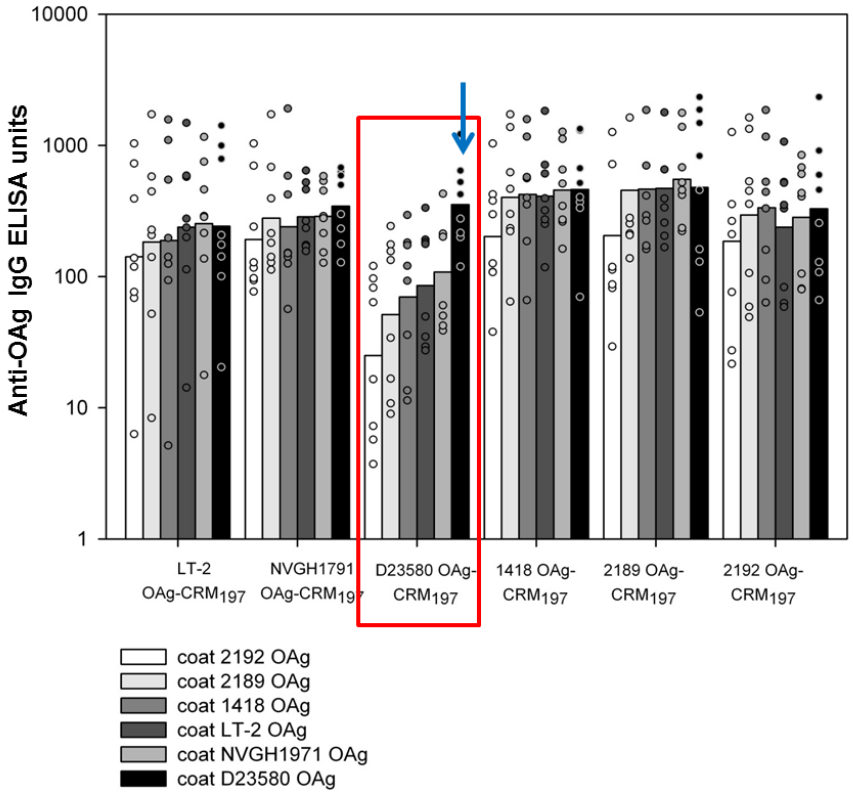

Figure 3.8 Anti-OAg IgG ELISA units against all the tested *S*. Thyphimurium OAg coating agents (day 42 sera, 8 µg/dose). D23580 conjugate elicited mostly strain-specific anti-OAg antibodies. Individual animals are represented by the scatter plots; horizontal bars represent Geometric Mean Units.

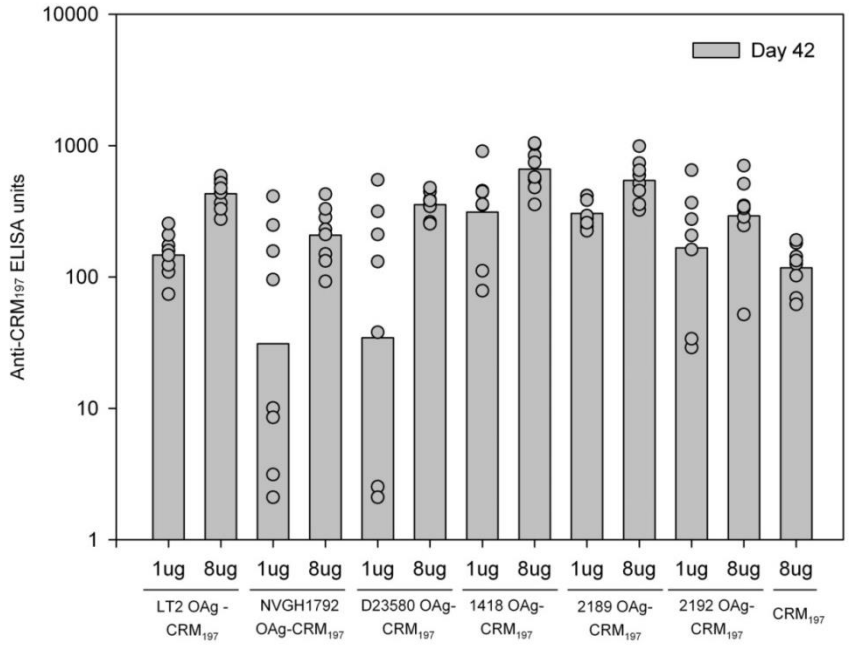

Figure 3.9 Anti-CRM_{197} IgG ELISA units using CRM_{197} as coating agent coating agents (day 42 sera). Individual animals are represented by the scatter plots; horizontal bars represent Geometric Mean Units.

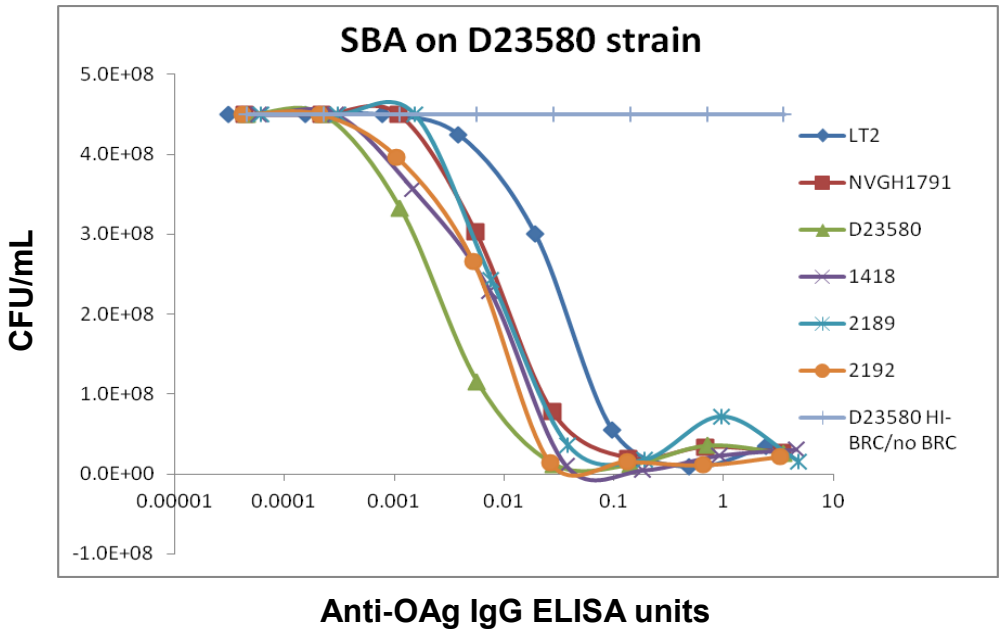

Figure 3.10 SBA performed with pooled mouse sera from different immunization groups (8 ug/dose, day 42) against D23580 strain. Data show bacterial growth inhibition by the immunized mice sera (heat-inactivated plus 50% BRS), normalized per anti-OAg antibody IgG ELISA units. SBA performed 3 times on 3 different days; graph represents the average of the triplicates.

S. Enteritidis

All *S.* Enteritidis conjugates were immunogenic in mice (Figure 3.11) and able to induce bactericidal activity. There was a large intergroup variation, with 1 non responder mouse in each group. This variability was reflected by anti CRM_{197} antibody levels, which resulted lower than those obtained with *S.* Typhimurium conjugates.
As expected, there was a lack of strain-specific responses (Figure 3.11), and this is not surprising considering the conjugates did not differ considerably in terms of OAg structural specificities (Table 3.5) in, although the anti-OAg IgG response induced by IV3453219 conjugate was lower at 8 ug/dose with respect to the other conjugates.

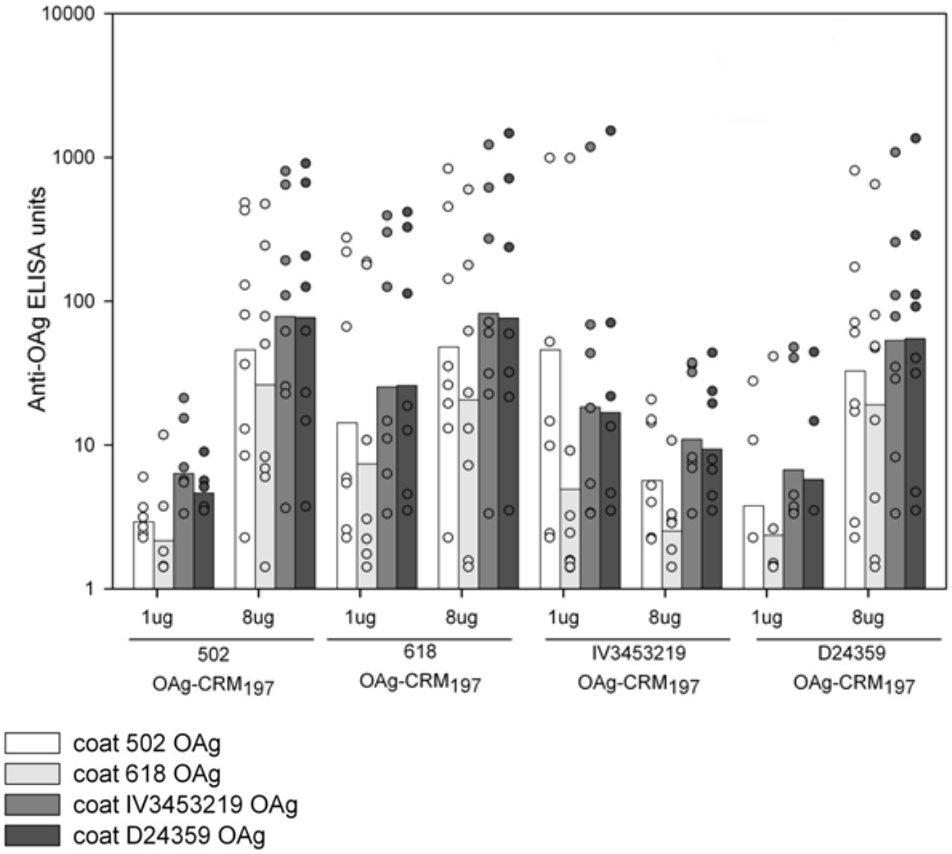

Figure 3.11 Anti-OAg IgG ELISA units against all the tested *S*. Enteritids OAg coating agents (day 42 sera). Individual animals are represented by the scatter points; horizontal bars represent Geometric Mean Units.

3.5 Discussion

As part of a NVGH project to develop a comprehensive conjugate vaccine against iNTS disease, OAg from different *S.* Typhimuirum and *S.* Enteritdis strains, major cause of iNTS infection in Africa, were fully characterized to investigate possible OAg heterogeneity related to the source and possible implication for the immunogenicity of corresponding conjugate vaccines.

S. Typhimurium OAg were extracted from two lab strains (LT2 and NVGH1791), three animal isolates (1418, 2192 and 2189) and one human isolate (D23580). As reported in Table 3.1, all purified OAg were similar in terms of MW distribution, with two main populations at average MW 80–87 and 28–31 kDa respectively. Only 2192 showed one main peak at average 34.5 kDa (Figure 3.1). Sugar analysis by HPAEC-PAD and GLC–MS confirmed the composition of the tetrasaccharide repeating unit as Man, Gal, Rha and Abe. The analysis also showed strain specific variable amounts of glucosylation, ranging from 8% to 84%. The structure of the repeating unit was confirmed by linkage analysis which showed that the terminal Glc present was linked 1→4 and/or 1→6 to Gal, depending on the strain. All the OAg were O-acetylated on C-2 Abe although to different extents depending on the strain, while D23580 was found to have additional OAc groups on C-2 and C-3 of Rha. The position of the OAc groups was established by GLC–MS (Figure 3.4) and NMR analysis (Figure 3.3). *S.* Enteritidis OAg were extracted from three animal isolates

(SA 502, IV3453219 and SA 618) and one human isolate (D24359). Contrary to what has been previously described (*204*) (*205*), *S.* Enteritidis isolates seemed to be more homogeneous than *S.* Typhimurium ones. In fact corresponding OAg were not only similar for average chain length (one prevalent population at average 29.6-32.6 kDa) but also for sugar composition, being all characterized by low glucosylation and O-acetylation levels and the same O-acetylation position. (Table 3.5)
The panel of analytical methods in place for OAg characterization performed on these samples will facilitate the screening of OAg structure and pattern of O-acetylation for LPS from new strains.
All the purified OAg were conjugated to CRM_{197} through the terminal KDO of the core region (Figure 3.6), in order to leave the OAg structure un-modified and look specifically at the impact of OAg specificities on the immunogenicity of the corresponding conjugates. It is known that saccharide structure is one of the parameter affecting the immunogenicity of conjugate vaccines (*122*). Few study have reported the impact of OAg O-acetylation on immunogenicity (*100*) (*98*) (*185*) and no studies have investigated on the impact of glucosylation level or position. The synthesized conjugates were characterized by a similar weight ratio of saccharide to protein, and the same carrier protein, conjugation chemistry, and MW distribution of the OAg (Table 3.6), so that differences in terms of immunogenicity can be attributed only to the different OAg structural specificities.
When tested in mice, all the conjugates induced anti-OAg IgG antibodies with bactericidal activity against different NTS strains. For *S.* Enteritidis no differences were found among the conjugates, in agreement with the homogeneous structure of these OAg. For *S*. Typhimurium conjugates, differently to what has been reported in the literature (*185*), O-acetylation on C-2 and C-3 Rha seemed to affect immunogenicity, generating strain-specific antibodies, which cross-reacted with other OAg strains to a lesser degree (Figure 3.8). Paralleling the strain-specificity found in ELISA, increased SBA was found when the homologous conjugate to D23580 strain was used (Figure 3.10).
Glucosylation of the OAg seems to be an important factor in inducing protection, with 1418 and 2189 conjugates, characterized by the highest glucosylation level showing stronger SBA toward a broader panel of endemic strains when compared to 2912 OAg similarly O-acetylated only on C-2 of Abe.
This work indicates that the selection of the strain as OAg source for glycoconjugate vaccine production can be important, as different strains may result in candidate vaccines with different immunogenicities and antibodies with potentially different cross-reactivities. A screening of a larger number of strains would probably highlight better the importance of the OAg structure in affecting the immunogenicity of NTS glycoconjugate vaccines.

4. Impact of conjugation chemistry on the design of *S*. Typhimurium conjugate vaccines

4.1 Abstract

Salmonella Typhimurium is major cause of invasive nontyphoidal *Salmonella* in Africa. Conjugation of *S.* Typhimurium OAg to an appropriate carrier protein constitutes a possible strategy for the development of a vaccine against this disease, for which no vaccines are currently available. Conjugation chemistry is one of the parameters that can affect the immunogenicity of glycoconjugate vaccines. Herein different conjugates were synthesized, using CRM_{197} as carrier protein, to look at the impact of this variable on the immunogenicity of *S.* Typhimurium conjugate vaccines in mice. Random derivatization along the OAg chain was compared with site-directed activation of the terminal KDO sugar. In particular, two different random approaches were used, based on the oxidation of the PS with sodium periodate ($NaIO_4$) and with 2.2.6.6-tetramethylpiperidin-1-oxyl (TEMPO), which differentially impacted on the structure and conformation of the OAg chain. With regard to the selective conjugation methods, linkers of different length were compared.
When tested in mice, all conjugates induced high levels of anti-OAg IgG antibodies with serum bactericidal activity. Similar anti-OAg antibodies titers were elicited independent of the chemistry used and a higher degree of saccharide derivatization did not impact negatively on the anti-OAg IgG response. Serum bactericidal activity of the antibodies induced by selective conjugates was similar independent of the length of the spacer used. Random conjugates elicited stronger bactericidal antibodies than selective ones, and an inverse correlation was found between degree of OAg modification and antibodies functional activity.

4.2 Introduction

In many parts of Africa, NTS is the leading cause of bacteremia. Incidence of disease caused by different serovars varies depending upon the country but *S.* Typhimurium is overall the main cause of invasive disease (*36*) ((*64*). Antibodies directed against the OAg mediate killing of NTS (*99*) (*206*) (*207*) and confer protection against infections, and OAg glycoconjugate vaccines have been proposed as a vaccine strategy against *Salmonella* (*98*) (*97*). (*208*) (*84*).
Synthesis of glycoconjugate vaccines requires covalent linkage of saccharide and protein components and the conjugation method used is one parameter that can affect the immunogenicity of the resulting vaccine (*122*).
Conjugation methods proposed so far, even if differing for the functional groups and linkers involved, follow two main approaches: one based on random linkage of the protein to the saccharide chain, and the other one based on coupling of the protein to one single point of the saccharide (*122*) (*209*) (*210*) (*168*). Conjugation strategy is dependent on the functional groups present on both the sugar and the protein, and on their size. The choice of conjugation strategy and linker used can affect efficiency of conjugation, saccharide to protein ratio and glycoconjugate size, with consequent impact on immunogenicity (*211*) (*212*) (*122*). Investigating the impact of different chemistries on the immunogenicity can also allow a rational structure-activity based design of next-generation conjugates.

Covalent linkage of PS is generally achieved by targeting the amino groups of lysines, the carboxylic groups of aspartic/glutamic acids or the sulfhydryl of cysteines on the protein.
Random approaches have been preferentially used for the conjugation of long carbohydrate antigens to proteins resulting in complex cross-linked and heterogeneous structures (Figure 4.1). Carboxylic or hydroxyl groups along the saccharide chain can be randomly activated by carbodiimide chemistry or cyanyilation respectively (*213*) (*214*). Alternatively, aldehydes generated on the PS by random oxidation can be used for reductive amination with the protein directly or with a linker (*215*).
Selective chemistries have been used for conjugation of shorter oligosaccharides, often obtained by partial hydrolysis of the native PS and fractionating a target MW population, and result in simplified and better defined structures of the final conjugates (Figure 4.1). Generally reductive amination of the terminal reducing sugar is performed, directly with the protein or more often using an appropriate spacer (*216*) (*98*).

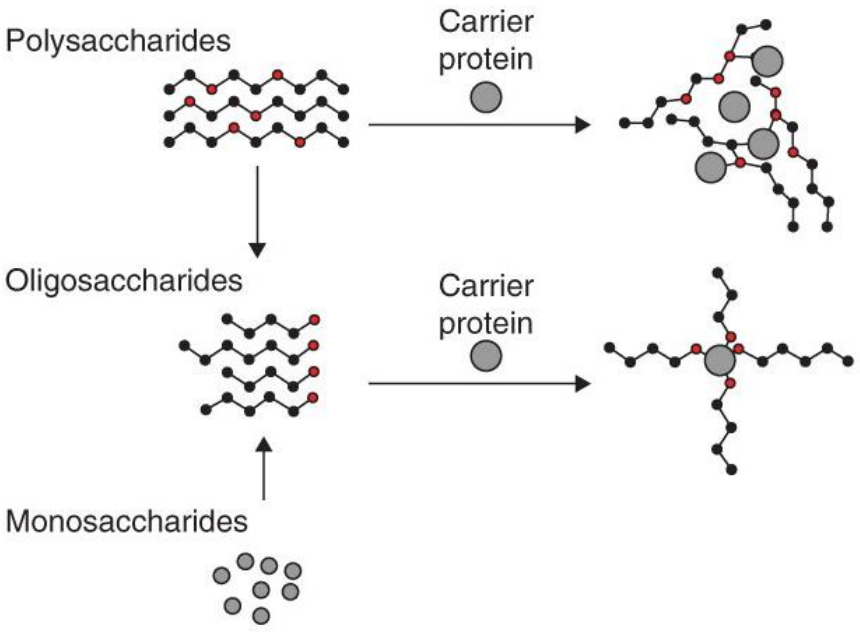

Figure 4.1 Schematic representation of different saccharide-protein chemical couplings (Figure reproduced from (*122*)).

Based on *Salmonella* OAg structure (Figure 4.1), few methods have been proposed for the synthesis of corresponding conjugate vaccines and few studies have investigated the impact of this parameter on immunogenicity (*98*) (*100*) (*180*) (*84*).
Random approaches are based on activation of the OH groups along the sugar chain by cyanilation using reagents such as cyanogen bromide (CNBr) or 1-Cyano-4-dimethylaminopyridinium tetrafluoroborate (CDAP), followed by direct linkage to the NH_2 groups on the protein or by linkage to the carrier after introduction of linkers such as ADH and cystamine (*98*) (*84*) (*100*). Selective conjugates have been obtained by using the carboxylic or the ketone group of the terminal KDO unit. Linkers like 2-(4-aminophenyl)-ethylamine, ADH, ADH/SIDEA, cystamine, diaminooxy cysteamine/N-(γ-maleimidobutyloxy)-sulfosuccinimide ester have been introduced by carbodiimide

chemistry or reductive amination on the COOH or C=O group respectively (*217*) (*98*) (*180*) (*84*).
Here we have compared different conjugation strategies for the linkage of *S.* Typhimurium OAg to CRM_{197} (*178*) as carrier protein and looked at the impact of the conjugation chemistries used on the immunogenicity of the resulting conjugates in mice. Two different oxidation methods and different degrees of oxidation have been compared, creating multiple points of attachment to the protein along the OAg chain, differently modifying the sugar structure (Figure 4.3a). Random chemistries have been compared with selective approaches, where only the terminal KDO unit of the sugar chain (Figure 4.3b) is involved in the linkage to the protein, leaving the OAg chain unmodified.

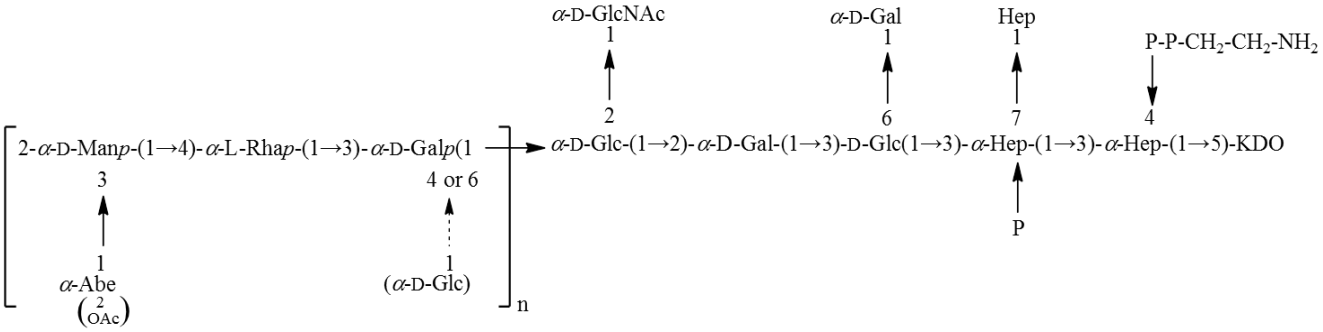

Figure 4.2 Structure of the *S.* Typhimurium OAg chain linked to the core region. Core region. Structure taken from (*218*).

a)

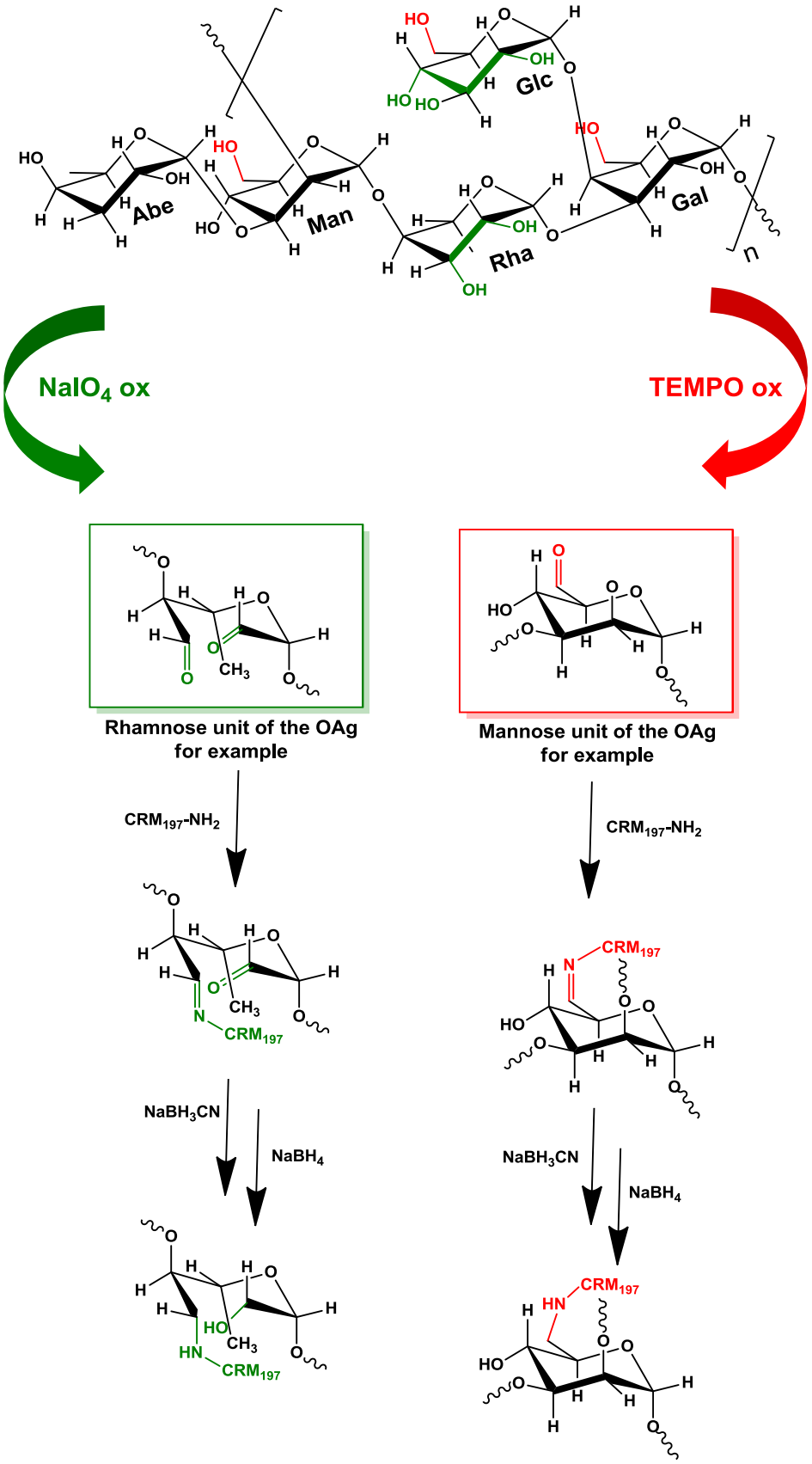
Abe
Man
Glc
Rha
Gal
n
NaIO4 ox
TEMPO ox
Rhamnose unit of the OAg for example
Mannose unit of the OAg for example
CRM197-NH2
CRM197-NH2
NaBH3CN
NaBH4
NaBH3CN
NaBH4
CRM197
CRM197

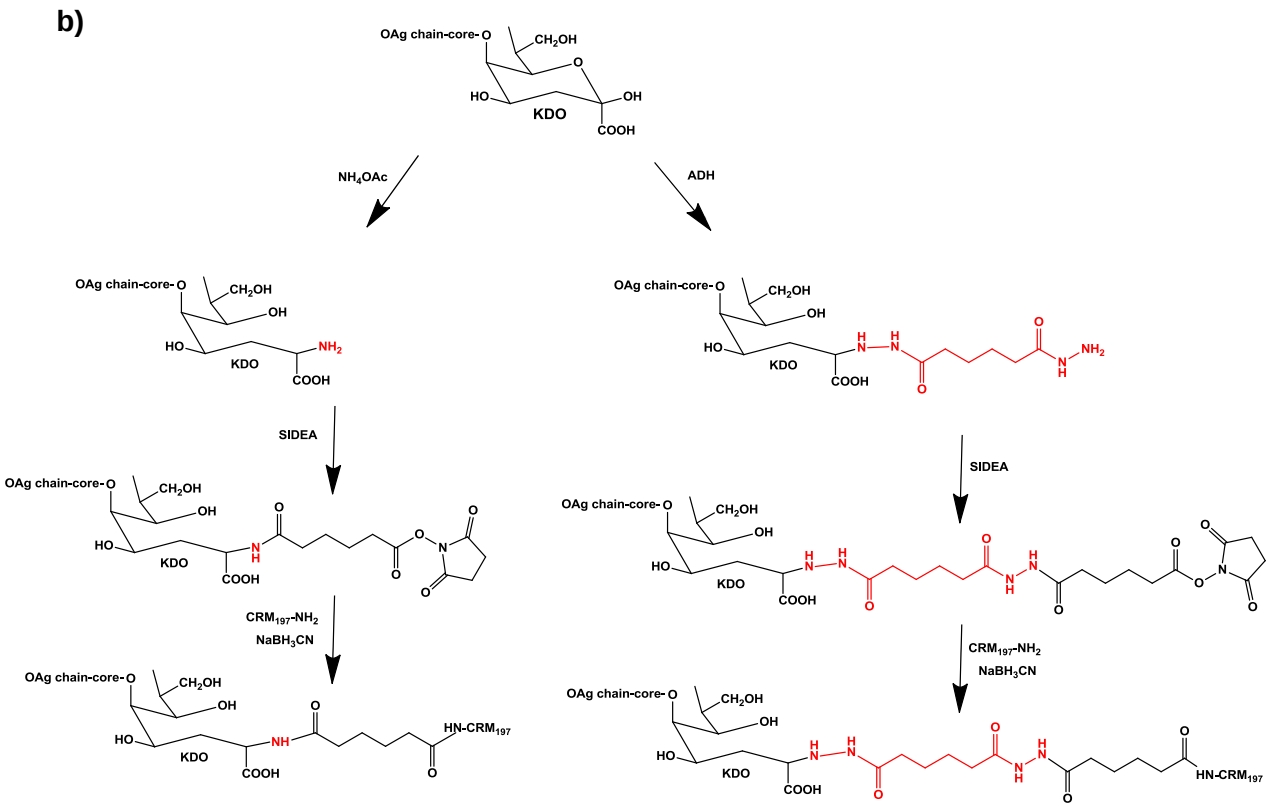

Figure 4.3 a) Structure of *S*. Typhimurium OAg chain and random derivatization by $NaIO_4$ or TEMPO oxidation. The $NaIO_4$-based oxidation affects vicinal diols to generate two aldehydes groups, opening the sugar ring. In the case of *S.* Typhimurium OAg, this reactivity can involve Rha and Glc residues. TEMPO oxidation targets primary alcohol groups, which in *S.* Typhimurium OAg are present in the sugar moieties of Man, Gal and Glc, one per monosaccharide. In both cases, the resulting aldehyde groups can then react with the lysine residues of the carrier protein to form a covalent C=N linkage, that is subsequently reduced to a stable C-N bond with $NaBH_3CN$. A further step of reduction with $NaBH_4$ was introduced to quench eventual unreacted C=O groups.
b) OAg selective derivatization of the reducing end unit KDO. Reductive amination of KDO with NH_4OAc or ADH, followed by SIDEA addition and conjugation to CRM_{197}. The two investigated chemistries differ for the spacer length.

4.3 Materials and methods

Reagents

The following chemicals were used in this study: triethylamine (TEA), adipic acid dihydrazide (ADH), sodium cyanoborohydride ($NaBH_3CN$), sodium borohydride ($NaBH_4$), sodium acetate (AcONa), dimethyl sulfoxide (DMSO), sodium phosphate monobasic (NaH_2PO_4), sodium chloride (NaCl), ammonium acetate (NH_4OAc), sodium bicarbonate ($NaHCO_3$), 2.2.6.6-tetramethylpiperidin-1-oxyl (TEMPO), trichloroisocyanuric acid (TCC), sodium periodate ($NaIO_4$), N,N-dimethylformamide (DMF), hydrochloric acid 37% (HCl) [Sigma]; acetonitrile (CH_3CN) [LC-MS Chromasolv]; adipic acid bis(N-hydroxysuccinimmide) (SIDEA) [PFANSTIEHL Laboratories]; absolute ethanol [Carlo Erba]. CRM_{197} was obtained from Novartis Vaccines and Diagnostics (NVD).

OAg purification and characterization

S. Typhimurium OAg were purified as previously described (*86*), after fermentation of the animal isolate 2192, obtained from the University of Calgary, or of the laboratory strain LT2, obtained from the Novartis Master Culture Collection. OAg preparations were characterized by protein content <1% (by micro BCA), nucleic acid content < 0.5% (by A_{260}), endotoxin level < 0.1 UI/µg (by LAL). OAg structures were fully elucidated, as reported in Chapter 1 (*203*). In particular, 2192 OAg, used for the synthesis of the conjugates, was 100% O-acetylated on C-2 Abe and had an average molecular weight (avMW) distribution of 20.5 KDa, determined from the molar ratio of Rha (OAg chain) to GlcNAc (core sugar) and sugar composition analysis by HPAEC-PAD and considering the level of O-acetylation by NMR analysis. OAg chains showed the presence of NH_2 groups (NH_2 to GlcNAc molar ratio % of 37.6), as detected by TNBS colorimetric method (*219, 220*), probably as pyrophosphoethanolamine residues in the core region (Figure 4.2).

Synthesis of OAg-CRM_{197} glycoconjugates

1) *OAg-ox$NaIO_4$-CRM_{197}: random activation of the OAg chain with $NaIO_4$ and conjugation to CRM_{197}*

OAg (10 mg/mL in AcONa 100 mM pH 5) was stirred for 2h in the dark with 3.75 mM $NaIO_4$. The mixture was desalted against water using a HiPrep™ 26/10 desalting column 53 mL, prepacked with Sephadex™ G-25 Superfine [GE Healthcare], and the pool eluted at the void volume of the column dried. The activated OAg was designated as OAg-ox$NaIO_4$. For conjugation to CRM_{197}, OAg-ox$NaIO_4$ was added to CRM_{197} in NaH_2PO_4 100 mM pH 7.2 to have a final concentration of 10 and 5 mg/mL respectively (OAg-ox$NaIO_4$:CRM_{197} = 2:1 w/w). $NaBH_3CN$ ($NaBH_3CN$:CRM_{197} = 1:1 w/w) was added immediately after, and the reaction mixture stirred ON at 37 °C. After this time, $NaBH_4$ (OAg-ox$NaIO_4$:$NaBH_4$ = 1:1 w/w) was added and the mixture was stirred at 37°C for 2h. The conjugate was designated as OAg-ox$NaIO_4$-CRM_{197}.

2) *OAg-oxTEMPO-CRM_{197}: random activation of the OAg chain with TEMPO and conjugation to CRM_{197}*

OAg (3 mg/mL, corresponding to [CH_2OH] of 7.69 mM) and $NaHCO_3$ (19.47 mg/mL, molar ratio $NaHCO_3$/CH_2OH = 30), were added to a stirred solution of TEMPO (0.06 mg/mL, molar ratio TEMPO/CH_2OH = 0.05) in DMF. The reaction was cooled to 0 °C and TCC (2.88 mg/mL, molar ratio TCC/CH_2OH = 1.6) was added. After 2 h of continuous stirring at 0 °C, the activated sugar was recovered from the reaction mixture by precipitation with EtOH (85% v/v in the final mixture). The pellet was washed twice with 100% EtOH (1.5 volumes with respect to the reaction mixture volume) and lyophilized. The activated OAg was designated as OAg-oxTEMPO2h. The same procedure, except for changing the reaction time from 2h to 12h, was used for the synthesis of OAg-oxTEMPO12h. For the reductive amination of OAg-oxTEMPO2h and OAg-oxTEMPO12h with CRM_{197}, the same conditions used for the conjugation of OAg-ox$NaIO_4$ were applied. The two corresponding conjugates were designated as OAg-oxTEMPO2h-CRM_{197} and OAg-oxTEMPO12h-CRM_{197} respectively.

3) *OAg-ADH-SIDEA-CRM_{197}: selective activation of the terminus KDO with ADH, followed by reaction with SIDEA and conjugation to CRM_{197}*

The synthesis of this conjugate was performed as described in the Chapter 1.

4) *OAg-NH_2-SIDEA-CRM_{197}: selective activation of the terminus KDO with NH_4OAc, followed by reaction with SIDEA and conjugation to CRM_{197}*

OAg was solubilized in 500 mM NH_4OAc pH 7.0 at a concentration of 40 mg/mL. $NaBH_3CN$ was added immediately ($NaBH_3CN$:OAg = 2:5 w/w). The solution was mixed at 30°C for 5 days. Reaction mixture was desalted against water on a G-25 column and OAg-NH_2 was dried. The introduction of the second linker SIDEA and conjugation to CRM_{197} were performed as described for OAg-ADH-SIDEA-CRM_{197} and the resulting conjugate was designed as OAg-NH_2-SIDEA-CRM_{197}.

Conjugates purification

All the conjugates were purified by hydrophobic interaction chromatography on a Phenyl HP column [GE Healthcare], loading 500 µg of protein for mL of resin in 50 mM NaH_2PO_4 3M NaCl pH 7.2. The purified conjugate was eluted in water and the collected fractions were dialysed against 10 mM NaH_2PO_4 pH 7.2.

Conjugates characterization

Total saccharide was quantified by phenol sulfuric assay (*195*), protein content by micro BCA (using BSA as standard and following manufacturer's instructions [Thermo Scientifics]) and the ratio of saccharide to protein calculated. OAg-CRM_{197} conjugates profiles were compared with free CRM_{197} by HPLC-SEC (see Chapter 1 for method description) and SDS-PAGE. Free protein was estimated by HPLC-SEC. A method for free saccharide determination is under development.

Derivatized OAg intermediates were all characterized by phenol sulfuric assay for sugar content and by HPLC-SEC for verifying aggregation or degradation after modification (see Chapter 1 for method description). The intermediates for the synthesis of OAg-ADH-SIDEA-CRM_{197} and OAg-NH-SIDEA-CRM_{197} were characterized as previously described (Chapter 1). 6-aminohexanoic acid was used as standard for NH_2 group quantification on OAg-NH_2 by TNBS assay.

Aldehyde groups introduced by oxidation with $NaIO_4$ or TEMPO were quantified by ^1H NMR, HPAEC-PAD or micro BCA using Glc as standard (*221*).

Sodium dodecyl sulfate-polyacrylamide gel electrophoresis (SDS-PAGE)

Conjugation mixtures were analyzed by SDS-PAGE for verifying conjugate formation before performing purification. 7% Tris-acetate gels (NuPAGE, Invitrogen) were used. The samples (5-20 µL with a protein content of 5-10 µg) were mixed with 0.5 M dithiothreitol (1/5 v/v) and NuPAGE LDS sample buffer (1/5 v/v). The mixtures were heated at 100°C for 1 min. The gel, containing loaded samples, was electrophoresed at 45 mA in NuPAGE Tris-Acetate SDS running buffer (20x, Invitrogen) and stained with Simply Blue Safe Stain (Invitrogen).

O-Ag chain sugar composition analysis by High-Performance Anion-Exchange Chromatography with Pulsed Amperometric Detection (HPAEC-PAD) (*203*)

OAg-chain sugar composition was estimated by HPAEC-PAD after acid hydrolysis of the OAg (free and conjugated) samples to release the monomers that constitute the

saccharide chain. Rha, Gal, Glc and Man present in the OAg chain were quantified by this method, together with GlcNAc present as a unique sugar in the core region. Analysis of OAg samples after oxidation with $NaIO_4$ allowed determining the % of Rha and Glc units oxidized, comparing the molar ratio of these monomers to Man before and after the oxidation.

^{1}H NMR spectroscopy (*203*)

Nuclear Magnetic Resonance (NMR) analysis was used as a confirmation of the identity of the OAg samples (typical signals of the OAg chain can be detected, confirming the presence of the characteristic sugars) and in particular for calculating the molar ratio of Rha to Abe by comparing the integrals of the two peaks corresponding to Rha-H6 and Abe-H6, at 1.36 and 1.23 ppm respectively. O-acetylation level of OAg samples before and after conjugation can be estimated by NMR too. NMR was also used to quantify the % of Rha units oxidized with $NaIO_4$ as the peak of Rha-H6 of modified Rha units shifts at lower ppm and overlapps the peak of Abe-H6 at 1.2 ppm. Comparing the integrals of the peaks at 1.36 and 1.23 ppm before and after oxidation, it was possible to quantify the % of Rha units modified.

Immunogenicity studies in mice

Seven groups of 8 C57BL/6 5-weeks female mice purchased from Charles River Laboratory and maintained at NVD Animal Care received three subcutaneous immunizations at 14 days-interval with 200 µL/dose of 1 µg of OAg (5 µg/mL).
Mice were bleed before first immunization (day 0) and on immunization days 14 and 28. Mice were scarified and sera collected 2 weeks after 3rd immunization, on day 42. All animal protocols were approved by the local animal ethical committee (approval N. AEC201018) and by the Italian Minister of Health in accordance with Italian laws.

Serum antibody analysis by ELISA

Serum IgG levels against both OAg and CRM_{197} were measured by ELISA (*222*) (*180*). Purified OAg from 2192 (5 µg/mL) and CRM_{197} (2 µg/mL) were used for ELISA coating. Mouse sera were diluted 1:200 in PBS containing 0.05% Tween 20 and 0.1% BSA. ELISA units were expressed relative to mouse anti-OAg or anti-CRM_{197} standard serum curves, with best 4 parameter fit determined by modified Hill Plot. One ELISA unit was defined as the reciprocal of the standard serum dilution that gives an absorbance value equal to 1 in this assay. Each mouse serum was run in triplicate on 3 different ELISA plates. Data are presented as scatter plots of individual mouse IgG ELISA units, and geometric mean of each group. IgM and IgG subclasses antibodies were detected using a similar ELISA procedure: all the secondary antibodies were diluted 1:1000 in PBS containing 0.05% Tween 20 and 0.1% BSA, incubated 30min at room temperature followed by a further incubation of 30min at room temperature of the tertiary antibody antigoat AP-labeled diluted 1:30000 in the same dilution buffer. As only anti-OAg IgG standard reference serum was available for specific unit determination, IgM and IgG subclasses antibodies are presented as ELISA absorbance values.

Serum bactericidal activity (SBA)

Equal volumes of day 42 mouse serum, belonging to the same immunization group, were pooled together for SBA experiments. *S.* Typhimurium D23580 strain was grown in Luria Bertani (LB) medium to log-phase (OD: 0.2), diluted 1:30,000 in SBA

buffer (50 mM phosphate; 0.041% $MgCl_2$ $6H_2O$; 33 mg/mL $CaCl_2$; 0.5% BSA) to approximately 3 X 10^3 colony forming units (CFU)/mL and distributed into sterile polystyrene U bottom 96-well microtiter plates (12.5 µL/well). To each well (final volume 50 µL, ~620 CFU/mL), serum samples serially diluted 1:3 (starting from 1:20-1:100 dilution) were added. Sera were heated at 56ºC for 30 min to inactivate endogenous complement. Active Baby Rabbit Complement (BRC, Pel-Freez lot 0405/lot 12521) used at 50% of the final volume was added to each well. BRC source, lot and percentage used in SBA reaction mixture were previously selected by lowest toxicity against *S.* Typhimurium. To evaluate possible nonspecific inhibitory effects of BRC or mouse serum, bacteria were also incubated with: a. the same tested sera plus heat-inactivated BRC (HI-BRC); b. sera alone (no BRC); c. SBA buffer and active BRC. Each sample and control was tested in triplicate. Seven microliter reaction mixtures from each well was spotted on LB-agar plates at time zero (T0) to assess initial colony forming units (CFU), and at 1.5 h (T90) after incubation at 37ºC. LB-agar plates were incubated overnight at 37ºC and resulting CFU were counted the following day. Bactericidal activity was determined as CFU counted in each pooled serum dilution with active/inactive BRC, compared with CFU of the same sera dilutions with no BRC. SBA graphs show the inhibition of bacterial growth as a function of anti-OAg ELISA units detected in each tested serum pool.

Flow cytometry

Bacteria were grown overnight in LB medium, diluted to OD: 0.17 and incubated in 1:200 diluted (PBS 1% BSA) serum samples (CFU: $3x10^6$ in 50 µL) for 1 h in ice. After washing with PBS, bacteria were incubated with secondary anti-mouse APC-labeled antibody (Invitrogen, 1:400 in PBS 1% BSA) for 1 in ice. After washing, bacteria were resuspended in 4% formaldehyde (130 µL) and then read using a FACS CANTO (BD Biosciences) flow cytometer (10,000 events recorded). Negative control was obtained by incubating bacteria with secondary antibody only. Values were obtained by dividing the geometric mean of fluorescent signals of positive bacteria compared to negative control.

4.4 Results

OAg oxidation with $NaIO_4$ and reductive amination with CRM_{197}

The $NaIO_4$-based oxidation affects vicinal diols to generate two aldehydes groups, opening the sugar ring. In the case of *S.* Typhimurium OAg, this reactivity can involve Rha and Glc residues (Figure 4.3a). The resulting aldehyde groups can hence react with the lysine residues of the carrier protein to form a covalent C=N linkage, that is subsequently reduced to a stable C-N bond with $NaBH_3CN$. A further step of reduction with $NaBH_4$ was introduced to quench eventual unreacted C=O groups.

Optimization of conjugation conditions working with LT2 OAg

OAg purified from *S*. Typhimurium LT2 (a lab strain) was used for testing different conditions for this conjugation approach. Different $NaIO_4$ concentrations were tested to obtain OAg with a different derivatization grade. With increasing concentration of $NaIO_4$, increasing % of activation were obtained (Table 4.1), expressed as molar ratio % of oxidized Rha to total Rha. LT2 OAg has a very low degree of glucosylation (molar ratio of Glc to Rha = 0.11) and % of activated repeating units was calculated looking at Rha units modified only, both by HPAEC-PAD and ^1H NMR (Figure 4.4). A

good correlation was found between the two methods used (Table 4.1). Higher OAg derivatization resulted in a shift of the peaks at lower MW, indicating partial depolymerization of the OAg chain after this treatment or a change in its conformation (Figure 4.5 and Table 4.1).

Table 4.1 OAg oxidation using different $NaIO_4$ concentration resulted in differently derivatized products

[$NaIO_4$] (mM)	% oxidized sugar recovery	% activation (HPAEC-PAD)	% activation (NMR)	Kd (HPLC-SEC)
1.87	87	4	2.8	0.19 and 0.30
3.75	92	14	12	0.20 and 0.31
7.5	92	35	35	0.22 and 0.34

% of activation was calculated as molar ratio % of oxidized Rha residues to total Rha. Kd values for the two main peaks of the underivatized OAg of 0.18 and 0.29.

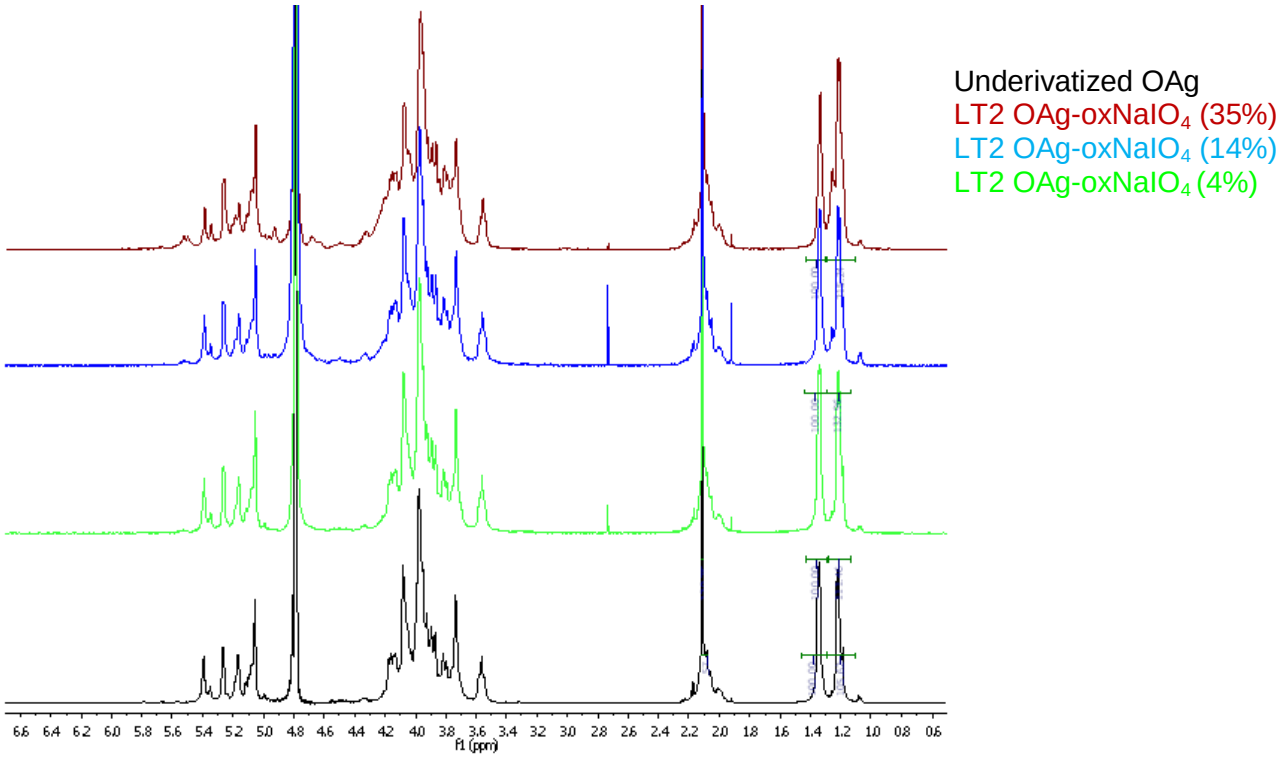

Figure 4.4 Characterization of LT2 OAg-oxNaIO$_4$ by ^{1}H NMR (RT, 500 MHz) in comparison to the corresponding underivatized OAg. Signal at 1.23 ppm corresponding to CH_3 Abe overlapped with CH_3 of modified Rha units in oxidized samples.

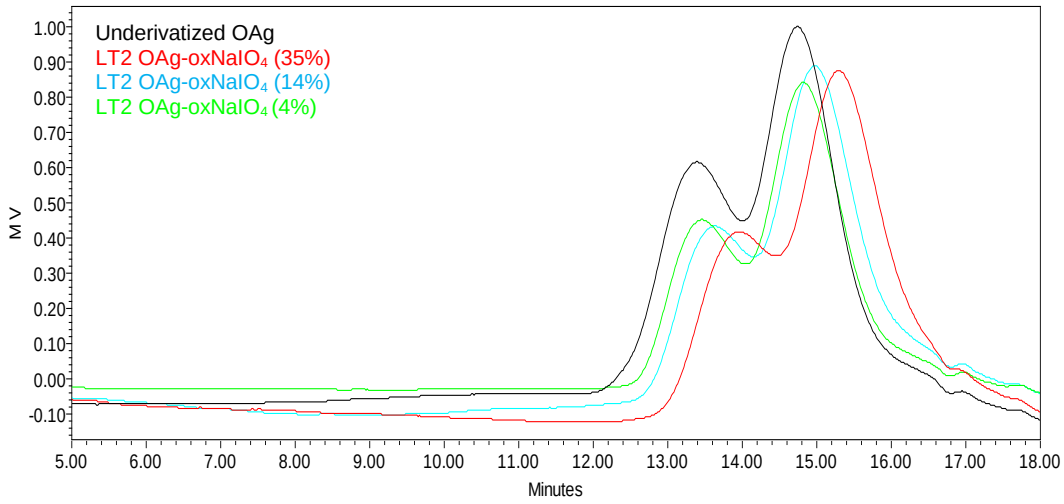

Figure 4.5 HPLC-SEC (dRI) chromatograms of the different products obtained by oxidation of LT2 OAg with $NaIO_4$. TSKgel 3000 PWXL column, 0.5 mL/min, 100 mM NaCl 100 mM NaH_2PO_4 5% CH_3CN pH 7.2; Vtot 23.29 min; V0 11.20 min

All the derivatized OAg obtained were tested for conjugation, to see if a different degree of derivatization could affect conjugation to the protein.
Different conjugation conditions were tested varying OAg to CRM_{197} ratio, the concentration of LT2 OAg-oxNaIO$_4$ and the concentration of CRM_{197} (Table 4.3). All the conjugations were performed in 100 mM Na_2HPO_4 pH 7.2 and adding $NaBH_3CN$ 1:1 w/w ratio with the OAg. Conjugation mixtures were gently mixed overnight at 37°C and then analyzed by SDS-PAGE (Figure 4.6) and HPLC-SEC to verify conjugate formation. Table 4.3 summarizes the results obtained. When SDS-PAGE and HPLC-SEC analysis did not show the presence of unconjugated protein in the mixture, conjugates were purified by HIC, and characterized.

Table 4.3 Conjugation performed with LT2 OAg-oxNaIO$_4$ and CRM$_{197}$

n° exp.	% oxidation OAg	OAg/CRM$_{197}$ (w/w)	[OAg] (mg/mL)	[CRM]$_{197}$ (mg/mL)	Free CRM$_{197}$ in the conj mixture	CRM$_{197}$ recovery in the purified conj (%)	OAg/CRM$_{197}$ in the conjugate (w/w)
1	**35%**	**2:1**	**10**	**5**	**No**	**70,1**	**0,54**
2	35%	1 :1	5	5	Yes		
3	35%	1:2	2,5	5	Yes		
4	35%	2:1	20	10	No	66,8	0,52
5	35%	2:1	40	20	No*	25,8	0,49
6	35%	1:2	5	10	Yes		
7	14%	1:2	5	10	Yes		
8	**14%**	**2:1**	**10**	**5**	**No**	**78**	**0,65**
9	4%	1:2	5	10	Yes*		
10	4%	2:1	10	5	No*	32,2	1,11

* protein precipitation was observed in the reaction mixture

Working with LT2 OAg-oxNaIO$_4$ with the highest degree of oxidation (35%), and with a protein concentration of 5 mg/mL, only the OAg/CRM$_{197}$ w/w ratio of 2:1 (exp. 1-3) allowed all protein conjugation. Maintaining the OAg to CRM$_{197}$ ratio constant and increasing CRM$_{197}$ concentration to 10 mg/mL did not make any difference (exp. 4 vs 1), while at 20 mg/mL (exp. 5), protein precipitation was observed, indicating that high reagent concentrations should be avoided. All the purified conjugates (exp 1, 4 and 5) were characterized by the same OAg to CRM$_{197}$ ratio of 0.5 (w/w) and when no precipitation happened, by similar saccharide and protein recoveries.
Also working with LT2 OAg-oxNaIO$_4$ 14% oxidized (exp. 7 and 8), all the protein was conjugated when a w/w ratio of OAg to CRM$_{197}$ of 2:1 was used in the reaction. With a ratio of 1:2, even increasing the protein concentration to 10 mg/mL, not all the protein was conjugated.
Using the same conditions in term of reagents concentration and OAg to CRM$_{197}$ ratio in the reaction mixture, the different % of OAg modification did not affect protein and OAg recoveries (exp. 1 and 8), like the OAg to CRM$_{197}$ ratio in the purified conjugates, which were similar. Working with the less derivatized LT2 OAg-oxNaIO$_4$ (4%), in both tested conditions (exp. 9-10), protein precipitation was observed, probably indicating that OAg activation was not sufficient for conjugation to CRM$_{197}$, which subsequently precipitated in the reaction conditions.
Activation of 14% seemed the most appropriate condition for assuring sufficient quantities of activated groups for conjugation, without altering consistently the OAg

chain structure, that could have a consequent negative impact on immunogenicity. This was selected as the condition for the production of the conjugate to test in mice.

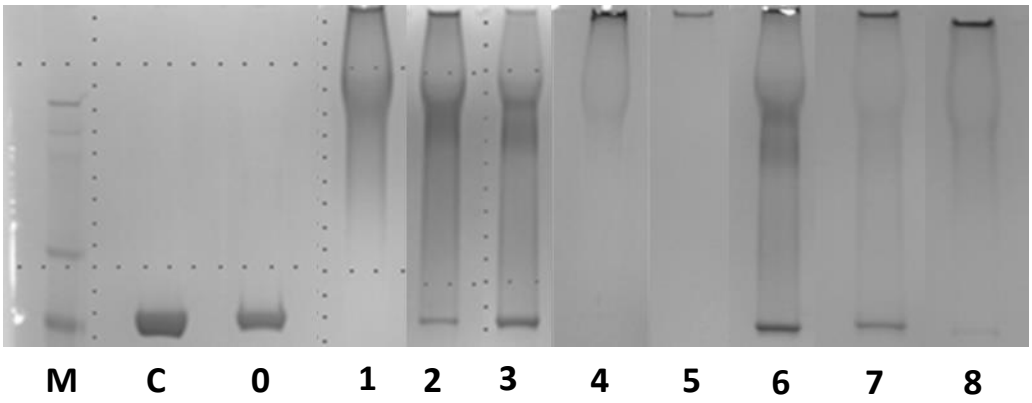

Figure 4.6 SDS-PAGE analysis of OAgox-CRM_{197} conjugation mixtures (1-8) in comparison to unconjugated CRM_{197} (C) and conjugation performed by direct reductive amination without oxidizing the sugar (0). Five μg of protein were loaded per well.

2192 OAg oxidation with $NaIO_4$ and conjugation to CRM_{197}

The HPLC-SEC profile of the oxidized 2192 in comparison with the underivatized OAg showed a shift of the main peak to a slightly lower MW. According to micro BCA, which constitutes a quick test to determine whether the oxidation has happened, 14% of OAg repeating units resulted derivatized (calculated as number of oxidized monomers/total Rha *100). HPAEC-PAD analysis stated that respectively 14% of the Rha and 6.4% of the Glc units were oxidized, corresponding to 15.5% of repeating units modified. NMR was not used in this case as it does not allow determination of the % of Glc oxidized present for 24% of OAg repeating units of 2192 OAg. Performing the conjugation reaction with conditions n° 8 reported in Table 4.3, all CRM_{197} was conjugated and residual free OAg was removed by purification through HIC. HPLC-SEC analysis showed the shift of the conjugate at HMW in comparison to free protein (Figure 4.7) and free OAg and was used for estimating conjugate MW distribution (Table 4.4).

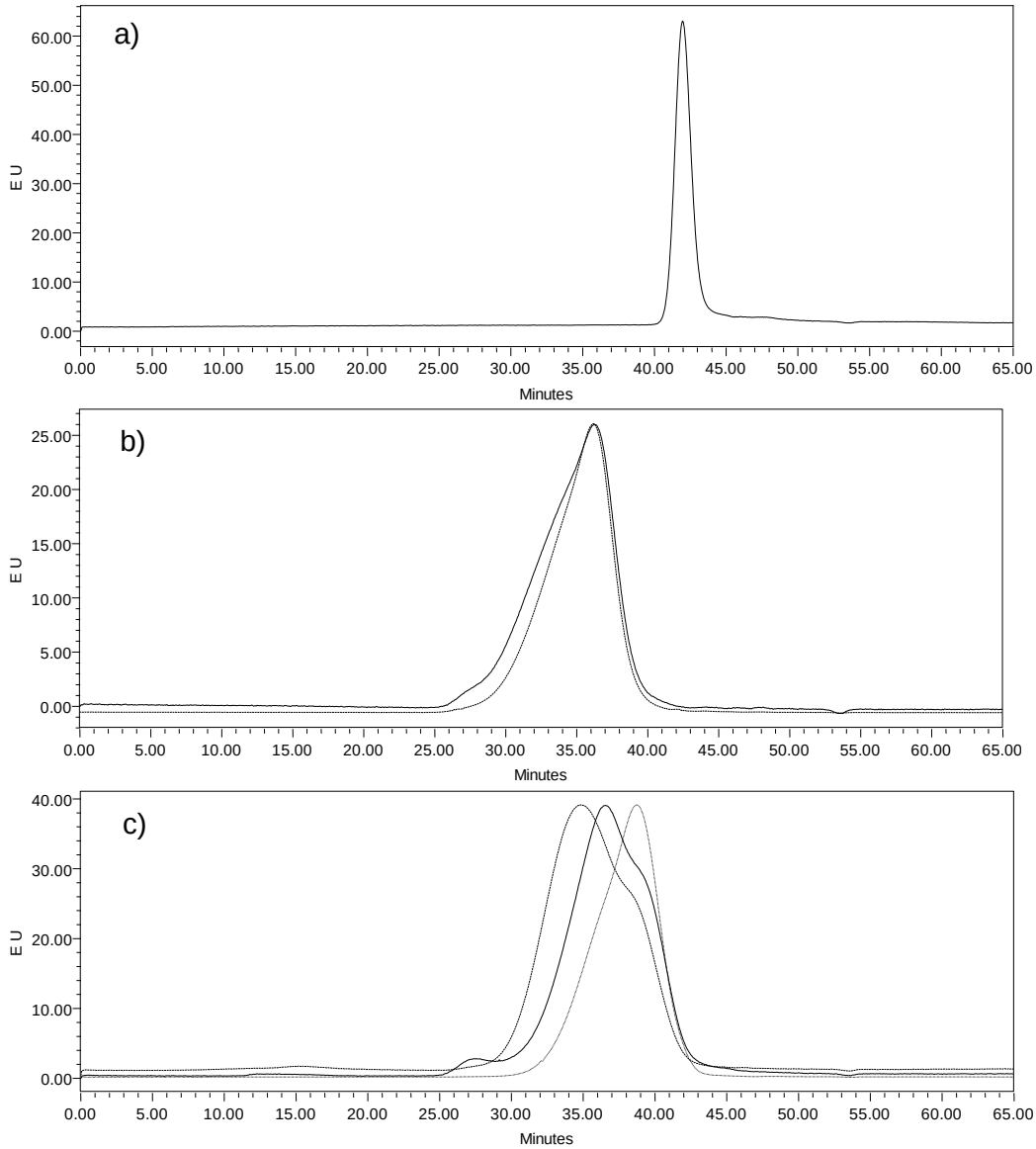

Figure 4.7 HPLC-SEC (fluorescence emission profiles) of free CRM_{197} (a); purified selective conjugates OAg-ADH-SIDEA-CRM_{197} (dashed line) and OAg-NH-SIDEA-CRM_{197} (solid line) (b); and random conjugates OAg-oxTEMPO2h-CRM_{197} (dashed line), OAg-oxTEMPO12h-CRM_{197} (solid line) and OAg-ox$NaIO_4$-CRM_{197} (dotted line). TSKgel 6000 PW + 5000 PW, 0.5 mL/min, 100 mM NaCl 100 mM NaH_2PO_4 5% CH_3CN pH 7.2; Vtot 49.004 min; V0 24.382 min.

Table 4.4 O:4,5-CRM_{197} conjugates generated using different chemistry

Conjugate	OAg/CRM_{197} (w/w)	OAg/CRM_{197} (mol/mol)	Kd conjugate (HPLC-SEC)
OAg-ox$NaIO_4$(14%*)-CRM_{197}	0.72	2.05	0.57
OAg-oxTEMPO2h(15%*)-CRM_{197}	0.56	1.6	0.44
OAg-oxTEMPO12h(36%*)-CRM_{197}	0.38	1.08	0.50
OAg-NH_2-SIDEA-CRM_{197}	1.42	4.05	0.50
OAg-ADH-SIDEA-CRM_{197}	1.74	4.96	0.49

Kd values were calculated on a TSKgel 6000 PW + 5000 PW, 0.5 mL/min, 100 mM NaCl 100 mM NaH_2PO_4 5% CH_3CN pH 7.2; Vtot 49.004 min; V0 24.382 min; Kd of free CRM_{197}: 0.72; Kd of free 2192 OAg: 0.67. * % repeating units oxidized calculated by micro BCA.

Is $NaBH_3CN$ able to reduce residual unreacted aldehydes groups on the sugar chains?

To verify if $NaBH_3CN$, used for the reductive amination of OAgox with CRM_{197}, was able to reduce residual unreacted aldehydes groups on the sugar chains, the reduction of OAg-ox$NaIO_4$ with $NaBH_3CN$ was performed using the same conditions adopted during the conjugation step, but without adding CRM_{197}. Aldehyde determination by micro BCA showed that carbonyl groups were not reduced. To quench the unreacted CHO groups remained after conjugation, $NaBH_4$ was tested as reducing agent. $NaBH_4$ was mixed with OAg-ox$NaIO_4$ ($NaBH_4$/OAg-ox$NaIO_4$ = 1:1 w/w) in NaH_2PO_4 100 mM pH 7.2 at 37°C, and the presence of aldehydes groups was verified after 2h and ON reaction. Already after 2h, there were no residual carbonyl groups. Analysis by HPAEC-PAD confirmed that the sugar composition of the OAg was not affected by this treatment. Therefore a 2h reduction step with $NaBH_4$ ($NaBH_4$/OAg-ox$NaIO_4$ = 1:1 w/w, 37 °C) was added after the ON conjugation by reductive amination. HPL-SEC profiles of the untreated and $NaBH_4$-reduced conjugates were identical (data not shown).

OAg oxidation with TEMPO and reductive amination with CRM_{197}

The oxidation of 2192 OAg with TEMPO was tested in order to have random formation of CHO groups along the chain without opening the sugar rings as oxidation with $NaIO_4$ does (Figure 4.3 a). TEMPO oxidation targets primary alcohols groups, which in *S.* Typhimurium OAg are present in the sugar moieties of Man, Gal

and Glc, one per monosaccharide. The resulting aldehyde groups can then react with the lysine residues of the carrier protein by reductive amination (Figure 4.3 a).
Oxidation of 2192 OAg with TEMPO was followed over time and the % of OAg monomers oxidized increased from 15% after 2h to 36% after 12h (as detected by micro BCA). HPLC-SEC analysis showed that OAg MW distribution remained unchanged after oxidation, even when the reaction was performed for longer times, differently from what was obtained with $NaIO_4$.
OAg-oxTEMPO with an average percentage number of oxidized repeating units of 36% (12h of reaction) and 15% (2h of reaction) were considered for further conjugation to CRM_{197}, to look also at the impact of OAg derivatization degree on the immunogenicity of the corresponding conjugates.
The same conditions for the conjugation and purification of OAg-ox$NaIO_4$ were applied and in both cases all CRM_{197} resulted conjugated in the reaction mixtures. Conjugates obtained using a less derivatized OAg (both after treatment with $NaIO_4$ or TEMPO) were characterized by a higher OAg to protein ratio respect with the conjugate obtained with the OAg more oxidized that was able to link more CRM_{197} molecules (Table 4.4).

Selective conjugation chemistries

The terminal KDO residue of the core region was used for selectively linking the OAg to the protein without modifying the OAg chain. In one case, reductive amination with ADH was followed by reaction with SIDEA and conjugation to CRM_{197} (Figure 4.3b). A similar chemistry was also evaluated where the first step of reductive amination was conducted with NH_4OAc, allowing the synthesis of a conjugate with a shorter linker than ADH-SIDEA (Figure 4.3b).
The reactivity of OAg-KDO with NH4OAc was tested at pH 4.5 and pH 7.0 (*124*) (*180*) (Table 4.5).

Table 4.5 OAg amination with NH_4OAc comparing different reaction conditions

[2192] (mg/mL)	[$NaBH_3CN$]/OAg w/w ratio	[NH_4OAc] (M)	pH	Reaction time (h)	% activated OAg (KDO)
40	1.2	0.5	4.5	3	37.6
				24	34.0
				120	44.3
40	2.5	0.5	7	3	66.8
				24	80.0
				120	97.5

Differently from ADH (*180*), NH_4OAc gave higher activation yields at pH 7.0, in line with what was expected based on the % of amino groups protonated at the two

different pH for the two different molecules (pKa NH_3 = 9.23, pKa ADH = 2.5). At pH 7.0, the activation degree was 67% after only 3h and 80% after 24h, indicating a higher reactivity of the KDO unit with respect to terminal reducing groups of other polysaccharide chains, that require longer reaction times and give often lower derivatization (*124*) (*223*).
For the synthesis of the corresponding conjugate, the reaction of 2192 OAg with NH_4OAc was performed for 5 days resulting in 90% of OAg chains activated and in a sugar recovery of 85%. Working with ADH, a sugar recovery of 80% was obtained with activation close to 100%, with free ADH < 5% in moles. The longer linker with the hydrazide functionality allowed performing the reaction in only 2h at pH 4.5. After the step of reductive amination, the second linker SIDEA was introduced in the same way for both the products. A sugar recovery >80% was obtained, with >90% of total NH_2 groups reacted with SIDEA and free SIDEA determined to be <10% in moles, for both OAg-NH_2 and OAg-ADH. TNBS analysis confirmed the presence of < 10% unreacted NH_2 groups. The same conjugation conditions were applied to OAg-NH_2-SIDEA and OAg-ADH-SIDEA. The analysis of the conjugation mixtures by HPLC-SEC confirmed conjugate formation without residual free protein in both cases. Unconjugated OAg was removed by HIC. The resulting conjugates were very similar in terms of OAg to CRM_{197} ratio (4-5 OAg chains linked per protein) and Kd values (Table 4.4, Figure 4.7). Both selective conjugates were characterized by a higher OAg to protein ratio than all the random conjugates (Table 4.4).

Immunogenicity study in mice of OAg-CRM_{197} comparing different conjugation chemistries

The synthesized conjugates were tested in mice, with three main objectives:

1. compare the immunogenicity of random and selective conjugates;
2. analyze the impact of linker chain length on the immunogenicity of conjugates obtained by selective linkage of the OAg through its terminal KDO unit;
3. evaluate if the degree of random modification of the OAg chain can have an impact on immunogenicity.

After three doses, all the conjugates generated high anti-2192 OAg IgG levels not statistically different among the groups (Figure 4.8a). Selective conjugates induced a similar anti-OAg IgG response compared with random conjugates and a stronger modification of the OAg chain did not negatively affect the immune response in mice. Also no differences were found regardless of the length of the linker when OAg-ADH-SIDEA-CRM_{197} was compared to OAg-NH_2-SIDEA-CRM_{197}.
Subclass antibody analysis showed that anti-2192 OAg IgG1 was the predominant subclass in sera from mice vaccinated with all the conjugates (Figure 4.8b), as expected for glycoconjugate antigens. No IgA was detected in any sera, while increased anti-2192 OAg IgM levels were detected at day 42 for OAg-TEMPOox conjugates with respect to the other groups (Figure 4.8c).
For all the conjugates, anti-CRM_{197} IgG levels were very low after the first injection and boosted after the second dose. Already after two doses, anti-CRM_{197} IgG responses for OAg-oxTEMPO-CRM_{197} conjugates were higher than for the other groups, in line with the higher dose of protein injected compared with the other groups (Figure 4.8d). However at day 42, differences were significant only between OAg-NH_2-SIDEA-CRM_{197} and OAg-ADH-SIDEA-CRM_{197} with OAg-oxTEMPO2h-CRM_{197} (p=0.0025).

a)

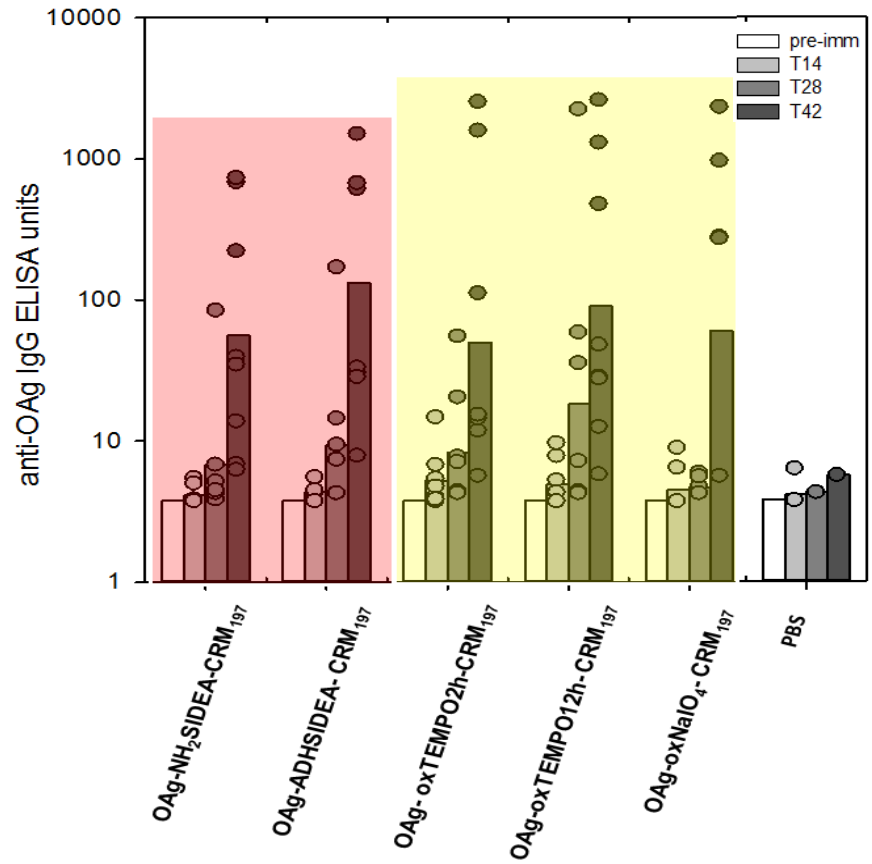

b)

IgG subclasses titers

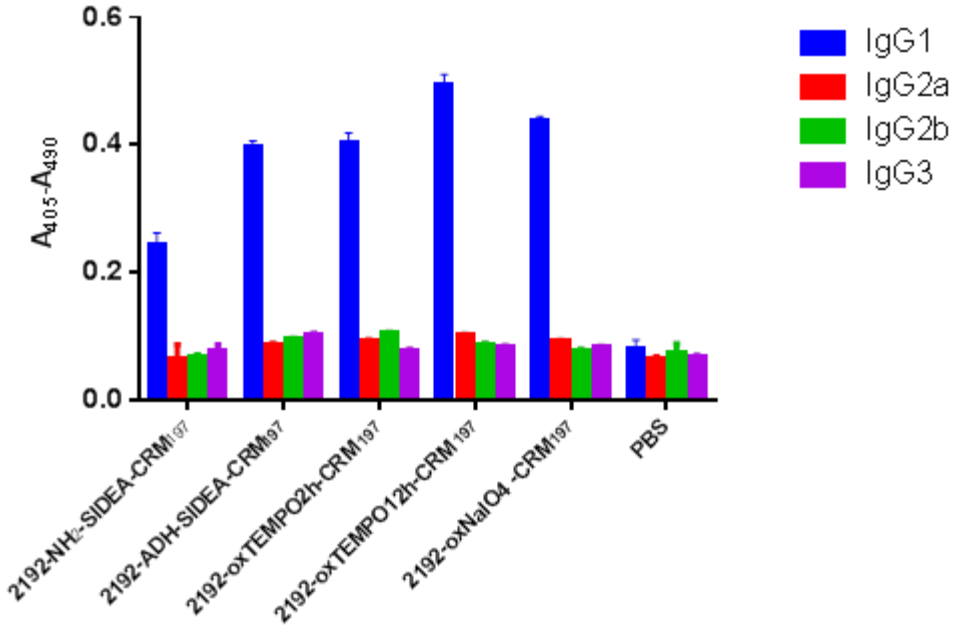

c)

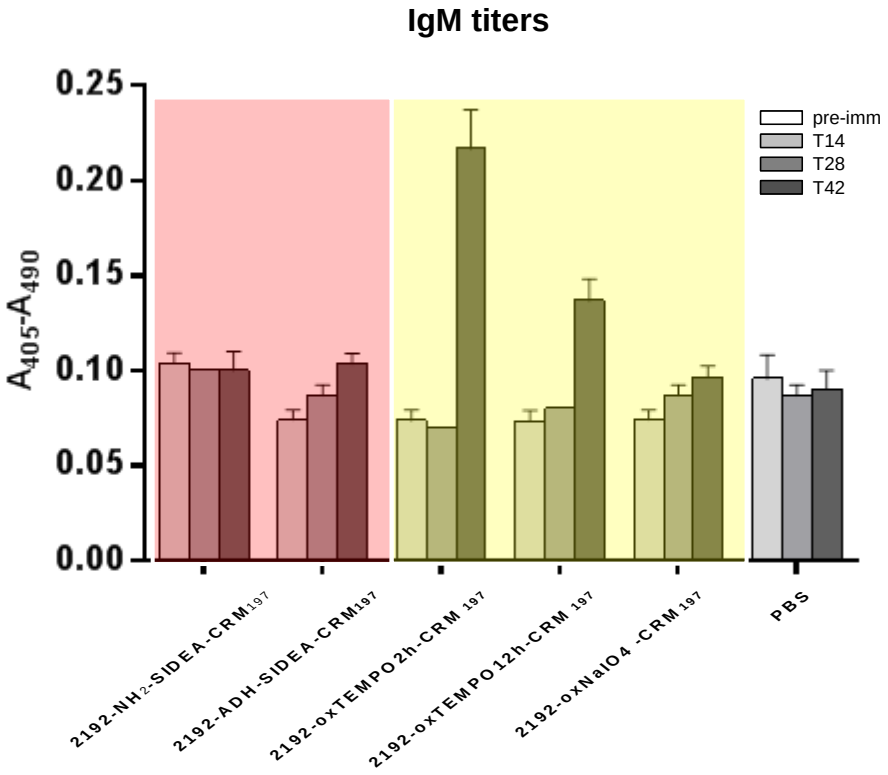

d)

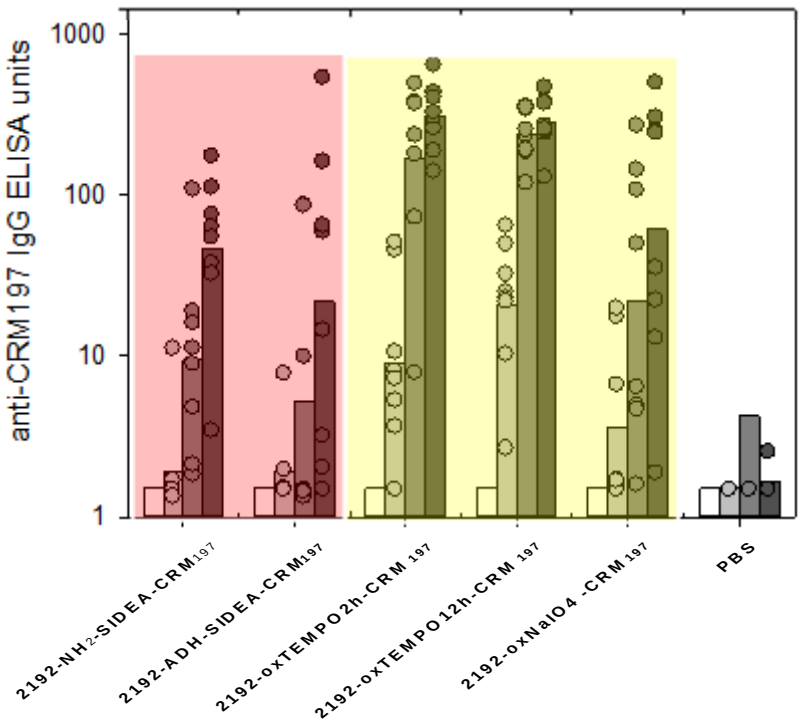

Figure 4.8 (a) Anti-OAg IgG ELISA units against 2192 OAg coating agent. Individual animals are represented by the points; horizontal bars represent Geometric Mean Units. (b) Anti-OAg IgG subclasses absorbance values against 2192 OAg coating agent (c) Anti-OAg IgM absorbance values against 2192 OAg coating agent. Horizontal bars represent Mean ± SD. (d). Anti-CRM_{197} IgG ELISA units against CRM_{197} coating agent.

To evaluate functional activity of elicited antibody, sera collected at day 42 were pooled and tested for SBA against *S.* Typhimurium D23580, a Malawian clinical isolate.. All the conjugates showed strong bactericidal activity with complete killing achieved with less than 0,01 IgG ELISA units, but with different extent depending on the conjugation chemistry used. To evaluate bactericidal specificity of the antibodies elicited by the various conjugates, inhibition of bacterial growth was plotted per anti-OAg IgG units as measured by ELISA. This highlights the different functional activity of antibodies independent of their absolute amount (Figure 4.9). Bactericidal activity of the antibodies induced by selective OAg-KDO conjugates was similar independent of the length of the spacer used, while all the random conjugates elicited stronger bacterial growth inhibition than the selective conjugates. Interestingly, heavier modifications of the OAg chain resulted in conjugates producing a weaker bactericidal activity. To evaluate possible differences in cell-surface binding, pooled sera at day 42 from mice immunized with the different conjugates were tested by FACS against the homologous 2192 and two additional heterologous strains (both invasive clinical isolates). As shown in Figure 4.10, all sera could bind the 3 strains, with a bigger shift of the signal observed for random conjugates. This result indicates that the increased SBA found with the random conjugates may be due to a stronger binding affinity of the antibodies generated by those conjugates.

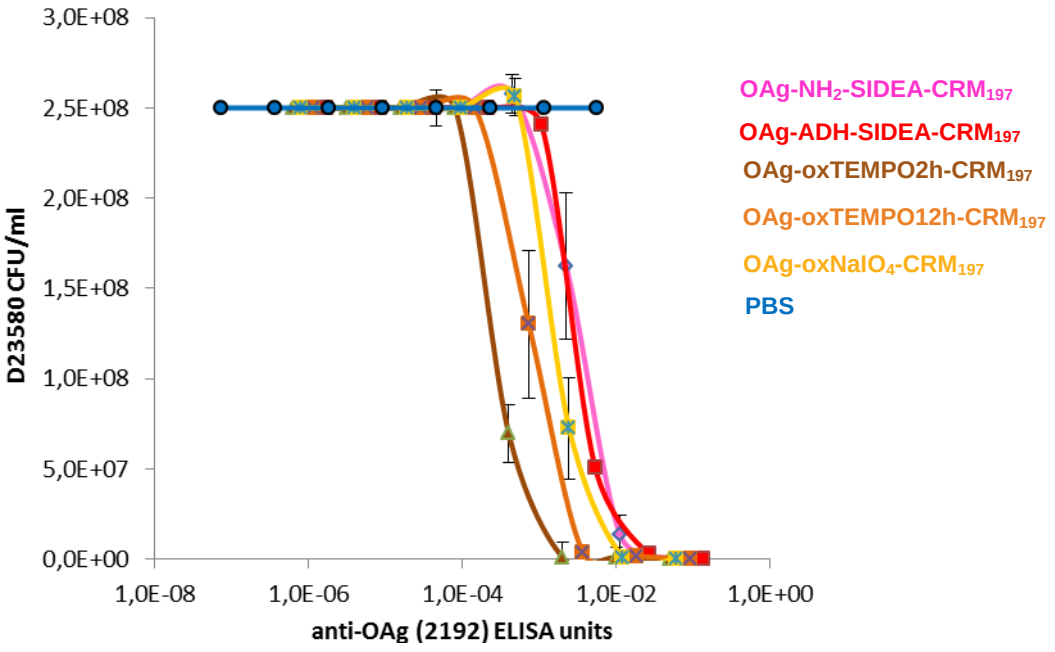

Figure 4.9 SBA analysis of pooled sera at day 42: CFU/mL of D23580 strain versus anti-OAg IgG ELISA units.

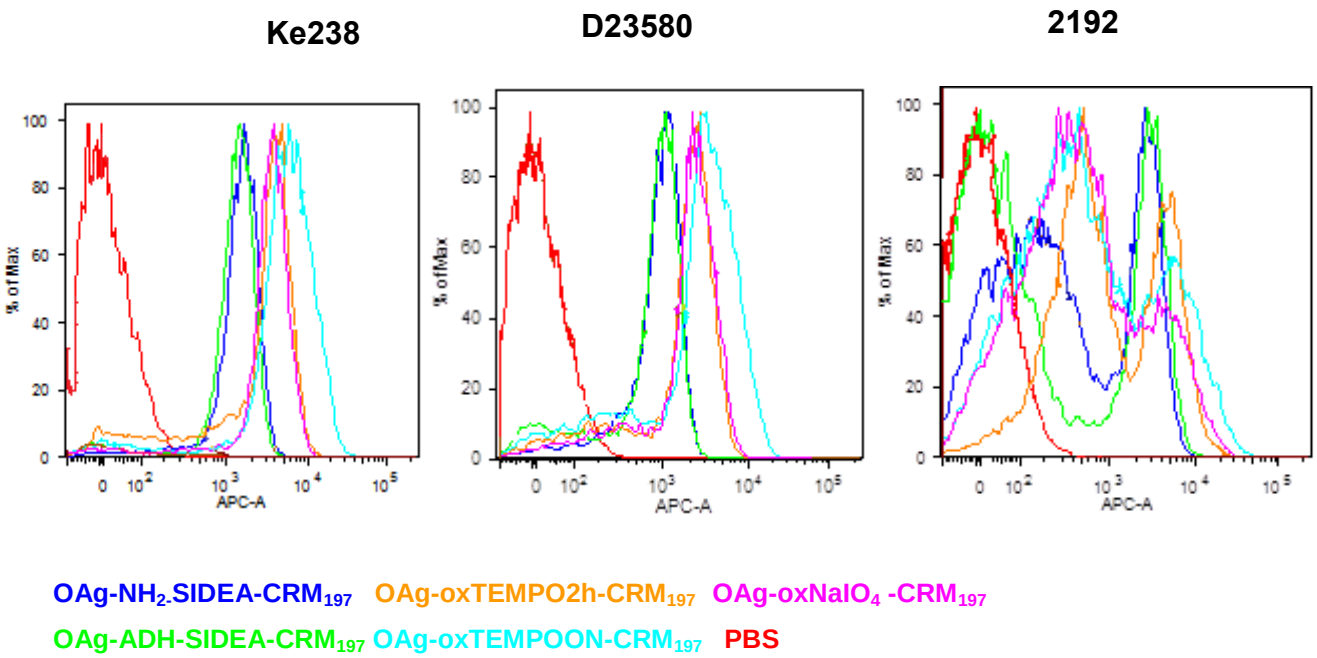

Figure 4.10 Flow cytometry analysis of surface staining of live Ke238, D23580 and 2192. Bacteria were stained with mice day 42 pooled immune sera raised against the different conjugates. Sera dilution is 1:200. Target bacteria were fixed after staining. Representative results of three experiments are shown.

4.5 Discussion

There is increasing awareness of the significance of NTS disease as a major public health concern in the developing world (Feasey *et al.*, 2012; MacLennan and Levine, 2013; Okoro *et al.*, 2012a). While responsible for gastroenteritis in high-income countries, NTS are a common cause of fatal invasive disease in low-income countries, particularly in Africa. Currently no vaccines are available against this disease and conjugation technology is one of the approaches followed at the moment for the development of a vaccine (*84*) (*85*) (*203*).

Conjugation chemistry is one of the parameters that can impact on the immunogenicity of the corresponding conjugate vaccines (*122*). In this study the immunogenicity in mice of *S.* Typhimurium OAg-CRM_{197} conjugate vaccines obtained by different methods has been investigated. Random derivatization along the sugar chain was compared with one-site linkage at the terminus of the core region. Regarding selective approach, the length of the spacer between the sugar and the protein moieties was evaluated. For the random approach, a milder oxidation by TEMPO was compared to oxidation with $NaIO_4$ that opens the sugar units impacting more on the OAg epitopes and conformation. Different percentages of OAg derivatization were also compared.

In general selective chemistry is preferred because of consistency of production and characterization of the final product, but suffers from lower yields in terms of OAg sugar recovery with respect to random approaches. From a process point of view, all the conjugation methods tested here resulted in no residual free protein in the conjugation mixture. In all the procedures the carrier protein was not derivatized, but one step less was required for the production of random conjugates with respect to

selective ones, even if sugar recoveries were good for all the derivatization steps performed. Much less OAg was required (w/w respect to the protein) for the random chemistries, with the advantage in terms of total sugar amount required for conjugation (about 1/5 of the sugar required for the selective approach). OAg conjugation yields did not improve much even when random chemistries were used (19-36% with respect to 15-17% for selective approaches), but consistently improved considering the total amount of sugar required for performing the reaction.
Random conjugates were all characterized by lower OAg to protein ratios than selective conjugates (Table 4.4), in line with the presence of more points of attachment for the protein along the sugar chain.
When tested in mice all the conjugates induced similar anti-OAg IgG antibodies titers independent from the chemistry used, and a strong modification along the sugar chain that could potentially impact on OAg epitopes integrity and conformation, did not negatively affect the immunogenicity. Random conjugates induced stronger bactericidal antibodies than selective ones, and FACS analysis confirmed that random derivatization did not impact on the ability of the corresponding conjugates to induce antibodies able to recognize structural epitopes. However, among the random conjugates, there was an inverse correlation between degree of derivatization and bactericidal activity of the antibodies induced. Although all the conjugates induced similar anti-IgG antibodies, the anti-OAg IgM levels were different, and were higher for TEMPO conjugates after three doses.
Simon et al., working on *S.* Enteritidis conjugates, did not find differences in terms of antibody response and protection comparing in mice flagellin monomers conjugates obtained by direct random linkage or selective chemistry on the terminal KDO with a long linker (*84*). Micoli et al. also found no differences in terms of IgG titers testing in mice *S.* Paratyphi A OAg conjugates obtained by selective ADH-SIDEA chemistry or by random activation through CDAP and using ADH as linker (*180*). In this case, selective conjugates gave stronger bactericidal titers than random ones (*180*). It is important to underline that random derivatization by CDAP can also create sugar cross-linking (*98*). Differently, it was found that *S.* Typhimurium OAg-TT and *S.* Paratyphi A OAg-CRM_{197} conjugates produced by random activation and ADH linker were more immunogenic in mice than when selective chemistry with ADH linked to the COOH group of KDO was used (*98*) (*180*). According to Watson, immunogenicity is also affected by the number of OAg units modified with ADH, resulting in different OAg to protein ratios in the conjugates too. In this study, the difference on the immunogenicity profile obtained could be related to the different amount of carrier protein injected for the different conjugates (higher for the random than for the selective conjugates at the same OAg dose) or to the different structure of the conjugate itself: a sun-structure for the selective conjugates with few points of linkage between the saccharide and the protein per molecule of conjugate, against a cross-linked heterogeneous structure for the random conjugates with possible formation of much more glycopeptides after processing in the B-cells. Recently it has been reported that T cell populations can recognize carbohydrate epitopes derived by APC processing of conjugate vaccines and that, when presented by MHCII, these epitopes recruit T cell help for the induction of adaptive immune responses. The outcome of this work suggests that vaccines with optimal, high-density presentation of carbohydrate epitopes could have a major role in prevention and control of many diseases (*142*). A random-like conjugate is likely to produce a higher number of glycan-peptide units than a selective one, and this could be related to the present results.

Different chemistries could also impact on the conformation of the conjugate components, impacting on the exposure of sugar and carrier epitopes. Furthermore, both the selective conjugates were characterized by the presence of a long linker between the sugar and the protein (NH_2-SIDEA or ADH-SIDEA), while no linker was used for the synthesis of the random conjugate and the presence of the linker could be an additional factor affecting immunogenicity (*100*) (*180*).
This study underlies the importance of conjugation chemistry in the design of *S.* Typhimurium OAg-based glycoconjugate vaccines, and suggests that a random strategy could be optimum. More investigations on the reasons behind this immunological outcome are currently ongoing in our lab. A better knowledge of the effective structure of the conjugates tested and the design of more defined conjugate vaccines could help to further understand the relation between conjugate structure and immunogenicity results.

5. Click chemistry: a powerful tool for the synthesis of glycoconjugate vaccines

5.1 Abstract

Well defined glycoconjugate vaccines, selectively modified not only on the saccharide but also on the protein component, are highly desirable in terms of consistency of production, optimal characterization of the vaccine and to facilitate studies of immunological mechanism. In this study we have looked for a powerful conjugation method that allows synthesis of such well-defined glycoconjugates, since selective chemistries are usually characterized by low conjugation efficiencies. The process was developed for the conjugation of *S.* Typhimurium OAg to CRM_{197} as carrier protein. Two strategies were initially investigated, both involving the linkage of the terminal KDO unit of the sugar to the protein: thiol chemistry and click chemistry. Thiol chemistry did not allow conjugation unless starting with a relative high number of linkers on the protein, while click chemistry allowed conjugate generation even when just one position on the protein was activated.
Another advantage of the click chemistry was the possibility to recycle unconjugated OAg and use it for the synthesis of a new batch of glycoconjugate. Furthermore a solid-phase conjugation method utilizing the carrier protein bound to an ion exchange matrix was developed. CRM_{197} was adsorbed to the matrix using a batch procedure, and the immobilized protein was then conjugated to the OAg. Unreacted OAg was easily recovered and used for further conjugation, while the conjugate was eluted from the resin pure from both free protein and free sugar. This process has great advantages in terms of cost for vaccine production, allowing unreacted sugar recovery and simplifying the purification of the conjugate itself.

5.2 Introduction

"Click chemistry is a set of powerful, virtually 100% reliable, selective reactions for the rapid synthesis of new compounds via heteroatom links (C-X-C)…" (*224*). One of these reactions, the Huisgen 1,3-dipolar cycloaddition (*225*), has become the most popular click reaction, especially because it can proceed rapidly at room temperature by employing copper as a catalyst (*226*) (*227*). It is characterized by mild reaction conditions, high yields and simple work-up, selectivity and specificity and can be usually performed in water. The possibility of applying click chemistry in bioconjugation was first demonstrated for the preparation of peptidotriazolels via solid state synthesis (37). One of the most important properties of the click chemistry is its bio-orthogonality. The azide moiety is absent in almost all naturally existing compounds, lacks reactivity with natural biomolecules and undergoes ligation only with a limited set of functionalities, such as alkyne groups. Despite some concerns about stability of azide derivatives, possible immunogenicity of the spacers used, the need for a toxic metal in some applications, and the alkyne homocoupling side reaction, this reaction is very likely to be greatly used in the design of future drugs and biomolecules due to its specificity and effectiveness.
Looking at the glycoconjugate vaccines licensed or in advanced development in the EU, US and WHO, it can be deduced that four main strategies of conjugations are generally used: reductive amination, active ester chemistry, thiol chemistry and

carbodiimide-mediated condensation (*127*). Conjugation often results in a mixture of glycoproteins due to the heterogeneity of the carbohydrate haptens and to the random activation along the sugar chains and on the protein. Resulting glycoforms may present diverse pharmacokinetic and immunological properties due to different epitope density and presentation. Hence, increasing attention has recently been made to control the conjugation site (*228*) (*127*) and provide products which are well-defined not only in their saccharide component but also in the attachment point to the protein (*228*) (*229*). In this sense, pre-activation of the carrier protein and of the sugar hapten with bio-orthogonal linkers, such as the alkyne and the azide moieties, can allow a selective control of the conjugation reaction.
The first aim of this work has been that to identify an efficient conjugation strategy that could allow conjugate formation targeting one single point of the saccharide chain and few points of attachment on the carrier protein. *S.* Typhimurium OAg and CRM_{197} have been used as models. The identification of this chemistry will then allow the production of very selective conjugates with few saccharide chains attached to specific points on the protein.
Click chemistry has proved to be a powerful tool in this sense, allowing the synthesis of conjugates where only one position on the protein was available for linkage to the KDO unit of the sugar chain. Furthermore azido and alkine groups involved in the click chemistry are not de-activated during the conjugation reaction so that unreacted components can be recycled and re-conjugated. In the specific case, reactions were performed to have all the protein conjugated and the OAg was recovered and successfully re-used for conjugation. After verifying this possibility, further work was done to set up a synthesis on solid phase with the advantage to recover the sugar and at the same time obtain a conjugate pure from free saccharide without further purification steps.

5.3 Material and methods

Reagents

The following chemicals were used in this study: cystamine dihydrocloride, 1-ethyl-3-(3-dimethylaminopropyl)carbodiimide (EDAC), (+)-sodium L-ascorbate, 2-(N-morpholino)ethanesulfonic acid (MES), N-hydroxysuccinimide (NHS), tris(2-carboxyethyl)phosphine hydrochloride solution (TCEP), propargylamine, copper(II) sulfate pentahydrate ($CuSO_4.5H_2O$), tris(3-hydroxypropyltriazolylmethyl)amine (THPTA), phosphate buffer solution (PBS), adipic acid dihydrazide (ADH), sodium cyanoborohydride ($NaBH_3CN$), dimethyl sulfoxide (DMSO), sodium phosphate monobasic (NaH_2PO_4) [Sigma]; triplex III (EDTA) [Merck]; N-[β-maleimidopropionic acid] hydrazide trifluoroacetic acid salt (BMPH) [Thermo]; *N*-[ε-maleimidocaproyloxy]succinimide ester (EMCS), succinimidyl 3-(bromoacetamido)propionate (SBAP), NHS-PEG_4-N_3 [Pierce], Click-easyTM BCN N-hydroxysuccinimide ester I [Berry & Associates]; DL-1,4-Dithiothreitol (DTT) [Invitrogen]. CRM_{197} was obtained from Novartis Vaccines and Diagnostics (NV&D).
The clinical isolate 2192 was grown and the corresponding OAg purified and characterized as described in the Chapter 1.

Synthesis and characterization of derivatized $CRM_{197}$$CRM_{197}$-BMPH via EDAC chemistry

10 mg of CRM_{197} were solubilized in MES 500 mM pH 6.0 (12 mg/mL); BMPH (42 mg/mL, molar ratio BMPH/COOH groups CRM_{197} = 10.42) and EDAC (3 mg/mL, molar ratio EDAC/COOH groups CRM_{197} = 1.15) were added. Mixture was stirred for 1h at RT, and then purified by desalting against NaH_2PO_4 100 mM EDTA 10 mM pH 7.0 on a HiPrep™ 26/10 desalting column 53 mL, prepacked with Sephadex™ G-25 Superfine (G25 53 mL) [GE Healthcare].

CRM_{197}-BMPH via EDAC/NHS chemistry

10 mg of protein were solubilized in MES 600 mM pH 6.0 (15.56 mg/mL); NHS (10.8 mg/mL, molar ratio NHS/COOH groups CRM_{197} = 5.36) and EDAC (6.2 mg/mL, molar ratio EDAC/COOH groups CRM_{197} = 1.83) were added and the solution mixed at RT for 1h. After this time, BMPH (2.8 mg/mL, molar ratio BMPH/COOH groups CRM_{197} = 0.53) was added and the solution stirred for 2h at RT. The mixture was purified by desalting on a PD-10 desalting column containing 8.3 ml of Sephadex™ G-25 Medium (PD 10) [GE Healthcare] against NaH_2PO_4 100 mM EDTA 1 mM pH 7.0.

CRM_{197}-EMCS

10 mg of CRM_{197} were solubilized in NaH_2PO_4 100 mM EDTA 1 mM pH 8.0 (4.7 mg/mL); EMCS was added (0.19 mg/mL, molar ratio EMCS/Lysine groups on CRM_{197} = 0.2) after being solubilized in DMSO (final DMSO concentration of 6% v/v). Mixture was stirred for 2h at RT, and then purified by desalting (G25 53 mL column) against NaH_2PO_4 100 mM EDTA 1 mM pH 7.0.

CRM_{197}-SBAP

10 mg of CRM_{197} were solubilized in NaH_2PO_4 100 mM EDTA 1 mM pH 8.0 (4.7 mg/mL); SBAP was added (0.3 mg/mL, molar ratio SBAP/Lysine groups on CRM_{197} = 0.3) after being solubilized in DMSO (final DMSO concentration of 4% v/v). Mixture was stirred for 3h at RT, and then purified by desalting (G25 53 mL column) against NaH_2PO_4 100 mM EDTA 1 mM pH 7.0.

Synthesis and characterization of CRM_{197}-N3

CMR_{197} (20 mg/mL) was solubilized in NaH_2PO_4 400 mM pH 7.2, and NHS-PEG4-N_3 was added (linker solubilized in DMSO with final DMSO concentration in the mixture of 1% v/v). Different amount of NHS-PEG4-N_3 were used to achieve a different degree of derivation on the protein with a molar ratio NHS-PEG4-N_3/Lysine groups CRM_{197} of 0.18, 0.26, 0.39, respectively. After mixing at RT for 8h, the mixture was purified by desalting on a G25 53 mL column against NaH_2PO_4 100mM pH 7.2.

Characterization of derivatized CRM_{197}

Protein content was estimated by micro BCA (using BSA as standard and following manufacturer's instructions [Thermo Scientifics]). HPLC-SEC analysis was used to compare derivatized protein with underivatized CRM_{197}. All samples were eluted on TSK gel G3000 PWXL column (30 cm x 7.8 mm; particle size 7 µm; cod. 808021) with TSK gel PWXL guard column (4.0 cm x 6.0 mm; particle size 12 µm; cod.808033) (Tosoh Bioscience). The mobile phase was 0.1 M NaCl, 0.1 M

NaH_2PO_4, 5% CH_3CN, pH 7.2 at the flow rate of 0.5 mL/min (isocratic method for 30 min). Void and bed volume calibration was performed with λ-DNA (λ-DNA Molecular Weight Marker III 0.12-21.2 Kbp, Roche) and sodium azide (NaN_3, Merck), respectively. Protein peaks were detected at 214 nm and 280 nm (UV detection) and using tryptophan fluorescence (emission spectrum at 336 nm, with excitation wavelength at 280 nm). Linker average loading on CRM_{197} was determined by MALDI-TOF analysis. For MALDI-TOF analysis, the protein was diafiltrated, using a Centricon-10 (Millipore), against NaH_2PO_4 10 mM pH 7.2. Two microliters of protein (at a concentration of 5 mg/mL) were mixed with 2 μL of a saturated solution of sinapinic acid in 50% acetonitrile solution containing 0.1% TFA. Two microliters of the mix was spotted on a MTP 384 stainless steel target (Bruker Daltonics GmbH, Bremen, Germany) and allowed to air-dry. Measurements were recorded on an Ultraflex III (Bruker GmBH) MALDI-TOF/TOF MS in linear mode. External calibration was performed by spotting 2 μL of protein calibration standard II (Bruker Daltonics) containing the following proteins: trypsinogen (23,982 Da), protein A (44,613 Da) and bovine serum albumin (66,431 Da). All mass spectra were recorded by summing up to 400 laser shots. The Flex Analysis software packages provided by the manufacturer were used for data processing.

Synthesis of OAg-cystamine-CRM_{197} conjugates

40 mg of 2192 OAg were solubilized in NaH_2PO_4 100 mM pH 7.0 (40 mg/mL) and then cystamine (110 mg/mL, cystamine/OAg (w/w) = 2.75) and $NaBH_3CN$ (61 mg/mL, $NaBH_3CN$/OAg (w/w) = 1.53) were added. The mixture was stirred for 3h at RT and then desalted against water on a G25 53 mL column. Cystamine disulfide bond was reduced by mixing the OAg at a concentration of 20 mg/mL with DTT 100 mM in NaH_2PO_4 100 mM EDTA 5 mM for 1h at RT. The derivatized OAg was purified by desalting on a G-25 53mL column against 10 mM NaH_2PO_4 5 mM EDTA pH 7.5. The amination reaction with cystamine was also performed at higher scale on 100 mg of OAg and the mixture purified by tangential flow filtration (10k 200 cm^2 Hydrosart membrane, 10 diafiltration cycles vs NaCl 1M, followed by 10 cycles against water).
Conjugation was performed solubilizing the derivatized protein in NaH_2PO_4 100 mM EDTA 1 mM pH 7.2 (10 mg/mL), and using a molar ratio of thiol groups to CRM_{197} of 30 to 1. After mixing ON at RT, the mixture was purified by size exclusion chromatography with a Sephacryl S-300 HR column 1.6 cm x 90 cm [GE Healthcare], eluting with PBS pH 7.2 at 0.5 mL/min.

Characterization of OAg-cystamine-CRM_{197} conjugates

Total saccharide content was quantified by phenol sulfuric assay (*195*), protein content by micro BCA and the ratio of saccharide to protein calculated. OAg-CRM_{197} conjugates profiles were compared with free CRM_{197} by HPLC-SEC (TSK gel 6000PW + TSK gel 5000PW, see chapter 1 for method description). Free protein was estimated by HPLC-SEC (TSK gel 6000PW + TSK gel 5000PW, see chapter 1 for method description), while a method for free saccharide determination is under development.
Derivatized OAg intermediates were all characterized by phenol sulfuric assay for sugar content and by HPLC-SEC for verifying aggregation or degradation after modification (TSK gel 3000PWXL, see chapter 1 for method description).

After the reaction with cystamine, the introduction of NH_2 groups was verified by TNBS colorimetric method (*201*) using 6-aminohexanoic acid as standard and subtracting the number of NH_2 groups already present on the un-derivatized OAg sample (Figure 4.2, Chapter 2). Percentage of OAg chains activated was calculated as moles of linked cystamine/moles of KDO (calculated by HPLC-SEC/semicarbazide assay (*86*)) %. After the reduction with DTT, introduction of SH groups was verified by Ellman analysis (*230*). Activation on the terminus KDO was calculated as moles of linked SH/moles of KDO %, while the ratio % between SH groups/ cystamine moles gave the efficiency of reduction reaction with DTT.

Synthesis of OAg-propargylamine-CRM_{197}

2192 OAg (40 mg) was solubilized in NaH_2PO_4 pH 7.0 (40 mg/mL); then propargylamine (27.5 mg/mL, propargylamine/OAg (w/w) = 0.67) and $NaBH_3CN$ (62.8 mg/mL, $NaBH_3CN$/OAg (w/w) = 1.53) were added. The reaction was stirred for 3h at RT and purified by desalting on a G25 53 mL column against water.
Conjugation was performed solubilizing CRM_{197}-N_3 (5 mg/mL, average of 5.2 Lysines activated) in NaH_2PO_4 400 mM pH 7.2 with THPTA 25 mM, sodium ascorbate 10 mM and $CuSO_4 \cdot 5H_2O$ 5mM, followed by OAg-propargylamine addition (molar ratio alkyne/N_3 = 5). Reaction was stirred at RT for 6h and conjugate formation followed by HPLC-SEC (TSK gel 6000PW + TSK gel 5000PW).

Synthesis of OAg-ADH-BCNesterI-CRM_{197}

2192 OAg (40 mg) was solubilized in AcONa 100 mM pH 4.5 (40 mg/mL), then ADH (48 mg/mL, ADH/OAg (w/w) = 1.2) and $NaBH_3CN$ (48 mg/mL, $NaBH_3CN$ /OAg (w/w) = 1.2) were added. The mixture was stirred for 2h at 30 °C and then purified by desalting on a G25 53 mL column against water.
For introduction of the second linker, Click easy BCN NHS ester I, OAg-ADH was dissolved in water/DMSO 1:9 (v/v) at a concentration of 50 mg/mL. When the derivatized OAg was completely solubilized, TEA was added (molar ratio TEA/total NH_2 groups = 5; total NH_2 groups included both phosphoethanolamine groups on the OAg and the hydrazide groups introduced with the linker ADH) and then Click easy BCN NHS ester I (molar ratio Click easy BCN NHS ester I/total NH_2 groups = 12). The solution was mixed at RT for 3h. The sample was purified by desalting on a G25 53 mL column against water.
For conjugation, CRM_{197}-N_3 was solubilized in PBS at a concentration of 10 mg/mL and OAg-ADH-BCNesterI added (molar ratio alkyne/N_3 = 4). Mixture was stirred for 6h at RT.
Conjugate purification was performed by hydrophobic interaction chromatography on a Phenyl HP column [GE Healthcare], loading 500 µg of protein for mL of resin in 50 mM NaH_2PO_4 3M NaCl pH 7.2. The purified conjugate was eluted in water and the collected fractions were dialysed against 10 mM NaH_2PO_4 pH 7.2.

Characterization of OAg-CRM_{197} conjugates via click chemistry

Total saccharide content was quantified by phenol sulfuric assay (*195*), protein content by micro BCA and the ratio of saccharide to protein calculated. OAg-CRM_{197} conjugates profiles were compared with free CRM_{197} by HPLC-SEC (TSK gel 6000PW + TSK gel 5000PW). Free protein was estimated by HPLC-SEC (TSK gel 6000PW + TSK gel 5000PW), while a method for free saccharide determination is under development.

Derivatized OAg intermediates were all characterized by phenol sulfuric assay for sugar content and by HPLC-SEC (TSK gel 3000PWXL) for verifying aggregation or degradation after modification.
After the reaction with ADH, the introduction of NH_2 groups was verified by TNBS colorimetric method (*201*) using ADH as standard and subtracting the number of NH_2 groups already present on the un-derivatized OAg sample. Free ADH was detected by RP-HPLC (*180*). Activation on the terminus KDO was calculated as moles of linked ADH/moles of KDO %, indicating the % of OAg chain activated. Total alkyne groups introduced with BCN ester I were quantified by TNBS considering the number of NH_2 groups remained after the derivatization. Percentage of derivatization with BCN ester I was calculated as molar ratio % of linked alkyne groups/total NH_2 groups by TNBS before derivatization, indicating the moles % of NH_2 groups activated with this reaction. Activation with propargylamine was not quantified as a method for alkyne quantification was not available. Derivatized OAg was directly used for glycoconjugation.

Recycle of unreacted OAg-ADH-BCNesterI and its further click glycoconjugation

After purification of the conjugate OAg-ADH-BCNesterI-CRM-N_3(LYS10) by HIC chromatography; unreacted OAg was recovered in the flow through fractions. They were desalted against water (G25 53 mL column) and re-conjugated to CRM_{197} using same conditions adopted in the first test of conjugation ([CRM_{197}-N_3(LYS10)] = 10 mg/mL in NaH_2PO_4 100 mM pH 7.2, alkyne:N_3 molar ratio = 4:1, 6h, RT). Conjugate formation was verified by HPLC-SEC (TSK gel 6000PW + TSK gel 5000PW).

Identification of conditions for conjugation on solid-phase

A physical mixture of 2192 OAg and CRM_{197} was run on a HiTrap 1mL Q FF [GE Healthcare], loading 500 µg of protein and 2 mg of sugar per mL of resin in 100 mM NaH_2PO_4 at respectively pH 7.0 or pH 8.0 buffer and increasing the NaCl concentration from 0 to 1 M in linear gradient. (20 column volumes). Different fractions were analyzed by HPLC-SEC (TSK gel 6000PW + TSK gel 5000PW), in comparison with free OAg and free CRM_{197}.

Click Conjugation on solid phase

The resin (Q Sepharose Fast Flow column [GE Healthcare]) was centrifuged to remove the storage solution (10000 rpm, 4 °C, 5 min), and washed two times with NaH_2PO_4 100 mM pH 8 (volume for washing equal to twice the volume of the resin). CRM_{197}-N_3(LYS7) (0.25 mg per mL of resin) was added at 0.5 mg/mL in NaH_2PO_4 100 mM pH 8. The mixture was gently stirred ON at 4°C. The supernatant was removed and the resin washed two times with NaH_2PO_4 100 mM pH 8.0 (washing volume equal to 2.5 times the volume of the resin). Supernatant and washing solutions were analyzed by micro BCA to estimate the amount of protein present in solution and by difference the amount of protein attached to the resin.
5 mg of 2192-ADH-BCNalkyne were solubilized in NaH_2PO_4 100 mM pH 8.0 and added to the resin (final OAg concentration of 50 mg/mL). The mixture was gently stirred ON at 4°C. The supernatant was recovered by centrifugation (10000 rpm, 4°C, 5 min), and the resin washed 5 times with 1 mL PBS to recover unreacted sugar . All the solutions were analyzed by HPLC-SEC (TSK gel 6000PW + TSK gel 5000PW). The conjugate was then eluted from the resin washing twice with 500 µL NaH_2PO_4

100 mM NaCl 1M pH 8.0 and recovered supernatant solutions pooled together and analyzed by HPLC-SEC (TSK gel 6000PW + TSK gel 5000PW).
Unreacted sugar recovered was used for a further conjugation test, adding the first supernatant recovered to fresh protein bound on the resin.

5.4 Results

Thiol conjugation chemistry

Thiol-conjugation chemistry was first tested as a possible conjugation approach. The KDO sugar was used for introducing cystamine as linker on one specific point of the OAg without modifying the OAg sugar chain and then the DDT-reduced form was used for binding the OAg to the carrier protein (Figure 5.1).
OAg derivatization with SH functionality was characterized by good reproducibility both in terms of sugar recovery and percentage of activation. In all the preparations, sugar recovery was >75% for both the first activation step and the reduction with DTT. After the activation with cystamine, TNBS analysis indicated that 70-80% of OAg chains were activated. After DDT reduction, the activation degree was also confirmed by the analysis of SH groups introduced. The reduction was always complete.

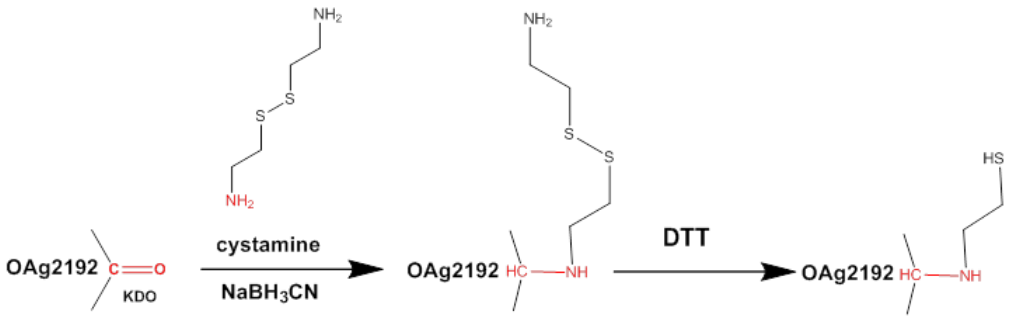

Figure 5.1 Introduction of thiol group on the reducing end of the sugar.

CRM_{197} was derivatized using different hetero bi-functional linkers, with a functional group able to react with the thiol unit on the OAg. Different amino acids were activated (Figure 5.2) with different protein loading (Figure 5.3). In all cases, protein recovery was >90%.Reaction of CRM_{197} with BMPH by EDAC chemistry resulted in the introduction of an average number of 3.4 linkers per protein. When NHS was added to EDAC for activating the COOH groups on the protein, trying to increase the activation degree, an average of 5.1 linkers was introduced. A higher number of linkers was introduced per mole of protein when derivatization was performed on Lysine residues: with an average number of 8 SBAP and 11.3 EMCS. (Figure 5.3)
Thiolated OAg was then conjugated to derivatized CRM_{197} where different amino acids were activated with different linker loading. Together with the modified proteins synthesized at NVGH, the conjugation was tested with CRM_{197} modified on tyrosines and lysines with low linker loading, 4.1 on tyrosine and 3.1 on lysines respectively (Figure 5.3), provided by Global Discovery chemistry (GDC) group in Boston.

Using this conjugation chemistry, it was not possible to obtain conjugate formation unless the linker loading on the protein was pretty high (at least an average of 8 linkers introduced per protein molecule).
The two conjugation reactions that succeeded, both based on lysine chemistry, indicated that a higher number of linkers per CRM_{197} resulted in a higher OAg to CRM_{197} ratio in the purified corresponding conjugate. However, the linkers used for the synthesis of these conjugates were different and an impact of the type of linker on conjugate formation cannot be excluded. In both cases all the protein was conjugated with residual un-reacted sugar chains. Even if the number of linkers per CRM_{197} was high (8 and 11.3) corresponding conjugates were characterized by a low OAg to protein molar ratio (1.6 and 2.7 respectively).

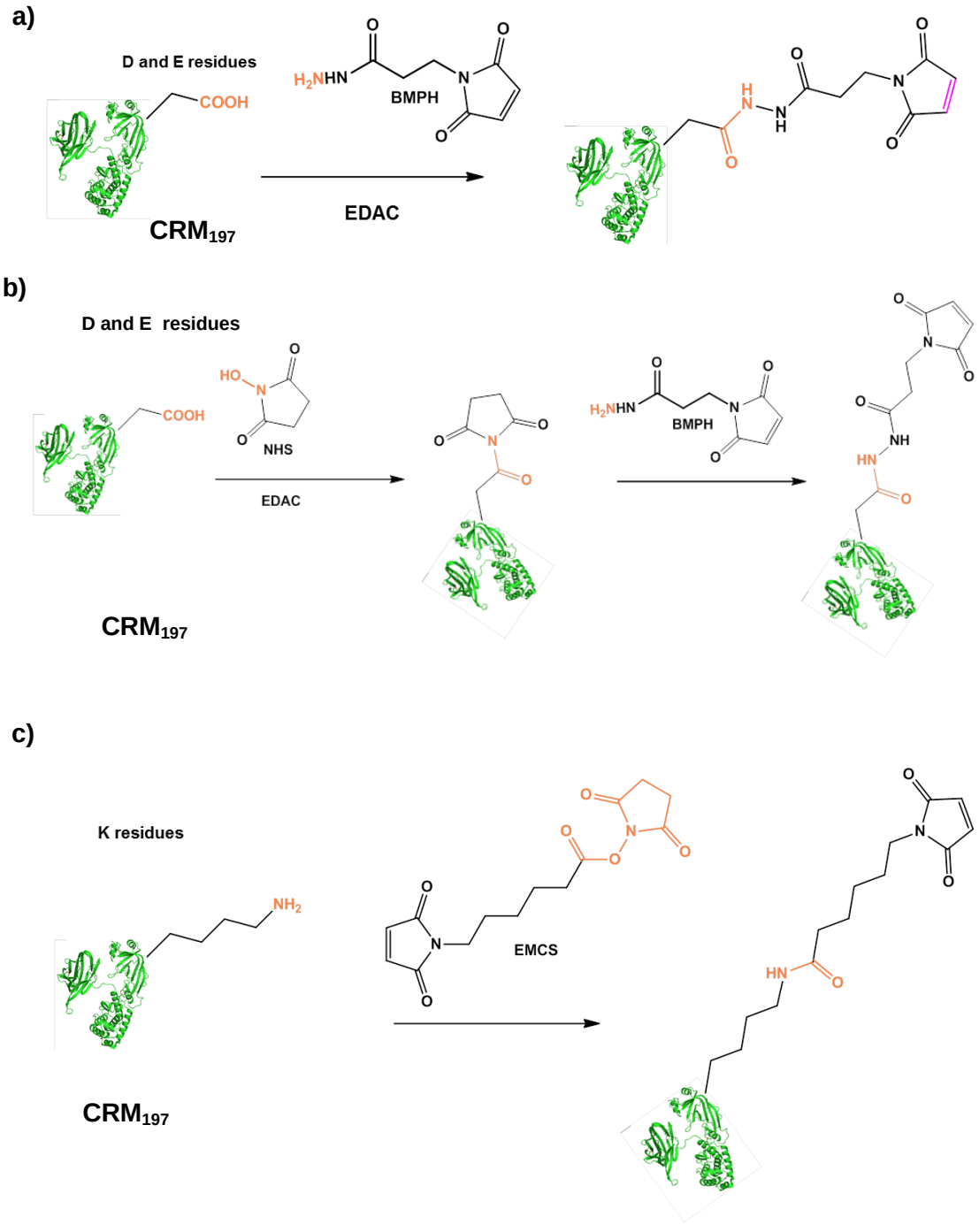

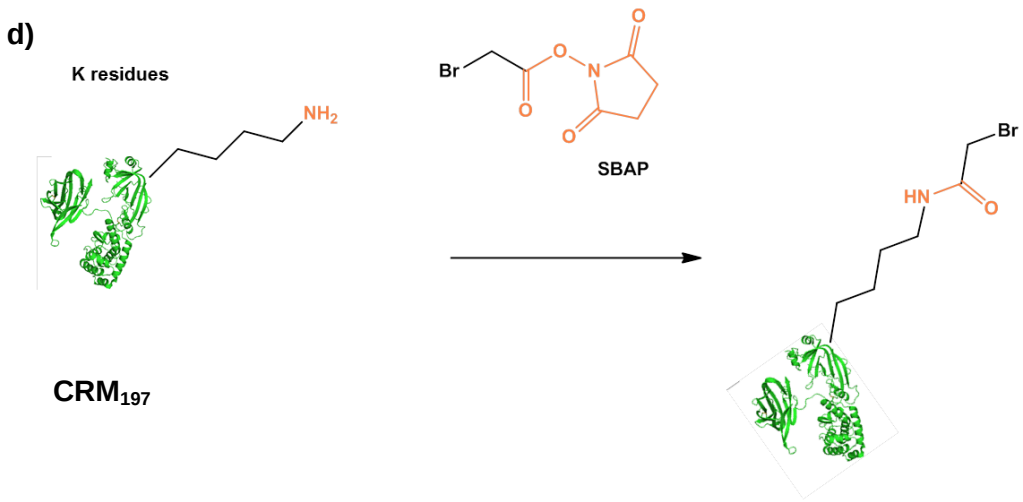

Figure 5.2 CRM_{197} was derivatized using different hetero bi-functional linkers able to react with thiol-activated OAg. **a)** CRM_{197}-COOH activation via EDAC with BMPH. **b)** CRM_{197}-COOH activation via EDAC/NHS with BMPH. **c)** CRM_{197}-NH_2 activation with EMCS. **d)** CRM_{197}-NH_2 activation with SBAP.

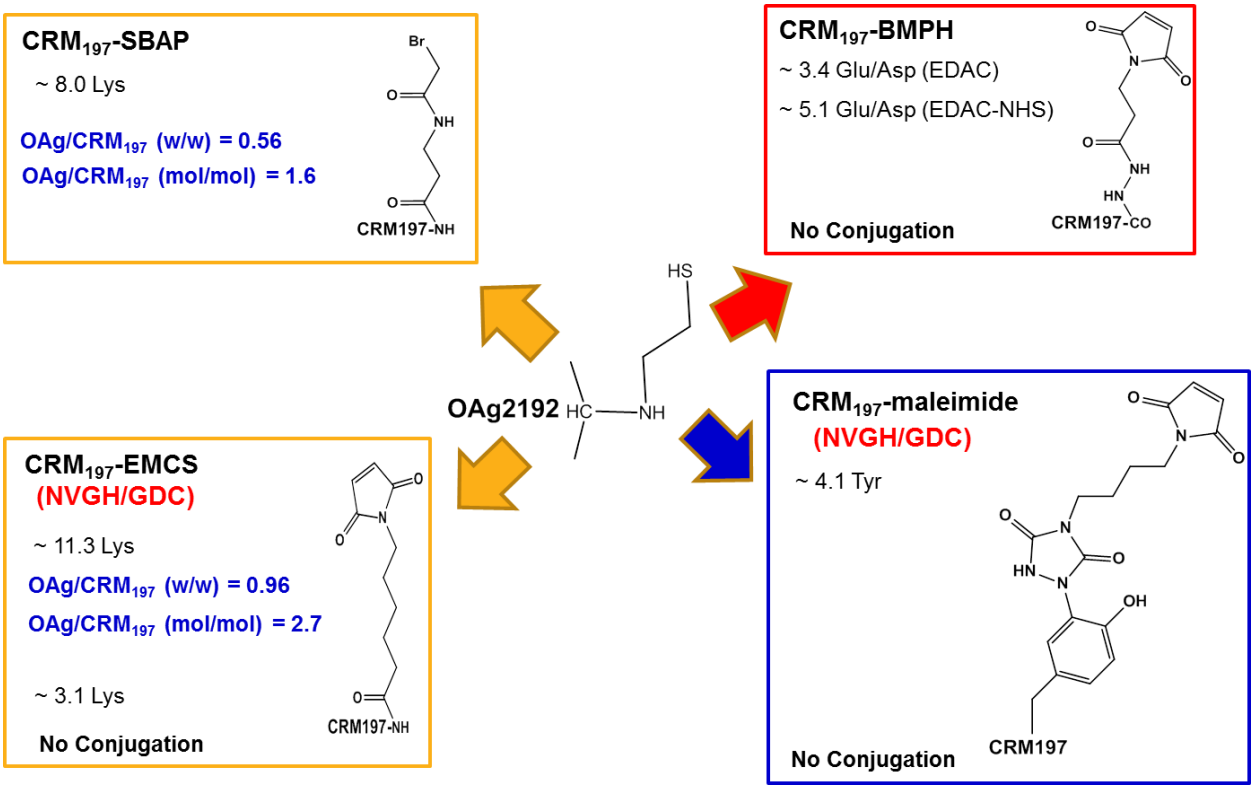

Figure 5.3 Thiol-conjugation chemistry for the synthesis of glycoconjugates targeting different amino acids on the protein.

Looking at the HPLC-SEC profiles (dRI) of the conjugation mixtures, even when conjugation was successful, the presence of a sugar population at higher MW was observed, probably deriving from oxidation of the thiolated OAg to generate a sugar dimer. Different methods were tried in order to avoid the generation of the oxidation product and hence of a unreactive OAg form, trying to see if this could then result in higher conjugation efficiency too. Conjugation of DTT-treated OAg-cystamine with

CMR_{197}-BMPH under N_2 caused precipitation of the protein; one-pot-two-step OAg-cystamine reduction with TCEP as reducing agent and conjugation to CRM_{197}-BMPH (5.2 linkers) did not work. When DTT-treated cystamine was conjugated with CRM_{197}-BMPH in the presence of TCEP, the formation of the disulfide aggregate was avoided, but the major part of the protein remained unconjugated.
In summary thiol conjugation strategies did not allow to get all the panel of wanted conjugates and it became needed to identify a different conjugation approach.

Click chemistry

There are two main ways of performing the click 1,3-dipolar reaction: by employing metal as a catalyst (usually copper), or alternatively lowering the activation barrier for [3+2] cycloaddition by employing intrinsically highly strained cyclic alkynes that readily react with azide groups. Both the approaches were initially compared for the reaction of 2192 OAg with CRM-N_3 (Figure 5.4). CRM_{197} was derivatized on lysine amino acids using NHS-PEG4-N_3 (Figure 5.5). Different loadings were obtained, in the range of 5-10 linker introduced per protein, depending on the amount of linker added. In all cases, protein recovery was >90%.

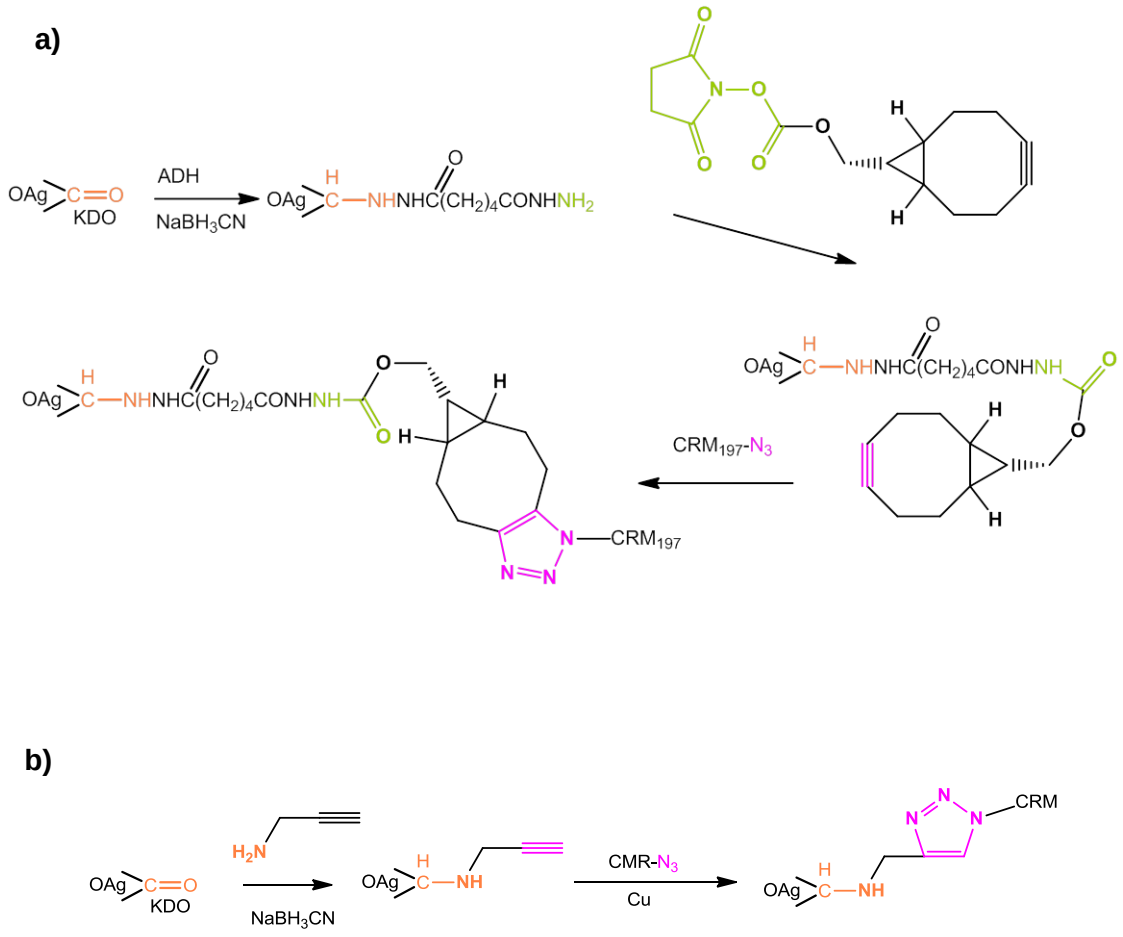

Figure 5.4 Two glycoconjugation strategies differing for the chemistry involved and the spacer length. a) Copper-free click reaction. b) Copper-catalyzed click reaction, using a shorter spacer.

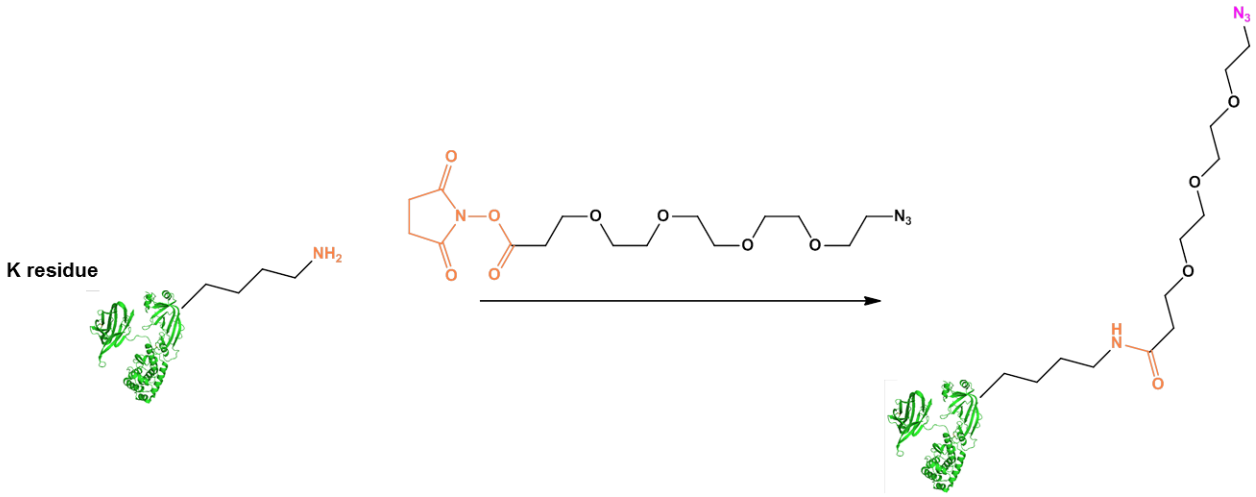

Figure 5.5 Modification of CRM_{197} with NHS-PEG4-N_3 to introduce azido groups on CRM_{197} and generate CRM_{197}-N_3.

For the copper click chemistry, the OAg was derivatized with propargylamine by reductive amination on the terminal KDO (Figure 5.4b). For the copper-free approach instead, the alkyne linker was introduced on the OAg-ADH, with activation >80% (Figure 5.4a).
CRM_{197} with an average number of 5.2 linkers introduced (CRM_{197}-N_3(LYS5.2)) was used at 5 mg/mL for comparing these two approaches. Despite a lower sugar to protein ratio, the copper free conjugation resulted more efficient (Table 5.1). Reaction time did not seem to have a strong impact on conjugate formation.

Table 5.1 Reaction conditions used for the comparison of the copper free and copper-catalyzed glycoconjugation reactions.

Copper	Alkyne:N_3 ratio (mol/mol)	Reaction time (h)	Conjugate (%)	Free CRM_{197} (%)
Yes	5	2	28	72
		4	36	64
		6	40	60
No	1	2	69	31
		4	75	25
		6	78	22

Conjugate and free CRM_{197}% calculated by comparing corresponding peak areas in HPLC-SEC fluorescence emission profiles on a TSK gel 6000-5000 PW column. Both reactions performed with [CRM_{197}-N_3(LYS5.2)] of 5 mg/mL at RT.

Because of the higher conjugation efficiency and to avoid the use of a toxic metal, the copper-free approach was selected for further experiments.
Maintaining protein concentration at 5 mg/mL and increasing the alkyne to N_3 molar ratio from 1 to 2, conjugation efficiency remained the same after 6h of reaction, with 78% of CRM_{197} conjugated according to the area of the peaks by HPLC-SEC (Table 5.2). Increasing protein concentration from 5 to 10 mg/mL and the alkyne to N_3 molar ratio from 2 to 4, conjugation was substantially complete. When a protein with a higher average number of linkers was used (from 5.2 to 10), no free CRM_{197} was detected in the conjugation mixture (Table 5.2 and Figure 5.6).

Table 5.2 Reaction conditions optimized for the copper free conjugation.

N_3 per CRM_{197}	**[CRM_{197}] (mg/mL)**	**Alkyne:N_3 (mol/mol)**	**Conjugate (%)**	**Free CRM_{197} (%)**
5.2	5	1:1	78	22
5.2	5	2:1	78	22
5.2	10	4:1	90	10
10	10	4:1	100	nd

Conjugate and free CRM_{197} % calculated by comparing corresponding peak areas in HPLC-SEC fluorescence emission profiles on a TSKgel 6000-5000 PW column. All the reactions performed at RT for 6h. nd: not detected.

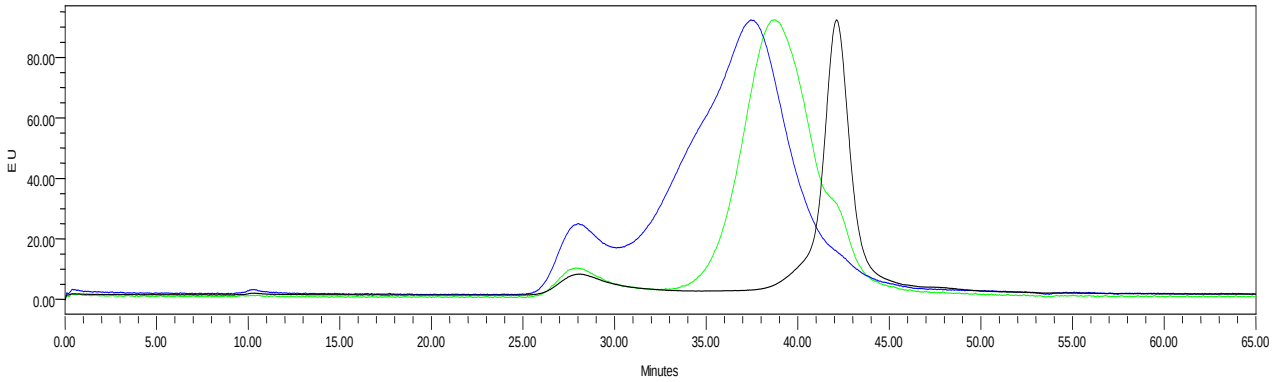

Figure 5.6 HPLC-SEC profiles of *OAg-ADH-BCNesterI-CRM_{197}* conjugation mixtures after 6h at RT, using CRM_{197}-N_3(LYS5.2) (green) or CRM_{197}-N_3(LYS10) (blue) at 10 mg/mL and with a alkyne to N_3 molar ratio of 4 in comparison to free CRM_{197} (black). TSKgel 6000 PW + 5000 PW columns, 0.5 mL/min, 100 mM NaCl 100 mM NaH_2PO_4 5% CH_3CN pH 7.2; Vtot 48.829 min; V0 24.125 min.

Optimal conditions identified by this work of screening via HPLC-SEC (protein concentration of 10 mg/mL with alkyne to azide molar ratio of 4) were used for the synthesis and purification of a conjugate.
CRM-N_3 with an average number of 7.1 linkers was used; all CRM_{197} resulted conjugated and residual free OAg was removed by purification through HIC. Table 5.3 showed the main features of the resulting conjugate.

Table 5.3 Main characteristics of OAg-CRM_{197} conjugate generated by using click chemistry.

Conjugate	OAg/CRM_{197} (w/w)	OAg/CRM_{197} (mol/mol)
OAg-ADH-BCNesterI-CRM_{197}(LYS7.1)	0.72	2.0

Similarly to what obtained by thiol chemistry activating lysine groups on CRM_{197}, also in this case the obtained conjugate was characterized by a low OAg to protein molar ratio (2.0), even if the protein was activated with an average of 7 linkers.

Conjugation of CRM_{197} with low linker loading to 2192 OAg by click chemistry

Conjugation conditions selected were tested for the conjugation of CRM_{197}-N_3 with lower average number of linkers per protein. CRM_{197}-N_3(TYR4.3) and CRM_{197}-N_3(LYS3.8) were successfully conjugated to OAg-ADH-BCNesterI obtaining respectively 91% and 81% conjugation yields (as quantified by comparing the area of conjugate and free protein peaks by HPLC-SEC). Furthermore, performing the conjugation with a protein with only one linker CRM_{197}-N_3(LYS1), 38% of CRM_{197} resulted conjugated after 6h (Table 4.4). Either in this case or when the activation loading on the protein was higher (Table 5.1, no copper reactions), the reaction proceeded fast, since no huge differences were seen after 2, 4 or 6h.

Table 5.4 Reaction conditions tested for the copper free conjugation with CRM_{197}-N_3(LYS1),.

Reaction time (h)	Conjugate (%)	Free CRM_{197} (%)
2	34	66
4	35	65
6	38	62

Conjugate and free CRM_{197} % calculated by comparing corresponding peak areas in HPLC-SEC fluorescence emission profiles on a TSKgel 6000-5000 PW column. Reaction performed over time at RT, with protein concentration of 10 mg/mL and alkyne to N_3 molar ratio of 4.

Click conjugation: recycle of the sugar

One of the advantages of the click chemistry is that the functional groups involved are not de-activated during the conjugation. This opens the possibility to recycle unreacted reagents. After purification of OAg-ADH-BCNesterI conjugate by HIC, unreacted OAg was recovered in the flow through, not containing traces of proteins, as verified by HPLC-SEC analysis. Flow through fractions were desalted against water (G25 53 mL column) and re-conjugated to CRM_{197}-N_3(LYS10) using same conjugation conditions adopted for the synthesis of the first batch (10 mg/mL protein concentration, alkyne to N_3 molar ratio of 4, RT, 6h). Conjugate formation was verified by HPLC-SEC and also in this case no traces of free protein in the reaction mixture were detected (Figure 5.7)

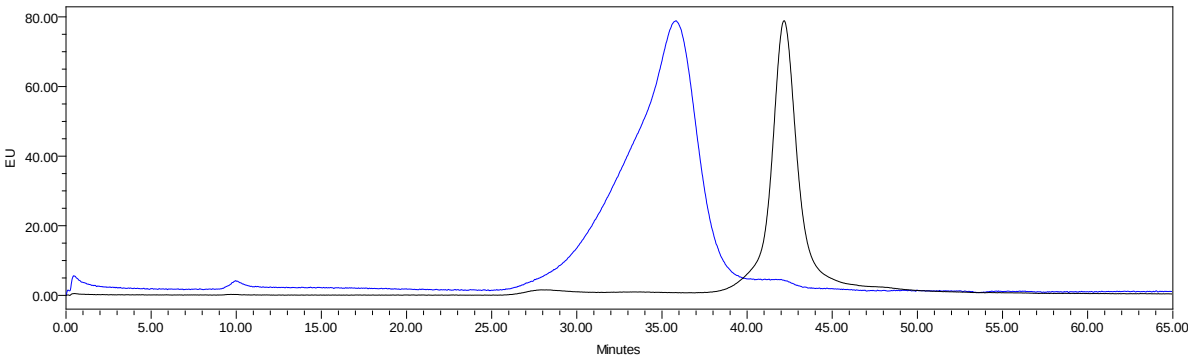

Figure 5.7 HPLC-SEC profile of the conjugation mixture obtained by reacting recycled OAg-ADH-BCNesterI with CRM-N_3(LYS10) (blue), in comparison with free protein (black). TSKgel 6000 PW + 5000 PW columns, 0.5 mL/min, 100 mM NaCl 100 mM NaH_2PO_4 5% CH_3CN pH 7.2; Vtot 48.829 min; V0 24.125 min.

Click conjugation on solid phase

The possibility to perform click conjugation on solid phase was investigated. As a first step, the best conditions for attaching the protein on the resin avoiding the linking of the sugar were identified, running a physical mixture of CRM_{197} and 2192 OAg on a Q Sepharose Fast Flow column. It was speculated that the behavior on the resin of 2912 OAg - CRM_{197} - and OAg-ADH-BCNesterI - CRM_{197}-N_3 was similar, since their structural modification is modest considering the interaction with this kind of resin. CRM_{197} resulted attached to the resin in 100 mM NaH_2PO_4 pH 8.0, while in these conditions 2192 OAg was recovered in the flow through. Increasing NaCl concentration, protein elution started at 100 mM salt concentration.
Conjugation on solid phase was performed in batch, using a Fast Flow Q resin. After incubating CRM_{197}-N_3(LYS7) on the resin ON at 4°C, analysis of the supernatant by micro BCA revealed 50% of protein bound. OAg-ADH-BCNesterI was then added (molar ratio alkyne/N_3 = 25) at a concentration of 50 mg/mL in 100 mM NaH_2PO_4 pH 8.0.
After ON at 4°C, analysis of the supernatant and washing PBS solutions by HPLC-SEC showed the presence of only unreacted OAg. The conjugate was eluted in 100 mM NaH_2PO_4 1M NaCl pH 8.0 and analysis by HPLC-SEC revealed that conjugation reaction was quantitative, with no free protein. No free OAg seemed to be present too (dRI detection by HPLC-SEC), however a more sensitive and accurate method will be used when a batch of conjugate produced by solid phase will be fully

characterized and tested in mice. In case the number of washing will be not enough to purify the conjugate, further steps will be added to the current procedure.
Interestingly, unreacted OAg recovered from the first supernatant was recycled for solid-phase conjugation with fresh resin-bounded CRM_{197}-N_3(LYS7). Although the sugar added in this experiment was lower (considering that part reacted in the first conjugation experiment), conjugation was again quantitative with no free CRM_{197} detected by HPLC-SEC in the eluted conjugate.

5.5 Discussion

The term click chemistry describes a set of reactions tailored to obtain high degree of selectivity and specificity, simple work-up, the possibility of carrying out experiments in eco-friendly conditions (such as at room temperature and in water) and with good yields (*224*). These are indeed important parameters to be considered in a strategy for the synthesis of functionalized compounds, in order to reduce the cost-effectiveness and to minimize the use and generation of hazardous substances. The emerging importance of click chemistry in many areas of science, such as bioconjugation, drug discovery material science and radiochemistry, underlies the unique specificities of this class of reactions (*231*) (*232*) (*233*) (*234*) (*235*). Recently, the click chemistry has been identified as a powerful method for the synthesis of glycoconjugates where few points of attachment are targeted on the protein too (*236*) (*127*). In this study this has been confirmed for the linkage of a longer sugar chain such as 2192 OAg (20.5 kDa) selectively activated on the terminal KDO unit to CRM_{197}. Copper-free chemistry was preferred because it gave better conjugation yields in preliminary tests and avoids the use of a toxic metal. Differently from the thiol chemistry tested, the click chemistry allowed the linkage of the terminal sugar end of the OAg chain to the protein with good conjugation yields (>80%) even when few linkers were present on the protein (average number of 4) and to have conjugate formation with just one linker on the protein (38% of CRM_{197} resulted conjugated). This finding opens the possibility of synthesizing a panel of well-defined OAg-CRM_{197} conjugates, targeting different amino acids on the protein. The insert of a different linker loading on the protein could also drive the number sugar of units attached per protein, with potential impact on the immunogenicity of the glycoconjugate. This is indeed an important goal not only for glycoconjugates development (consistency of production, better characterization and rational design of optimal candidate vaccines), but also to gain a better understanding about the complex mechanism of conjugate vaccines in vivo.
In order to further exploit the potentiality of the click chemistry, unreacted OAg, having alkyne groups not de-activated during conjugation, was successfully recycled for conjugation. In addition, the possibility to perform conjugation in solid phase was verified. Solid-phase bioconjugation has been previously reported for the synthesis of peptides directly on carrier proteins (*237*), conjugation to carrier proteins pre-adsorbed to aluminum hydroxide (*238*), and by ion exchange matrix adsorbed carrier proteins (*239*). Here, CRM_{197} was adsorbed to an anion exchange matrix using a batch procedure, and the immobilized protein was then conjugated to the OAg. Unreacted OAg was easily recovered and used for further conjugation, while the conjugate was eluted from the resin pure from both free protein and free sugar. The absence of free protein in the eluted conjugate confirmed the efficiency of this conjugation strategy. In this way, the purification of the conjugate is reduced to a simple washing/elution procedure, where unreacted sugar is removed from the resin-

bound conjugate, and the matrix-bound conjugate can be then simply eluted and use for immunization.

When the conjugates are intended for use as vaccines, removal of unconjugated saccharide is particularly important to obtain consistent products without affecting the immune response too. Several methods are in use for the separation of free saccharide from conjugate vaccines. These methods often involve complex steps, and some of them may result in the selection of sub-populations of conjugates. This may result in low recoveries and reduction of immunogenicity of the purified conjugate preparations. There is thus a need for further and improved processes for purifying saccharide-protein conjugates, and particularly for processes that would be simple, requiring the minimum number of steps between conjugation and purification, resulting in minimal selection of sub-populations of conjugates retaining effective immunogenicity. The possibility of recycling the unreacted sugar for further conjugation adds cost-effectiveness to the entire process.

To sum up, a conjugation methodology that allows the synthesis of highly defined OAg glycoconjugate vaccines with good yields was developed. The process has great advantages in terms of cost for vaccine production, allowing unreacted sugar recovery and making easy the purification of the conjugate.

6. Discussion

Vaccination has had an unparalleled impact on global health (*240*) and vaccines have the greatest potential for further improvement in health in the poorest countries of the world (*50*). Infectious diseases account for around half of all deaths in these countries with around 90% of this mortality being attributed to diarrheal and respiratory diseases, AIDS, tuberculosis, malaria and measles (*2*).

Glycoconjugate vaccines are among the safest and more efficacious vaccines developed during the last 30 years against infectious diseases. They have been developed to improve the immunogenicity of polysaccharide vaccines which are T-cell independent, poorly immunogenic in infants and young children < 2 years of age (*241*) (*242*) and do not induce immunological memory (*243*). It is likely that glycoconjugates will replace all polysaccharide vaccines in the next future (*179*). There is no other example where the introduction of a new approach to vaccine development has had such a rapid and positive effect in preventing infections by a series of human pathogens (*244*) and this accomplishment has triggered studies on new possible applications such as therapeutic vaccines for cancer and Alzheimer and conjugate vaccines for drug abuse, which are currently under development (*245*) (*246*) (*247*).

In addition to effectiveness and safety profile, there are other features of glycoconjugate vaccines that contribute to their success. The lack of interference with other routine vaccination together with the ability to induce herd protection by reducing nasopharyngeal carriage are also important parameters that contribute to improving the final cost-benefit ratio.

Following the use of *Haemophilus influenzae* type b (Hib), *Meningococcus* group C (MenC) and pneumococcal glycoconjugate vaccines in national immunization programmes, drastic reductions in serious infections in target risk groups, especially infants, children and adolescents, have been observed (*179*). Following the licensure of MenACWY and PCV13-CRM_{197} conjugates, robust protection has been observed in adults and elderly (*248*) (*249*) (*250*). The Hib-MenCY-TT vaccine, which has been licensed by the FDA in June 2012, now offers broader protection against MenY disease from as early as 6 weeks of life (*251*).

As yet there is still the need for more investment in glycoconjugate vaccines which protect against neglected enteric diseases, such as typhoid fever, shigellosis and infection with enterotoxigenic *E. coli* and nontyphoidal *Salmonella*, which pose a significant threat to millions of children, especially in the developing world. Tiered pricing and subsidization of vaccines by public-private partnerships and non-profit organizations would be crucial in addressing persisting inequities in vaccine availability between industrialized and developing countries (*179*). Continued surveillance following introduction of glycoconjugates in national immunization programs is also crucial to detect changes in the epidemiology of infectious diseases and in guiding appropriate interventions, since it is reported that conjugate vaccines may exert an increased selection pressure favoring a capsular switch. In the future, multivalent vaccine approaches targeting different well conserved antigens will be probably necessary to counteract further serotype replacement. Genome mining and reverse vaccinology are alternative technologies that have been successfully exploited to design a promising recombinant protein based vaccine (*252*). If their affordability as protein carrier will be confirmed, glycoconjugates that use homologous pathogen protective antigens (e.g., flagellins, porins for *Salmonella*) as carrier proteins can enhance protection by concomitantly eliciting immune responses

to a second relevant antigen, thereby providing greater protective efficacy than conjugates constructed with heterologous carrier proteins (e.g., tetanus toxoid, CRM_{197}) (*84*).
Currently two vaccines are widely licensed targeting *S.* Typhi: the live attenuated vaccine, Ty21a, and the Vi capsular PS vaccine, but neither is licensed for use in children under the age of two years. New vaccines, such as glycoconjugates, new generation live attenuated and protein based vaccines (Martin, 2012; McGregor et al., 2013; Szu, 2013), are currently under development against enteric disease, including *S.* Paratyphi A for which no vaccine is currently available (*55*), and hold promise for the future availability of these vaccines for use in endemic areas. Whereas licensed vaccines are available to prevent typhoid fever, no vaccines are available against NTS serovars.
NTS, with the most common serovars being Typhimurium and Enteritidis, typically cause gastroenteritis in healthy children and adults in industrialized countries but in certain hosts (e.g., young infants, the elderly, immunocompromised individuals) they also cause invasive infections. The situation is much more complicated in many regions of sub-Saharan Africa, where they are important cause of invasive bacterial disease, especially among children with less than three years of age (*71*) (*72*) (*73*) (*74*) (*75*) and HIV infected individuals (*65*) (*76*). Prior to the introduction of programmatic immunization with Hib or *Streptococcus pneumoniae* conjugate vaccines in countries of sub-Saharan Africa, invasive NTS disease was as common as invasive Hib or pneumococcal disease (*66*) (*253*) (*254*) (*255*) (*256*) (*257*).
Despite being a significant global health problem, NTS is surprisingly an underestimated disease. This is probably related with the very diverse clinical presentation of this illness which makes diagnosis and treatment a challenge for health-care workers in low-resource setting (*36*) (*77*). In addition, blood culture and microbiological diagnosis of *Salmonella* require technical expertise and investment in infrastructure, consumables, and quality control, all of which must be strengthened (*78*). In a recent study around 90% of invasive NTS isolates in Malawi have been found to be multidrug resistant (*63*), emphasizing the need for development of alternative interventions.
The OAg of LPS is the main surface polysaccharide for NTS species. OAg are poor immunogens in animal models and do not generate immunologic memory (*100*) (*84*) (*98*). Conjugation of *Salmonella* OAg to appropriate carrier proteins results in vaccines that have been effective in generating anti-OAg antibodies in animal models protecting against mortality in the mouse model of lethal *Salmonella* (*101*) (*102*) (*103*) (*98*) (*84*).
Glycoconjugate vaccines in development against NTS are at preclinical stage. However, Phase 1 and 2 clinical trials of another *Salmonella* OAg-based glycoconjugate vaccine, *S*. Paratyphi A linked to TT as carrier protein, was shown to be safe and immunogenic in Vietnamese adults and children (*100*) (*208*), demonstrating the goodness of this approach.
However there are some issues regarding the use of OAg-based conjugate vaccines to prevent invasive NTS diseases, related to the activity and ability of OAg antibodies to confer protection in humans, and whether antibodies to an OAg-based vaccine made with purified OAg from one serovar cross-protect against other serovars within the same O serogroup (*258*).
Although *Salmonella* are intracellular pathogens, they are vulnerable while extracellular when IgG and IgM directed against the surface polysaccharides of *Salmonella* can bind them leading to bacteriolysis or opsonophagocytosis. The

importance of serum immunity is highlighted by the increased virulence seen for *Salmonella* that can evade the alternative pathway of complement through alteration in the length and structure of their OAg and expression of the resistance to complement killing (*rck*) gene (*259*) (*260*) (*261*) (*262*). Antibodies to *Salmonella* surface carbohydrates mediate opsonophagocytosis through Fc receptors on phagocytes that can kill by oxidative burst (*95*). Activation of the antibody mediated complement pathway by IgM and IgG can also kill directly via formation of the C9 membrane attack complex; surface deposition of C3b also enhances opsonophagocytosis (*71*) (*263*).

Antibody to *S.* Typhimurium LPS from HIV positive individuals in Africa was shown to interfere with complement mediated bactericidal killing of a serum sensitive prototype African *S.* Typhimurium strain (*83*). Anti LPS IgG however does not interfere with opsonophagocytosis and oxidative burst in human neutrophils with either complement resistant or sensitive *S.* Typhimurium strains (*95*). NTS isolates from the blood also frequently display marked resistance to complement mediated bactericidal killing (*264*). Further work is needed to better define the role of anti-OAg in serum bactericidal and opsonophagocytic killing in immunity to invasive NTS infection in humans. While glycoconjugates are set to make a major impact, the possibility of serovar replacement and the challenge of invasive NTS disease among HIV-infected Africans, where lack of antibodies to *Salmonella* is not the issue, support the development of new generation vaccines. These include new live-attenuated, protein-based and GMMA-based vaccines, which could potentially induce broader protection together with *Salmonella*-specific T cell responses.

Several variables can affect the immunogenicity of a glycoconjugate vaccine. Parameters like saccharide chain length, saccharide to protein ratio in the purified conjugate, conjugation chemistry, the nature of the linkers used for saccharide and/or protein derivatization and of the protein carrier confer to the glycoconjugate different physico-chemical characteristics that may result in different immunological properties. A rational understanding of the effects of these different parameters could lead to improved rational design of glycoconjugate vaccines, with consequent enhanced vaccine efficacy and long term protection. However, this is not trivial for different reasons. First, the immune response is highly antigen dependent, and so contrasting findings can be obtained working with different sugar haptens. In addition, studies performed so far have compared the immunogenicity of vaccines differing for multiple parameters at the same time, making therefore difficult to assign the relative importance of the single variable to the immunogenicity. Moreover, parameters like saccharide chain length, saccharide to protein ratio and conjugation chemistry are strongly interconnected complicating the look for a clear correlation. Because of this complexity, the relative importance of each variable should be investigated for each carbohydrate antigen, whenever a glycoconjugate vaccine is under development.

As part of a NVGH project to develop a comprehensive conjugate vaccine against invasive NTS disease, OAg from different *S.* Typhimurium and *S.* Enteritidis strains, major cause of invasive NTS in Africa, were fully characterized and the impact of OAg heterogeneity on the immunogenicity of corresponding conjugate vaccines evaluated in mice.

NTS OAg were extracted from different sources: lab strains, animal and human isolates. *S.* Typhimurium OAg showed a similar bimodal molecular weight distribution, but differed with respect to the amount and position of O-acetylation and glucosylation. For D23580 strain, a clinical isolate from Malawi, O-acetyl groups were found not only on C-2 of abequose (factor 5 specificity), but also on C-2 and C-3 of

Rhamnose. Glucose was found to be linked 1→4 or 1→6 to galactose in different amounts according to the strain of origin. *S.* Enteritidis isolates were more structurally homogeneous, being all characterized by low glucosylation and O-acetylation levels and the same O-acetylation position.

Glycoconjugates were synthesized using CRM_{197} as carrier protein by a selective derivatization on the KDO moiety of the OAg, allowing the rational design of structurally defined conjugates which differed uniquely for their OAg fine specificities. All NTS glycoconjugates resulted immunogenic in mice and able to elicit bactericidal antibodies. OAg fine specificities seemed to influence glycoconjugate immunogenicity. In particular, the presence of additional O-acetyl groups on rhamnose for *S*. Typhimurium D23580 OAg resulted in the production of strain-specific anti-OAg antibodies. O-acetylation and glucosylation seemed also to have an impact on the bactericidal activity when antibodies produced in mice were tested against a broad panel of *S.* Typhimurium endemic strains. This work underlines how the selection of the strain as OAg source for glycoconjugate vaccine production can be important, as different strains may result in candidate vaccines inducing antibodies with potentially different cross-reactivities and different immunogenicity. A screening of a bigger number of strains would probably highlight better on the importance of the OAg structure in affecting the immunogenicity of NTS glycoconjugate vaccines.

To investigate on the impact of conjugation chemistry on the immunogenicity of *S.* Typhimurium glycoconjugate vaccines, conjugates obtained by different random derivatizations along the sugar chain or selective activation of the KDO introducing linkers of different length were compared in mice. All the conjugates induced high anti-OAg IgG antibodies with strong serum bactericidal activity. However, random conjugates induced stronger bactericidal antibodies than selective ones, and FACS analysis confirmed that the random derivation did not impact on the ability of the corresponding conjugates to induce antibodies able to recognize structural epitopes. However, an inverse correlation between the degree of OAg chain modification and the ability of elicited antibodies to protect against the infection was found.

In the development of a vaccine it is important also to consider the product yield, the total number of steps involved in the process and the issues related to the purification and characterization of starting materials, intermediates and final vaccine. Random chemistry can be preferred also in terms of manufacturing process: less number of steps and higher conjugation yield, even if the complexity of the resulting cross-linked structures make more difficult the vaccine characterization.

The synthesis of structurally defined, homogeneous glycoconjugate vaccines is desirable not only for production but also as biochemical tools to study conjugates processing by the immune system. The development of methods which allow saccharide coupling to precise amino acids of proteins/peptides with controlled saccharide/protein ratio can be a key aspect of the structure–activity relationships (SARs) (*127*). Moreover, new insights coming from immunology demonstrate that the connectivity between the saccharide and the protein may be crucial to the immunogenicity of carbohydrate-based conjugate vaccines (*160*).

The synthesis of well-defined glycoconjugates requires powerful conjugation chemistry. Two strategies were initially investigated for the conjugation of *S.* Typhimurium OAg to CRM_{197}, both involving the linkage of the terminal KDO unit of the sugar to the protein: thiol chemistry and click chemistry. Thiol chemistry did not allow conjugation unless starting with a relative high number of linkers on the protein, while click chemistry allowed conjugate generation even when just one position on

the protein was activated. Another advantage of the click chemistry was the possibility to recycle unconjugated OAg and use it for the synthesis of a new batch of glycoconjugate. Furthermore a solid-phase conjugation method utilizing the carrier protein bound to an ion exchange matrix was developed. This methodology holds promise for a big impact on reducing the cost and the complexity of vaccine production, since it allows the recycling of unreacted sugar and it simplifies the conjugate purification.
Using this conjugation methodology, in the near future we are planning to selectively target different amino acids on CRM_{197} (Figure 6.1) and introducing a precise number of different sugar chains per protein in selective positions.

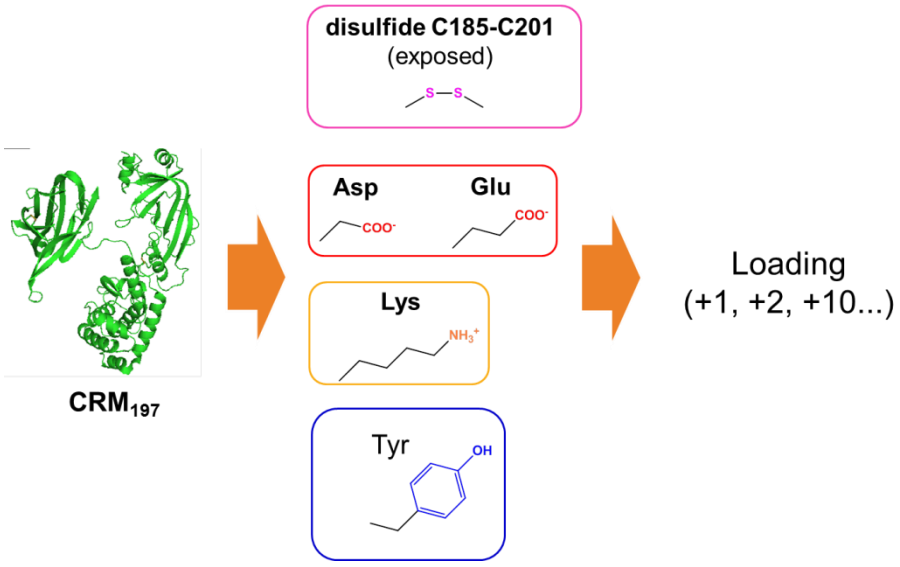

Figure 6.1 Different amino acids of CRM_{197} can be activated with different loading

These conjugates will represent the first example of well-defined glycoconjugate vaccines against NTS, selective on both saccharide and protein component. The impact of these highly structural-defined conjugates on the immunogenicity and the possibility to control OAg/protein ratio are very attracting.
In addition to the relevance on the development of NTS glycoconjugate based vaccines, this study can add useful informations about factors that influence antigen presentation, processing, and cooperation between B and T cells and drive the rational design of the next generation conjugate vaccines.

7. Bibliography

1. C. J. L. Murray, A. D. Lopez. The global burden of disease - a comprehensive assessment of mortality and disability form diseases, injuries and risk factors in 1990 and projected to 2020 (1996).
2. World Health Organization GS.The global burden of disease (GBD): 2004 update. (2008).
3. World Health Organization GS. Global Health Observatory Data Repository. Cause-specific mortality 2008 (2012).
4. M. Moran *et al.*, *PLoS. Med.* **6**, e30 (2009).
5. World Health Organization GS. CSDH (2008). Closing the gap in a generation: health equity through action on the social determinants of health. Final Report of the Commission on Social Determinants of Health (2008).
6. World Health Organization GS. World Health Organization, Global burden of disease (GBD) 2002 estimates (2004).
7. World Health Organization GS. Children: reducing mortality (2012).
8. M. P. Girard, D. Steele, C. L. Chaignat, M. P. Kieny, *Vaccine* **24**, 2732 (2006).
9. C.A. Siegrist. General aspects of vaccination: Vaccines Immunology. From *Vaccines 5th edition*, pp. 17-36 (2008).
10. K. Murphy. Basic concept in immunology. From *Immunobiology 8th edition,* pp. 1-37 (2012).
11. N. R. Cooper, G. R. Nemerow, *J. Invest Dermatol.* **83**, 121s (1984).
12. R. Bacchetta, S. Gregori, M. G. Roncarolo, *Autoimmun. Rev.* **4**, 491 (2005).
13. A. K. Palucka *et al.*, *Adv. Exp. Med. Biol.* **560**, 105 (2005).
14. K. Hoebe, E. Janssen, B. Beutler, *Nat. Immunol.* **5**, 971 (2004).
15. J. U. Igietseme, F. O. Eko, Q. He, C. M. Black, *Expert. Rev. Vaccines.* **3**, 23 (2004).
16. A. Weintraub, *Carbohydr. Res.* **338**, 2539 (2003).
17. C. J. Lee, L. H. Lee, C. S. Lu, A. Wu, *Adv. Exp. Med. Biol.* **491**, 453 (2001).
18. O. Finco, R. Rappuoli, *Front Immunol.* **5**, 12 (2014).
19. S. A. Plotkin, *Nat. Med.* **11**, S5 (2005).
20. K. Murphy. Manipulation of the Immune Response. From *Immunobiology 8th edition,* pp. 669-681 (2012).
21. Tong A. 8th International Conference on Typhoid Fever and Other Invasive Salmonelloses - Draft Estimated Global Burden of Invasive non-typhoidal Salmonelloses, pp. 31-32 (2013).
22. M. Kosek, C. Bern, R. L. Guerrant, *Bull. World Health Organ* **81**, 197 (2003).
23. World Health Organization GS. UNICEF/WHO, Diarrhoea: Why children are still dying and what can be done (2009).
24. J. W. Ahs, W. Tao, J. Löfgren, B. C. Forsberg, *The Open Infectious Diseases Journal* **4**, 113 (2010).
25. B. Lorntz *et al.*, *Pediatr. Infect. Dis. J.* **25**, 513 (2006).
26. S. R. Moore *et al.*, *Int. J. Epidemiol.* **30**, 1457 (2001).
27. A. A. Lima, *Curr. Opin. Infect. Dis.* **14**, 547 (2001).
28. World Health Organization GS. Initiative for Vaccines Research, Diarrhoeal Diseases - Updated February 2009 (2009)
29. B. Rowe, L. R. Ward, E. J. Threlfall, *Clin. Infect. Dis.* **24 Suppl 1**, S106 (1997).
30. B. V. Krishna, A. B. Patil, M. R. Chandrasekhar, *Trans. R. Soc. Trop. Med. Hyg.* **100**, 224 (2006).

31. C. M. Parry, T. T. Hien, G. Dougan, N. J. White, J. J. Farrar, *N. Engl. J. Med.* **347**, 1770 (2002).
32. M. K. Bhan, R. Bahl, S. Bhatnagar, *Lancet* **366**, 749 (2005).
33. Skerman VBD, McGowan V, Sneath PHA, *Int J Syst Bacteriol.* **30**, 225 (1980).
34. Gaffky G, *Zur Aetiologie des abdominaltyphus.Mittheilungen aus dem kaiserlichen Gesundheitsante*, pp. 372-420 (1984).
35. Z. A. Bhutta, M. I. Khan, S. B. Soofi, R. L. Ochiai, *Adv. Exp. Med. Biol.* **697**, 17 (2011).
36. N. A. Feasey, G. Dougan, R. A. Kingsley, R. S. Heyderman, M. A. Gordon, *Lancet* **379**, 2489 (2012).
37. J. Deen *et al.*, *Lancet Infect. Dis.* **12**, 480 (2012).
38. R. L. Ochiai *et al.*, *Emerg. Infect. Dis.* **11**, 1764 (2005).
39. J. A. Crump, S. P. Luby, E. D. Mintz, *Bull. World Health Organ* **82**, 346 (2004).
40. A. Sinha *et al.*, *Lancet* **354**, 734 (1999).
41. S. K. Saha *et al.*, *Pediatr. Infect. Dis. J.* **20**, 521 (2001).
42. W. A. Brooks *et al.*, *Emerg. Infect Dis* **11**, 326 (2005).
43. R. Germanier, E. Fuer, *J. Infect. Dis.* **131**, 553 (1975).
44. A. Fraser, M. Paul, E. Goldberg, C. J. Acosta, L. Leibovici. *Vaccine* **25**, 45 (2007).
45. M. M. Levine *et al.*, *Clin. Infect. Dis.* **45 Suppl 1**, S24 (2007).
46. S. H. Pakkanen, J. M. Kantele, A. Kantele, *Vaccine* **30**, 6047 (2012).
47. R. Wahid, R. Simon, S. J. Zafar, M. M. Levine, M. B. Sztein, *Clin. Vaccine Immunol.* **19**, 825 (2012).
48. A. Kantele, S. H. Pakkanen, R. Karttunen, J. M. Kantele, *PLoS One* **8**, e60583 (2013).
49. A. J. Pollard, K. P. Perrett, P. C. Beverley, *Nat. Rev. Immunol.* **9**, 213 (2009).
50. C. A. MacLennan, *Semin. Immunol.* **25**, 114 (2013).
51. D. Sur *et al.*, *N. Engl. J. Med.* **361**, 335 (2009).
52. M. I. Khan *et al.*, *Vaccine* **30**, 5389 (2012).
53. J. R. Murphy *et al.*, *Infect. Immun.* **59**, 4291 (1991).
54. J. Poolman, R. Borrow, *Expert Rev. Vaccines.* **10**, 307 (2011).
55. S. Sahastrabuddhe, R. Carbis, T. F. Wierzba, R. L. Ochiai, *Expert. Rev. Vaccines.* **12**, 1021 (2013).
56. L. B. Martin, *Curr. Opin. Infect. Dis.* **25**, 489 (2012).
57. A. C. McGregor, C. S. Waddington, A. J. Pollard, *Curr. Opin. Infect. Dis.* **26**, 254 (2013).
58. S. C. Szu, *Expert. Rev. Vaccines.* **12**, 1273 (2013).
59. A. Podda *et al.*, *J. Infect. Dev. Ctries.* **4**, 404 (2010).
60. K. B. Laupland *et al.*, *BMC. Infect. Dis.* **10**, 95 (2010).
61. M. A. Gordon, *J Infect.* **56**, 413 (2008).
62. B. Sigauque *et al.*, *Pediatr. Infect. Dis. J.* **28**, 108 (2009).
63. M. A. Gordon *et al.*, *Clin. Infect. Dis.* **46**, 963 (2008).
64. E. A. Reddy, A. V. Shaw, J. A. Crump, *Lancet Infect. Dis.* **10**, 417 (2010).
65. C. F. Gilks *et al.*, *Lancet* **336**, 545 (1990).
66. J. A. Berkley *et al.*, *N. Engl. J Med* **352**, 39 (2005).
67. E. A. Reddy, A. V. Shaw, J. A. Crump, *Lancet Infect. Dis.* **10**, 417 (2010).
68. J. Wadula *et al.*, *Pediatr. Infect. Dis. J* **25**, 843 (2006).
69. G. Beyene *et al.*, *J Infect. Dev. Ctries.* **5**, 23 (2011).

70. S. M. Tennant *et al.*, *PLoS. Negl. Trop. Dis.* **4**, e621 (2010).
71. C. A. MacLennan *et al.*, *J. Clin. Invest* **118**, 1553 (2008).
72. N. A. Feasey *et al.*, *Emerg. Infect. Dis.* **16**, 1448 (2010).
73. D. C. Mabey, A. Brown, B. M. Greenwood, *J. Infect. Dis.* **155**, 1319 (1987).
74. J. C. Calis *et al.*, *N. Engl. J. Med.* **358**, 888 (2008).
75. H. Bachou, T. Tylleskar, D. H. Kaddu-Mulindwa, J. K. Tumwine, *BMC. Infect. Dis.* **6**, 160 (2006).
76. M. A. Gordon *et al.*, *AIDS* **16**, 1633 (2002).
77. C. A. MacLennan, M. M. Levine, *Expert. Rev. Anti. Infect. Ther.* **11**, 443 (2013).
78. J. D. Clemens, *Emerg. Infect. Dis.* **15**, e2 (2009).
79. M. Raffatellu *et al.*, *Nat. Med.* **14**, 421 (2008).
80. S. M. Tennant, Y. Zhang, J. E. Galen, C. D. Geddes, M. M. Levine, *PLoS. One.* **6**, e18700 (2011).
81. R. A. Kingsley *et al.*, *Genome Res.* **19**, 2279 (2009).
82. G. Dougan, V. John, S. Palmer, P. Mastroeni, *Immunol. Rev.* **240**, 196 (2011).
83. C. A. MacLennan *et al.*, *Science* **328**, 508 (2010).
84. R. Simon *et al.*, *Infect. Immun.* **79**, 4240 (2011).
85. R. Simon *et al.*, *PLoS. One.* **8**, e64680 (2013).
86. F. Micoli *et al.*, *Anal. Biochem.* **434**, 136 (2013).
87. Z. Hindle *et al.*, *Infect. Immun.* **70**, 3457 (2002).
88. S. M. Tennant *et al.*, *Infect. Immun.* **79**, 4175 (2011).
89. J. Choi, D. Shin, S. Ryu, *Vaccine* **28**, 6436 (2010).
90. U. S. Allam, M. G. Krishna, A. Lahiri, O. Joy, D. Chakravortty, *PLoS One* **6**, e16667 (2011).
91. M. Pesciaroli *et al.*, *Vaccine* **29**, 1783 (2011).
92. V. Vishwakarma *et al.*, *PLoS One* **7**, e52043 (2012).
93. C. Gil-Cruz *et al.*, *Proceedings Of The National Academy Of Sciences Of The United States Of America* **106**, 9803 (2009).
94. S. F. Berlanda *et al.*, *Mol. Cell Proteomics.* **7**, 473 (2008).
95. E. N. Gondwe *et al.*, *Proc. Natl. Acad. Sci. U. S. A* **107**, 3070 (2010).
96. C. Whitfield, N. Kaniuk, E. Frirdich, *J. Endotoxin. Res.* **9**, 244 (2003).
97. E. Konadu, J. Shiloach, D. A. Bryla, J. B. Robbins, S. C. Szu, *Infect. Immun.* **64**, 2709 (1996).
98. D. C. Watson, J. B. Robbins, S. C. Szu, *Infect. Immun.* **60**, 4679 (1992).
99. S. Rondini *et al.*, *Microb. Pathog.* **63**, 19 (2013).
100. E. Konadu, J. Shiloach, D. A. Bryla, J. B. Robbins, S. C. Szu, *Infect Immun* **64**, 2709 (1996).
101. S. B. Svenson, A. A. Lindberg, *Infect. Immun.* **32**, 490 (1981).
102. S. B. Svenson, M. Nurminen, A. A. Lindberg, *Infect. Immun.* **25**, 863 (1979).
103. H. J. Jorbeck, S. B. Svenson, A. A. Lindberg, *Infect. Immun.* **32**, 497 (1981).
104. A. Kantele, S. H. Pakkanen, A. Siitonen, R. Karttunen, J. M. Kantele, *Vaccine* **30**, 7238 (2012).
105. J. E. Galen, R. Simon, R. K. Ernst, *Expert. Rev. Vaccines.* **10**, 1679 (2011).
106. R. Simon *et al.*, *Infect Immun* **79**, 4240 (2011).
107. R. Simon *et al.*, *PLoS. One.* **8**, e64680 (2013).
108. A. F. Cunningham *et al.*, **178**, 6200 (2007).
109. H. Toobak *et al.*, *Biologicals* **41**, 224 (2013).

110. M. J. Kuehn, N. C. Kesty, *Genes Dev.* **19**, 2645 (2005).
111. T. J. Beveridge, *J. Bacteriol.* **181**, 4725 (1999).
112. T. N. Ellis, M. J. Kuehn, *Microbiol. Mol. Biol. Rev.* **74**, 81 (2010).
113. C. R. Raetz, C. M. Reynolds, M. S. Trent, R. E. Bishop, *Annu. Rev. Biochem.* **76**, 295 (2007).
114. Y. S. Ovodov, *Biochemistry (Mosc.)* **71**, 937 (2006).
115. F. Y. Avci, D. L. Kasper, *Annu. Rev. Immunol.* **28**, 107 (2010).
116. C. M. Taylor, I. S. Roberts, *Contrib. Microbiol.* **12**, 55 (2005).
117. M. Finland, W. D. Sutliff, *J Exp. Med.* **55**, 853 (1932).
118. C. M. Macleod, R. G. Hodges, *J Exp. Med.* **82**, 445 (1945).
119. M. S. Artenstein *et al.*, *N. Engl. J Med.* **282**, 417 (1970).
120. R. Gold, M. S. Artenstein, *Bull. World Health Organ* **45**, 279 (1971).
121. C. Jones, *An. Acad. Bras. Cienc.* **77**, 293 (2005).
122. P. Costantino, R. Rappuoli, F. Berti, *Expert. Opin. Drug Discov.* **6**, 1045 (2011).
123. O. T. Avery, W. F. Goebel, *J Exp. Med.* **50**, 533 (1929).
124. P. Costantino *et al.*, *Vaccine* **10**, 691 (1992).
125. R. Eby, *Pharm. Biotechnol.* **6**, 695 (1995).
126. L. C. Paoletti, D. L. Kasper, *Expert. Opin. Biol. Ther.* **3**, 975 (2003).
127. R. Adamo *et al.*, *Chem. Sci.* **4**, 2995 (2013).
128. Z. Lai, J. R. Schreiber, *Vaccine* **27**, 3137 (2009).
129. G. Ada, D. Isaacs, *Clin. Microbiol. Infect.* **9**, 79 (2003).
130. D. F. Kelly, A. J. Pollard, E. R. Moxon, *JAMA* **294**, 3019 (2005).
131. F. Borriello *et al.*, *Immunity.* **6**, 303 (1997).
132. H. K. Guttormsen *et al.*, *Infect. Immun.* **67**, 6375 (1999).
133. M. Guirola *et al.*, *FEMS Immunol. Med Microbiol* **46**, 169 (2006).
134. H. K. Guttormsen, L. M. Wetzler, R. W. Finberg, D. L. Kasper, *Infect. Immun.* **66**, 2026 (1998).
135. R. A. Insel, P. W. Anderson, *J Exp. Med* **163**, 262 (1986).
136. M. E. Pichichero, *Pediatrics* **124**, 1633 (2009).
137. S. G. Tangye, D. T. Avery, E. K. Deenick, P. D. Hodgkin, *J Immunol.* **170**, 686 (2003).
138. D. Goldblatt, A. R. Vaz, E. Miller, *J Infect. Dis.* **177**, 1112 (1998).
139. B. A. Cobb, D. L. Kasper, *Cell Microbiol* **7**, 1398 (2005).
140. A. Tzianabos, J. Y. Wang, D. L. Kasper, *Carbohydr. Res.* **338**, 2531 (2003).
141. C. D. Velez, C. J. Lewis, D. L. Kasper, B. A. Cobb, *Immunology* **127**, 73 (2009).
142. F. Y. Avci, X. Li, M. Tsuji, D. L. Kasper, *Nat. Med.* **17**, 1602 (2011).
143. N. Petrovsky, J. C. Aguilar, *Immunol. Cell Biol.* **82**, 488 (2004).
144. R. K. Gupta, *Adv. Drug Deliv. Rev.* **32**, 155 (1998).
145. T. A. Reese *et al.*, *Nature* **447**, 92 (2007).
146. A. C. Allison, G. Gregoriadis, *Recent Results Cancer Res.* 58 (1976).
147. Y. L. Huang *et al.*, *Proc. Natl. Acad. Sci. U. S. A* **110**, 2517 (2013).
148. E. M. Long, B. Millen, P. Kubes, S. M. Robbins, *PLoS. One.* **4**, e5601 (2009).
149. M. Roman *et al.*, *Nat. Med.* **3**, 849 (1997).
150. E. K. Chea *et al.*, *J Am. Chem. Soc.* **134**, 13448 (2012).
151. M. Singh *et al.*, *Hum. Vaccin. Immunother.* **8**, 486 (2012).
152. V. Verez-Bencomo *et al.*, *Science* **305**, 522 (2004).
153. P. H. Seeberger, *Chem. Soc. Rev.* **37**, 19 (2008).

154. F. A. Jaipuri, N. L. Pohl, *Org. Biomol. Chem.* **6**, 2686 (2008).
155. R. Adamo *et al.*, *ACS Chem. Biol.* **7**, 1420 (2012).
156. C. M. Szymanski, R. Yao, C. P. Ewing, T. J. Trust, P. Guerry, *Mol. Microbiol.* **32**, 1022 (1999).
157. J. Kelly *et al.*, *J Bacteriol.* **188**, 2427 (2006).
158. M. F. Feldman *et al.*, *Proc. Natl. Acad. Sci. U. S. A* **102**, 3016 (2005).
159. J. Ihssen *et al.*, *Microb. Cell Fact.* **9**, 61 (2010).
160. F. Y. Avci, *Curr. Top. Med. Chem.* **13**, 2535 (2013).
161. M. N. Kweon, *Curr. Opin. Infect. Dis.* **21**, 313 (2008).
162. V. Pozsgay *et al.*, *Proc. Natl. Acad. Sci. U. S. A* **96**, 5194 (1999).
163. J. B. Robbins *et al.*, *Proc. Natl. Acad. Sci. U. S. A* **106**, 7974 (2009).
164. J. Kubler-Kielb *et al.*, *Carbohydr. Res.* **345**, 1600 (2010).
165. A. Phalipon *et al.*, *J. Immunol.* **182**, 2241 (2009).
166. P. Chong *et al.*, *Infect. Immun.* **65**, 4918 (1997).
167. C. C. Peeters *et al.*, *Infect. Immun.* **60**, 1826 (1992).
168. V. Pozsgay, *Adv. Carbohydr. Chem. Biochem.* **56**, 153 (2000).
169. R. K. Gupta, S. C. Szu, R. A. Finkelstein, J. B. Robbins, *Infect. Immun.* **60**, 3201 (1992).
170. I. Jacques, G. Dubray, *Vaccine* **9**, 559 (1991).
171. R. K. Gupta, W. Egan, D. A. Bryla, J. B. Robbins, S. C. Szu, *Infect. Immun.* **63**, 2805 (1995).
172. R. Saksena, X. Ma, T. K. Wade, P. Kovac, W. F. Wade, *FEMS Immunol. Med. Microbiol.* **47**, 116 (2006).
173. P. Anderson, M. E. Pichichero, R. A. Insel, *J. Clin. Invest* **76**, 52 (1985).
174. F. Mawas *et al.*, *Infect. Immun.* **70**, 5107 (2002).
175. J. H. Passwell *et al.*, *Infect. Immun.* **69**, 1351 (2001).
176. D. Pavliakova *et al.*, *Infect. Immun.* **67**, 5526 (1999).
177. R. Simon *et al.*, *Infect. Immun.* **79**, 4240 (2011).
178. M. Broker, P. Costantino, L. DeTora, E. D. McIntosh, R. Rappuoli, *Biologicals* **39**, 195 (2011).
179. D. Pace, *Expert. Opin. Biol. Ther.* **13**, 11 (2013).
180. F. Micoli *et al.*, *PLoS. One.* **7**, e47039 (2012).
181. I. M. Helander, A. P. Moran, P. H. Makela, *Mol. Microbiol* **6**, 2857 (1992).
182. C. G. Hellerqvist, B.Lindberg, S.Svensson, T.Holme, A.A.Lindberg, *Carbohydr. Res.* **9**, 237 (1969).
183. C. G. Hellerqvist, B.Lindberg, S.Svensson, T.Holme, A.A.Lindberg, *Carbohydr. Res.* **8**, 43 (1968).
184. C. G. Hellerqvist, B. Lindberg, S. Svensson, T. Holme, A. A. Lindberg, *Acta Chem. Scand.* **23**, 1588 (1969).
185. R. Wollin, B. A. Stocker, A. A. Lindberg, *J. Bacteriol.* **169**, 1003 (1987).
186. D. S. Berry, F. Lynn, C. H. Lee, C. E. Frasch, M. C. Bash, *Infect. Immun.* **70**, 3707 (2002).
187. S. K. Gudlavalleti *et al.*, *Vaccine* **25**, 7972 (2007).
188. A. I. Fattom, J. Sarwar, L. Basham, S. Ennifar, R. Naso, *Infect. Immun.* **66**, 4588 (1998).
189. F. Michon *et al.*, *Dev. Biol. (Basel)* **103**, 151 (2000).
190. P. C. Fusco, E. K. Farley, C. H. Huang, S. Moore, F. Michon, *Clin. Vaccine Immunol.* **14**, 577 (2007).

191. P. Beltran *et al.*, *Proc. Natl. Acad. Sci. U. S. A* **85**, 7753 (1988).
192. P. Beltran *et al.*, *J Gen. Microbiol* **137**, 601 (1991).
193. K. Lilleegen, *Acta Pathol. Microbiol Scand.* **27**, 625 (1950).
194. S. Rondini *et al.*, *Clin. Vaccine Immunol.* **18**, 460 (2011).
195. M. Dubois, K. A. Giles, J. K. Hamilton JK, P.A. Rebers, F. Smith, *Analytical Chemistry* **28**, 350 (1956).
196. P. Albersheim, D. J. Nevins, P. D. English, A. Karr, *Carbohydr. Res.* **5**, 340 (1967).
197. P. J. Harris, R. J. Henry, A. B. Blakeney, B. A. Stone, *Carbohydr. Res.* **127**, 59 (1984).
198. D. P.Sweet , R. H.Shapiro, P. Albersheim, *Carbohydr. Res.* **40**, 217 (1975).
199. G. J. Gerwig, J. P. Kamerling, J. F. G. Vliegenthart, *Carbohydr. Res.* **62**, 349 (1978).
200. P. Prehm *et al.*, *Carbohydr. Res.* **78**, 372 (1980).
201. D. W. Palmer, T. Peters, Jr., *Clin. Chem.* **15**, 891 (1969).
202. N. I. Carlin, S. B. Svenson, A. A. Lindberg, *Microb. Pathog.* **2**, 171 (1987).
203. F. Micoli *et al.*, *Carbohydr. Res.* **385**, 1 (2014).
204. C. T. Parker, E. Liebana, D. J. Henzler, J. Guard-Petter, *Environ. Microbiol.* **3**, 332 (2001).
205. J. Guard-Petter, C. T. Parker, K. Asokan, R. W. Carlson, *Appl. Environ. Microbiol.* **65**, 2195 (1999).
206. E. Trebicka, S. Jacob, W. Pirzai, B. P. Hurley, B. J. Cherayil, *Clin. Vaccine Immunol.* **20**, 1491 (2013).
207. C. A. MacLennan, S. M. Tennant, *Clin. Vaccine Immunol.* **20**, 1487 (2013).
208. E. Y. Konadu *et al.*, *Infect. Immun.* **68**, 1529 (2000).
209. C. Jones, *An. Acad. Bras. Cienc.* **77**, 293 (2005).
210. C. E. Frasch, *Vaccine* **27**, 6468 (2009).
211. T. Carmenate *et al.*, *FEMS Immunol. Med. Microbiol.* **40**, 193 (2004).
212. E. C. Beuvery, K. A. vd, V. Kanhai, A. B. Leussink, *Vaccine* **1**, 31 (1983).
213. R. Schneerson, O. Barrera, A. Sutton, J. B. Robbins, *J. Exp. Med.* **152**, 361 (1980).
214. R. Prymula, L. Schuerman, *Expert. Rev. Vaccines.* **8**, 1479 (2009).
215. W. Zou, H. J. Jennings. Preparation og glycoconjugate vaccines. From *Carbohydrate-Based Vaccines and Immunotherapies*, pp.55-88 (2009).
216. M. Broker, P. M. Dull, R. Rappuoli, P. Costantino, *Vaccine* **27**, 5574 (2009).
217. S. B. Svenson, A. A. Lindberg, *J Immunol. Methods* **25**, 323 (1979).
218. P. E. Jansson, A. A. Lindberg, B. Lindberg, R. Wollin, *Eur. J Biochem.* **115**, 571 (1981).
219. K. Satake, T. Okuyamna, M. Ohashi, T. Shinoda, *J.Biochem*. **47**, 5 (1960).
220. D. W. Palmer, T. Peters, Jr., *Clin. Chem.* **15**, 891 (1969).
221. P. J. Meeuwsen, J. P. Vincken, G. Beldman, A. G. Voragen, *J Biosci. Bioeng.* **89**, 107 (2000).
222. S. Rondini *et al.*, *Clin Vaccine Immunol* **18**, 460 (2011).
223. F. Micoli *et al.*, *Proc. Natl. Acad. Sci. U. S. A* **110**, 19077 (2013).
224. H. C. Kolb, M. G. Finn, K. B. Sharpless, *Angew. Chem. Int. Ed Engl.* **40**, 11 (2001).
225. R. Huisgen, *Angewandte chemie international ediiton* **2**, 633 (1963).
226. C. W. Tornoe, C. Christensen, M. Meldal, *J. Org. Chem.* **67**, 3057 (2002).
227. V. V. Rostovtsev, L. G. Green, V. V. Fokin, K. B. Sharpless, *Angew. Chem. Int Ed Engl.* **41**, 2596 (2002).
228. G. J. Bernardes, B. Castagner, P. H. Seeberger, *ACS Chem. Biol.* **4**, 703 (2009).

229. E. J. Grayson *et al.*, *Angew. Chem. Int Ed Engl.* **50**, 4127 (2011).
230. G. L. Ellman, *Arch. Biochem. Biophys.* **82**, 70 (1959).
231. H. C. Kolb, K. B. Sharpless, *Drug Discov. Today* **8**, 1128 (2003).
232. J. E. Moses, A. D. Moorhouse, *Chem. Soc. Rev.* **36**, 1249 (2007).
233. H. W. Binder, R. Sachsenhofer, *Macromol. Rapid. Commun.* **28**, 15 (2008).
234. C. D. Hein, X. M. Liu, D. Wang, *Pharm. Res.* **25**, 2216 (2008).
235. D. Zeng, B. M. Zeglis, J. S. Lewis, C. J. Anderson, *J Nucl. Med.* **54**, 829 (2013).
236. Q.-Y. Hu *et al.*, *Chem. Sci.* **4**, 3827 (2013).
237. P. R. Hansen, A. Holm, G. Houen, *Int J Pept. Protein Res.* **41**, 237 (1993).
238. G. Houen, M. H. Jakobsen, C. Svaerke, C. Koch, V. Barkholt, *J Immunol. Methods* **206**, 125 (1997).
239. G. Houen, D. T. Olsen, P. R. Hansen, K. B. Petersen, V. Barkholt, *Bioconjug. Chem.* **14**, 75 (2003).
240. S. A. Plotkin, *Clin. Vaccine Immunol.* **16**, 1709 (2009).
241. D. Pace, *Expert. Rev. Vaccines.* **8**, 529 (2009).
242. D. M. Granoff, A. J. Pollard, *Pediatr. Infect. Dis. J* **26**, 716 (2007).
243. D. Pace, *Curr. Opin. Mol. Ther.* **11**, 692 (2009).
244. G. Ada, D. Isaacs, *Clin. Microbiol Infect.* **9**, 79 (2003).
245. S. Hakomori, *Adv. Exp. Med. Biol.* **491**, 369 (2001).
246. B. Winblad *et al.*, *Lancet Neurol.* **11**, 597 (2012).
247. B. M. Kinsey, D. C. Jackson, F. M. Orson, *Immunol. Cell Biol.* **87**, 309 (2009).
248. M. D. Snape *et al.*, *Pediatr. Infect. Dis. J* **29**, e80 (2010).
249. Y. Al-Mazrou *et al.*, *Infect. Immun.* **73**, 2932 (2005).
250. L. Ostergaard, E. Lebacq, J. Poolman, G. Maechler, D. Boutriau, *Vaccine* **27**, 161 (2009).
251. J. M. Miller, N. Mesaros, M. Van Der Wielen, Y. Baine, *Adv. Prev. Med.* **2011**, 846756 (2011).
252. D. Serruto, M. J. Bottomley, S. Ram, M. M. Giuliani, R. Rappuoli, *Vaccine* **30 Suppl 2**, B87 (2012).
253. S. Kariuki *et al.*, *J Med. Microbiol.* **55**, 585 (2006).
254. S. Kariuki *et al.*, *BMC. Microbiol.* **6**, 101 (2006).
255. I. Mandomando *et al.*, *Trop. Med. Int Health* **14**, 1467 (2009).
256. A. L. Walsh, A. J. Phiri, S. M. Graham, E. M. Molyneux, M. E. Molyneux, *Pediatr. Infect. Dis. J* **19**, 312 (2000).
257. G. Enwere *et al.*, *Pediatr. Infect. Dis. J* **25**, 700 (2006).
258. R. Simon, M. M. Levine, *Hum. Vaccin. Immunother.* **8**, 494 (2012).
259. E. J. Heffernan, J. Harwood, J. Fierer, D. Guiney, *J Bacteriol.* **174**, 84 (1992).
260. N. Grossman *et al.*, *J Bacteriol.* **169**, 856 (1987).
261. C. J. Liang-Takasaki, N. Grossman, L. Leive, *J Immunol.* **130**, 1867 (1983).
262. C. J. Liang-Takasaki, H. Saxen, P. H. Makela, L. Leive, *Infect. Immun.* **41**, 563 (1983).
263. A. Casadevall, L. A. Pirofski, *Adv. Immunol.* **91**, 1 (2006).
264. R. J. Roantree, L. A. Rantz, *J Clin. Invest* **39**, 72 (1960).

8. Annex

Communications

Poster presentations:

- Structural variability of *Salmonella* Typhimurium and *Salmonella* Enteritidis O-antigens and impact on the immunogenicity of glycoconjugate vaccines. *G. Stefanetti, S. Rondini, L. Lanzilao, M. Gavini, S. Londero, P. Cescutti, N. Ravenscroft, A. Saul, C.A. MacLennan, F. Micoli.*
  (Gordon Research Conference: *Carbohydrates 2013.* West Dover (VT), US)
- Impact of O-antigen structure and conjugation chemistry on the immunogenicity of glycoconjugate vaccines against nontyphoidal Salmonella.
  G. Stefanetti, S. Rondini, L. Lanzilao, M. Gavini, S. Londero, P. Cescutti, N. Ravenscroft, A. Saul, C.A. MacLennan, F. Micoli.
  (Research Days 2013, NV&D, Novartis campus, Siena, IT).

Oral presentations:

- Impact of *Salmonella* Typhimurium O-antigen structure on the immunogenicity of conjugate vaccines.
  G. Stefanetti.
  (XIII convegno-scuola sulla chimica dei carboidrati, certosa di Pontignano (SI), IT)
- Impact of *Salmonella* Typhimurium O-antigen structure on the immunogenicity of conjugate vaccines.
  G. Stefanetti.
  (German Cancer Research Centre DKFZ, PhD Retreat 2012, Weil der Stadt, DE).
- Impact of Salmonella Typhimurium O-Antigen structure on the immunogenicity of conjugate vaccines
  G. Stefanetti.
  (Novartis PhD students Workshop 2012, NV&D, Novartis campus, Siena, IT).
- Impact of conjugation chemistry in the design of iNTS glycoconjugate vaccines
  G. Stefanetti.
  (Novartis PhD students Workshop 2013, NV&D, Novartis campus, Siena, IT).

Publication:

Structural analysis of O-polysaccharide chains extracted from different Salmonella Typhimurium strains.
Francesca Micoli, Neil Ravenscroft , Paola Cescutti, Giuseppe Stefanetti, Silvia Londero, Simona Rondini, Calman A. MacLennan.
(Carbohydrate Research 385 (2014) 1–8)

First author publications:

Screening of S. Typhimurium and S. Enteritidis as source of O-antigen for glycoconjugate vaccines against NTS.
(Manuscript in preparation)

Impact of conjugation chemistry on the immunogenicity of S. Typhimurium conjugate vaccines.
(Manuscript in preparation)

Click chemistry: a powerful tool for the synthesis of glycoconjugate vaccines.
(Manuscript in preparation)

Courses, Conferences and Scientific Visits

Courses:

- How to write a paper (2012, Novartis Academy course, Keith Veitch, Head of Publications, Novartis Pharma, Novartis campus, Siena).
- Enhancing your presentation skills (2010, NIBR training course, Novartis campus, Siena).
- Master in Vaccinology: vaccine immunology and preclinical research Novartis Vaccines and Diagnostic (NVD). (2011, NV&D Master in Vaccinology, Novartis campus, Siena).

Conferences:

- Novartis-Harvard meeting: Minisimposium on Vaccines and Host-Pathogen Interactions (2012, Novartis campus, Siena, IT).
- XIII convegno - scuola sulla chimica dei carboidrati (2012, certosa di Pontignano, (SI), IT).
- German Cancer Research Centre DKFZ- PhD Retreat (2012, Weil der Stadt, DE).
- Gordon Research Conference: *Carbohydrates* (*2013,* West Dover, US).

Scientific Visits:

- September, 12th - 23rd, 2012: visiting student at the University of Trieste for GLC and GLC-MS analysis on OAg samples. Supervisor: Dr. Paola Cescutti and Prof. Roberto Rizzo.

Acknowledgments

It would not have been possible to work during these 3 years and to write this doctoral thesis without the help and support of the people around me, to only some of whom it is possible to give particular mention here.
First of all, a big thank to my main supervisor Francesca. We have had a unique experience: my first and only (I guess) as a PhD student and your first of many (I am sure) as a PhD mentor. You have been a very good, careful and passionate supervisor. Thanks for all you have taught me in these years and for the time you have dedicated to me. I have been remarkably impressed by your strong commitment and skills, thanks a lot also for the trust and for the freedom you have given me whenever I wanted to try new things.
Many thanks also to my second supervisor Cal for the helpful feedbacks, wise suggestions and positive discussions during this period. Thanks for your strong support and for your careful revision of the thesis. I am looking forward for the next social event to enjoy together!
A special thank goes to Allan. I have very much enjoyed all the time we have met and discussed about science. Your passion and your outstanding competences have been a source of inspiration for me. Thanks for being a great example of visionary scientist always thinking and looking ahead.
Many thanks to my good friend Massimiliano for introducing me to the lab techniques during Francesca's maternity leave. Although it was just for one year, I have definitely enjoyed our time together in the lab. A big acknowledgment goes to Luisa, my ELISA's teacher, and to Simona for their support for the immunological assays. Thanks also Simona for you revision of some chapters of the thesis.
I am grateful to Prof. Roberto Rizzo and Paola Cescutti, which kindly hosted me at the University of Trieste, and to our collaborators Prof. Neil Ravenscroft, Roberto Adamo and the GDC group in Boston. I would also like to thank the Novartis PhD Academy coordinators, Prof. Enzo Scarlato and Ilaria Ferlenghi, the director of the Doctoral School at the University of Naples, Prof. Giovanni Sannia, Paolo Costantino and Francesco Berti, members of my PhD committee, for their helpful guide and suggestions. Thanks also Ilaria for the opportunity you give me to join the German Cancer Research Centre DKFZ- PhD Retreat, it is because of you than one fine day I will win the gold medal in the water-skiing Olympic Games competition.
Big thanks to Ivan and Carlo for sharing their valuable expertise with me and to my lab&office mates Renzo and Melissa. Thanks also to Federico, Emilia and Oscar for their support and company. Thanks Yunshan for all the immunology-related discussions we have had and for giving me the big honor to be a "brother-in-law".
A big thank to all my NVGH colleagues and friends. Thank you, guys, I have enjoyed (almost) every seconds spent with you. A special mention goes to my friends Omar, Eleonora, Francesco, Francesca N., Robert (forza inter amigo!!!), Anna Maria, Antonio, Jochen, Arianna, Mariagrazia, Angela, Anna, Lynda, Chris and Oliver, for all the good time we have spent together. Thanks to my BAT colleagues Jochen, Osvaldo, Ivan, Simona, Breda and Silvia: it was a hard job, but someone had to do it. Thanks also to my former roommates Antonio, Michelangelo and Dario.
A special mention for my music partners: Osvaldo (again!) in the "PFM", "I ragazzi fotonici" Paolo and Stefano, and the "Accademia musicale di canto moderno". During these years we have been playing very hard, thanks for showing me once again that if you do something you love, you never work a day in your life.
Finally, I want to thank my greatest discovery (sorry click chemistry, it is not you…) here in NVGH, Mariaelena. Thanks for all the moments we are having together, for the time spent discussing about ZPSs and MAPPs assays and for teaching me the basis of molecular biology.
Above all, thanks to my parents and to my family for your continuative and unconditional support, without you nothing would have been possible. To you I dedicate this thesis.

Carbohydrate Research 385 (2014) 1–8

Contents lists available at ScienceDirect

Carbohydrate Research

journal homepage: www.elsevier.com/locate/carres

Note

Structural analysis of O-polysaccharide chains extracted from different *Salmonella* Typhimurium strains

Francesca Micoli [a,*], Neil Ravenscroft [b], Paola Cescutti [c], Giuseppe Stefanetti [a], Silvia Londero [c], Simona Rondini [a], Calman A. MacLennan [a,d]

[a] *Novartis Vaccines Institute for Global Health, Via Fiorentina 1, I-53100 Siena, Italy*
[b] *Department of Chemistry, University of Cape Town, Rondebosch 7701, South Africa*
[c] *Dipartimento di Scienze della Vita, Ed. C11, Università di Trieste, via L. Giorgieri 1, 34127 Trieste, Italy*
[d] *Medical Research Council Centre for Immune Regulation, Institute of Biomedical Research, School of Immunity and Infection, College of Medicine and Dental Sciences, University of Birmingham, Birmingham B15 2TT, UK*

ARTICLE INFO

Article history:
Received 26 October 2013
Received in revised form 3 December 2013
Accepted 4 December 2013
Available online 11 December 2013

Keywords:
Salmonella Typhimurium
O-Polysaccharide
Bacterial polysaccharide structure

ABSTRACT

Salmonella Typhimurium is the major cause of invasive nontyphoidal *Salmonella* disease in Africa, with high mortality among children and HIV-infected individuals. Currently, no vaccine is available for use in humans. Antibodies directed against the O-polysaccharide of the lipopolysaccharide molecule of *Salmonella* mediate bacterial killing and are protective, and conjugation of the O-polysaccharide to a carrier protein represents a possible strategy for vaccine development.

Here we have purified the O-polysaccharide from six different strains of *S.* Typhimurium and fully characterized them using analytical methods including HPLC–SEC, HPAEC-PAD, GC, GC–MS, 1D and 2D NMR spectroscopy. All the O-polysaccharide samples showed a similar bimodal molecular mass distribution, but differed with respect to the amount and position of O-acetylation and glucosylation. For some strains, *O*-acetyl groups were found not only on C-2 of abequose (factor 5 specificity), but also on C-2 and C-3 of rhamnose; glucose was found to be linked 1→4 or 1→6 to galactose in different amounts according to the strain of origin.

This structural variability could have an impact on the immunogenicity of corresponding glycoconjugate vaccines and different strains need to be evaluated in order to identify the appropriate source of O-polysaccharide to use for the development of a candidate conjugate vaccine with broad coverage against *S.* Typhimurium.

Salmonella Typhimurium is the main *Salmonella* serovar responsible for invasive nontyphoidal *Salmonella* (NTS) disease in Africa.[1,2] The case fatality rate for bacteremia caused by NTS is 20–25% for children[1,3] and increases to 50% for children with NTS meningitis.[4] Young children with malaria, anaemia and malnutrition[5–9] and HIV infected individuals[10,11] are particularly affected. The most recent multisite data on the incidence of *Salmonella* bacteremia among African children, from the RTS,S-AS01 malaria vaccine Phase 3 trials, gives rates of around 500/100,000 children/year.[12] These incidence rates are similar to those reported from a recent single-site study from Mozambique, that found an incidence of 388/100,000 in children under one year and 262/100,000 in those aged one to five years.[13] There is no distinctive clinical syndrome association with this disease,[1,3] making diagnosis and treatment a challenge for health-care workers in low-resource settings. Around 90% of invasive NTS isolates in Malawi have been found to be multidrug resistant,[14] emphasizing the need for development of alternative interventions.

Salmonella lipopolysaccharide (LPS) is both a virulence factor and a target for protective antibodies. Lipid A is linked to the 3-deoxy-D-manno-octulosonic acid (KDO) terminus of the conserved core region,[15] which in turn is attached to the O-polysaccharide chain. Lipid A is highly conserved and has endotoxic activity, while the O-polysaccharide chain differs between species and is responsible for the serological specificity of bacteria. Antibodies directed towards the O-polysaccharide mediate killing of NTS[16–18] and confer protection against NTS infections, and O-polysaccharide glycoconjugate vaccines have been proposed as a vaccine strategy against *Salmonella*.[19–22]

The *S.* Typhimurium O-polysaccharide chain is a polymer of tetrasaccharide repeating units. →2)-β-D-Man*p*-(1→4)-β-L-Rha*p*-(1→3)-α-D-Gal*p*-(1→, common to *Salmonella* A, B and D, constitutes the backbone, associated with the factor 12 specificity of the Kauffmann–White scheme.[23] The serogroup B specificity is conferred by the α-D-Abe*p*, an α-3,6-dideoxyhexose (1→3) linked

* Corresponding author. Tel.: +39 0577 539087; fax: +39 0577 243540.
E-mail address: francesca.micoli@novartis.com (F. Micoli).

0008-6215/$ - see front matter © 2013 Elsevier Ltd. All rights reserved.
http://dx.doi.org/10.1016/j.carres.2013.12.003

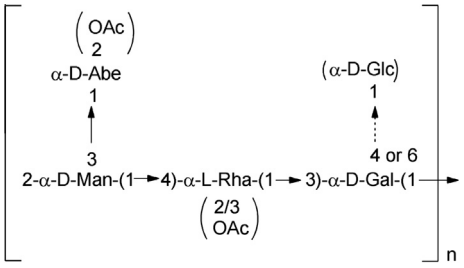

Figure 1. Structure of the repeating unit of *S.* Typhimurium O-polysaccharide. The structural features that vary with the strain of origin are shown in curved brackets.

to the mannose (Man) of the backbone (Fig. 1). This side chain confers the factor 4 specificity.[23]

Bacterial LPS can demonstrate high levels of heterogeneity, particularly LPS from *S.* Typhimurium. O-Polysaccharide can vary in chain length and other modifications, like glucosylation and O-acetylation of the repeating units, which can constitute additional specific O-polysaccharide factors.[24] For *S.* Typhimurium, the abequose (Abe) may be 2-O-acetylated, which adds O:5 specificity in the Kauffman–White scheme. Wollin et al.[25] reported the O-acetylation of C-2 and C-3 of rhamnose (Rha) as a new, hitherto unknown modification of *S.* Typhimurium O-polysaccharide chain. Galactose (Gal) may be α(1→6) or α(1→4) glucosylated, giving the factor 1 or factor 12_2 specificity, respectively.[23,24,26]

Here O-polysaccharide chains purified from six different strains of *S.* Typhimurium have been fully characterized to verify how much the O-polysaccharide structure can differ according to the strain of origin. Two of the structures have been fully elucidated by use of NMR spectroscopy.

The results obtained have confirmed the structural variability of LPS expressed by different isolates of *S.* Typhimurium which will have an impact on the selection of *S.* Typhimurium strains for O-polysaccharide conjugate vaccine development.

1. Results

All purified O-polysaccharide samples exhibited high levels of purity, with protein and nucleic acid content <1% (weight to weight respect to the sugar) and endotoxin level <0.1 EU/μg of sugar, indicating complete removal of the lipid A.

A similar bimodal molecular mass (MM) distribution (Fig. S1) was obtained for all O-polysaccharide strains except for 2192; the K_d values are listed in Table 1. Using dextrans as calibrants, the average MM for the species of higher (HMM) and lower MM (LMM) were in the range of 80–87 and 28–30 kDa, respectively, whereas the O-polysaccharide from strain 2192 showed one main population with an average MM of 34.5 kDa. However, based on the average degree of polymerization (DP) and the mass contribution from O-acetylation, the average MM for this homogeneous sample was 20.5 kDa. The average DP was determined from the molar ratio of Rha (O-polysaccharide chain) to GlcNAc (core sugar) from sugar composition analysis by High-Performance Anion-Exchange Chromatography with Pulsed Amperometric Detection (HPAEC-PAD) and the level of O-acetylation was determined by NMR analysis.

Sugar composition analysis by HPAEC-PAD confirmed the presence of Rha, Gal and Man, the sugars constituting the backbone of the O-polysaccharide chain, in a ratio 1:1:1 for all O-polysaccharides examined, while a variable amount of glucosylation was found depending on the origin of the O-polysaccharide strain (Table 1). This composition was confirmed by Gas Liquid Chromatography (GLC) analysis of the alditol acetates derivatives (Table S1). In the absence of a monomer standard, Abe was quantified by ^{1}H NMR analysis which yielded the expected molar ratio of 1:1 with respect to Man for all samples (Fig. 1).

The linkage positions for the constituent sugars of the O-polysaccharide samples were determined by GLC and GLC–MS of the partially-methylated alditol acetate (PMAA) derivatives (Table 2). As expected,[26] the O-polysaccharide chains from all sources contained terminal non-reducing 3,6 dideoxyhexose, identified as Abe by NMR (t-Abe), 4-linked Rha (4-Rha), terminal non-reducing glucose (t-Glc) (its peak overlaps with that of 4-Rha and was not quantified in samples with a low level of glucosylation), 3-linked Gal (3-Gal), 2,3 linked Man (2,3-Man). Glc was found to be linked to Gal in position 4 or 6, in different amounts according to the

Table 2
Determination of glycosidic linkages in *S.* Typhimurium O-polysaccharide by GLC–MS of PMAA derivatives

Linkage	RRT[a]	1418	2189	2192	D23580	LT2	NVGH1792
t-Abe[b]	0.45	0.16	0.05	0.42	0.07	0.15	0.46
4-Rha	0.72	0.87	0.84	1.12	1.00	1.40	1.00
t-Glc	0.73	0.63	0.29	nd[c]	nd[c]	nd[c]	nd[c]
3-Gal	0.91	0.22	0.56	0.91	0.76	0.85	1.10
2,3-Man	1.00	1.00	1.00	1.00	1.00	1.00	1.00
3,4-Gal	1.03	~0.05	0.37	0.10	0.26	~0.04	~0.04
3,6-Gal	1.14	0.59	0.06	0.08	—	—	—

[a] Relative retention time
[b] t-Abe = the amount of this derivative is underestimated because it is acid labile.
[c] nd = not determined because t-Glc peak overlaps with that of 4-Rha and was not quantified in samples with a low level of glucosylation.

Table 1
Main differences detected for O-polysaccharide purified from different *S.* Typhimurium strains

O-Polysaccharide source	Glc%	Glc linkage	OAc on Rha	% OAc	K_d (avMM)
1418	84	1→4 Gal (8%) 1→6 Gal (92%)	No	73	0.16 and 0.28 (87.0 and 30.4 kDa)
2189	51	1→4 Gal (86%) 1→6 Gal (14%)	No	58	0.17 and 0.27 (80.8 and 31.6 kDa)
2192	24	1→4 Gal (56%) 1→6 Gal (44%)	No	100	0.26 (34.5 kDa)
D23580	39	1→4 Gal	Yes	142	0.17 and 0.28 (82.6 and 28.3 kDa)
LT2	11	1→4 Gal	No	65	0.17 and 0.28 (82.6 and 28.3 kDa)
NVGH1792	8	1→4 Gal	Yes	149	0.17 and 0.28 (82.6 and 28.3 kDa)

Glucosylation level calculated as molar ratio % to Man by HPAEC-PAD analysis. Glc linkage to Gal determined by GLC–MS analysis of PMAA derivatives. O-Acetylation level calculated by ^{1}H NMR of de-O-acetylated samples (integral of acetate ion peak compared to Rha-H6 peak). K_d values calculated after HPLC–SEC analysis on TSK gel 3000 PWXL column (flow rate: 0.5 mL/min; eluent: 100 mM NaH_2PO_4 100 mM NaCl 5% CH_3CN pH 7.2 using λ-DNA and NaN_3 for determining void volume and total volume, respectively). Average molecular mass (avMM) expressed in kDa using dextrans as standards on the TSK gel 3000 PWXL column. HPLC–SEC profiles are shown in Figure S1.

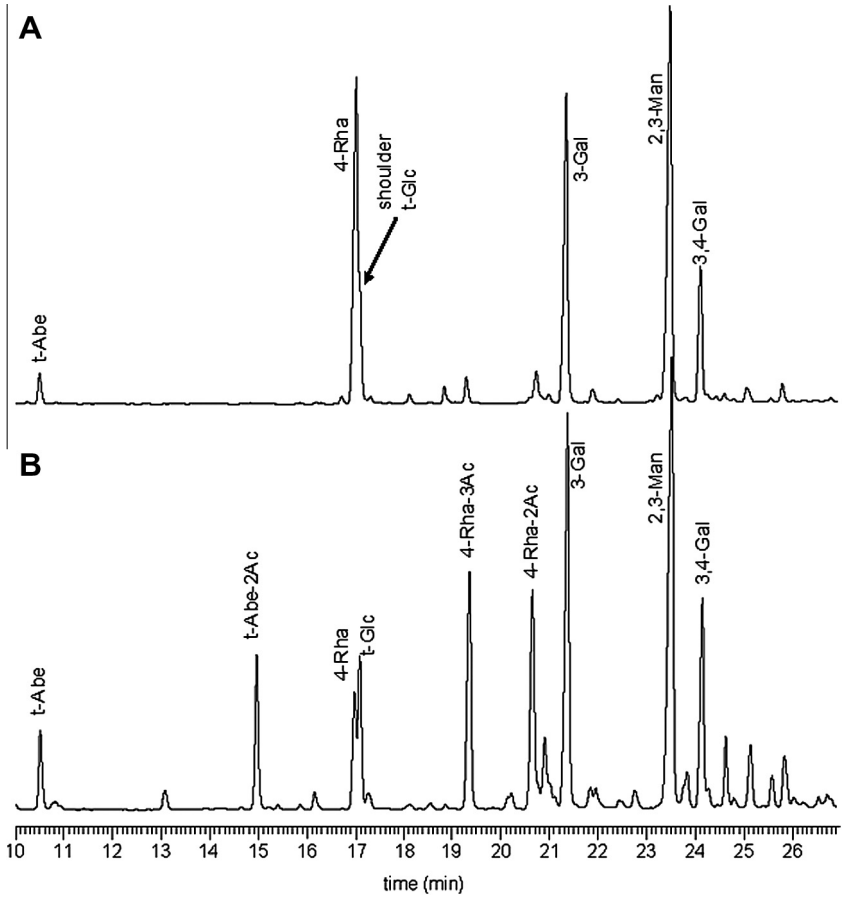

Figure 2. GLC chromatograms of the PMAA derivatives from D23580 OAg obtained without (A) and with (B) retention of *O*-acetyl position. Peak assignments are reported: t-Abe = terminal non-reducing Abe; t-Abe-2Ac = terminal non-reducing Abe acetylated on C-2. The numbers indicate the position of hydroxyl functions engaged in linkages. Similar chromatograms were obtained for the other O-polysaccharide and the results are summarized in Table 3.

strain of origin. LT2, D23580 and NVGH1792 had Glc linked 1→4 to Gal, as shown by the presence of 3,4-Gal (Table 2). For 1418 O-polysaccharide, Glc was predominantly linked 1→6 to Gal, as shown by the presence of 3,6-Gal rather than 3,4-Gal (Table 2), while the opposite was found for 2189 O-polysaccharide. 2192 sample showed equal amounts of Glc linked 1→4 and 1→6. The amount of t-Glc determined was variable in the different O-polysaccharide samples[27] and the sum of 3,4-Gal and 3,6-Gal for each sample was in agreement with the total amount of Glc determined by GLC analysis of the alditol acetates (Table S1). The results are consistent with the structural variations reported for the *S.* Typhimurium O-polysaccharide[23,24,26]; the structure of the general repeating unit is shown in Figure 1.

GLC analysis of the chiral glycosides of all the O-polysaccharide samples showed that the hexoses were in the D absolute configuration and Rha in the L absolute configuration. As before, the absence of a standard meant that this analysis could not be performed for Abe, and its D configuration was established by NMR glycosylation shifts.

Analysis by ^{1}H NMR performed after the addition of 200 mM NaOD[28] revealed different O-acetylation levels according to the source of O-polysaccharide (Table 1). In D_2O all samples contained the characteristic signal near 2.13 ppm assigned to OAc on C-2 Abe, with D23580 and NVGH1792 O-polysaccharide having additional OAc signals at 2.23 and 2.19 ppm. In order to determine the position of these additional *O*-acetyl groups and to confirm that OAc on Abe was at C-2, the O-polysaccharides were permethylated following the method of Prehm,[29] which leaves the *O*-acetyl groups in their native positions. Analysis of the corresponding PMAA derivatives was performed by GLC and GLC–MS. Figure 2 shows the GLC chromatograms of the PMAA derivatives for the D23580 O-polysaccharide, as an example, obtained without (A) and with (B) retention of the *O*-acetyl groups. Comparison of the two chromatograms showed that new peaks were present when PMAA derivatives were obtained with retention of *O*-acetyl position. 2-Abe was a new signal, confirming esterification with *O*-acetyl on C-2 of the terminal Abe. In addition, the expected 4-Rha, 3,4-Rha and 2,4-Rha were also present, indicating partial esterification of the 4-linked Rha on C-2 or C-3. Separation of the 4-Rha into three derivatives also resulted in the partial separation of the peak assigned to t-Glc from that of 4-Rha. In the chromatogram obtained without retention of *O*-acetyl groups (Fig. 2A), t-Glc was a shoulder on the side of the 4-Rha peak and therefore its integration was not possible (Table 2).

Table 3
Deduced OAc position and quantification of substitution based on the relative molar ratios of O-polysaccharide PMAA derivatives obtained with and without retention of *O*-acetyl substituents

Residue	1418	2189	2192	D23580	LT2	NVGH1792
t-Abe	48%	63%	20%	37%	37%	20%
t-Abe-2Ac	52%	37%	80%	63%	63%	80%
4-Rha	100%	100%	100%	22%	100%	13%
4-Rha-3Ac	–	–	–	43%	–	48%
4-Rha-2Ac	–	–	–	35%	–	39%

This analysis was performed on all the O-polysaccharide samples (Table 3) and confirmed the results from ^{1}H NMR analysis (Table 1): all O-polysaccharides were variably O-acetylated on C-2 Abe, whereas only the D23580 and NVGH1792 O-polysaccharides had additional OAc groups on Rha (Table 3). According to the analysis, OAc were on C-2 and C-3 of Rha (Fig. 1).

The structure of the O-polysaccharide produced by *S.* Typhimurium strains 2192 and D23580 was investigated by use of 1D and 2D NMR spectroscopy as these samples are representative of OAg O-acetylated only on C-2 Abe and on Abe with additional O-acetylation on C-2 and C-3 Rha, respectively. Both samples analysed contained low levels of glucose. The O-acetylation was demonstrated by *O*-acetyl signals at 2.11 ppm (for strain 2192, Fig. 3A) and 2.23, 2.19 and 2.13 ppm (for strain D23580, Fig. 4A) and the associated ring protons in the anomeric region of the spectra. Due to the spectral complexity introduced by O-acetylation, the structure (linkages and sequence) of the sugar backbone was first elucidated by analysis of the corresponding de-O-acetylated samples (Supplementary information). The ^{1}H and ^{13}C NMR spectra of the O-polysaccharide 2192 showed key spectral differences arising from O-acetylation (Fig. 3, Table 4). Comparison of the relative areas of the *O*-acetyl singlet at 2.11 ppm (and H-3 of Abe) compared to H-6 of Rha and Abe indicated approximately 95% O-acetylation. Use of COSY, TOCSY and HSQC (Fig. S2) experiments permitted full assignment of the O-acetylated repeating unit and showed the presence of a single *O*-acetyl group on C-2 of Abe (cross-peak H-2/C-2 of Abe2Ac at 5.09/68.0 ppm). Some of the minor peaks due to the presence of the unacetylated repeating unit are labelled in Figure 3C. The major spectral differences between O-polysaccharide 2192 and the de-O-acetylated polysaccharide are the expected deshielding of H-1 (+0.19 ppm) and H-2 (+1.1 ppm) and C-2 (+3.2 ppm) of Abe (at the position of substitution) and shielding of the adjacent carbons C-1 (−2.7 ppm) and C-3 (−3.0 ppm).[30] In addition, H-1 of α-Man was deshielded from 5.31 ppm (de-OAc 2192) to 5.39 ppm for 2192, otherwise O-acetylation resulted in only minor chemical shift differences for the other residues. The assignments (Table 4) for the major repeating unit [→2)[α-D-Abe*p*2Ac-(1→3)]-α-D-Man*p*-(1→4)-α-L-Rha*p*-(1→3)-α-D-Gal*p*-(1→] agree with those reported for the same O-acetylated repeating unit isolated from several species of *Edwardsiella tarda* and recently for *Salmonella enterica*.[31,32]

Comparison of the ^{1}H and ^{13}C NMR spectra of O-polysaccharide D23580 with 2192 showed additional *O*-acetyl signals at 2.23 and 2.19 ppm for O-polysaccharide of D23580 and several other spectral differences arising from O-acetylation (Fig. 4). Comparison of the relative peak areas of the total O-acetate signal to H-6 of Rha and Abe for de-O-acetylated D23580 sample indicated a total of 150–180% O-acetylation per repeating unit. The major *O*-acetyl

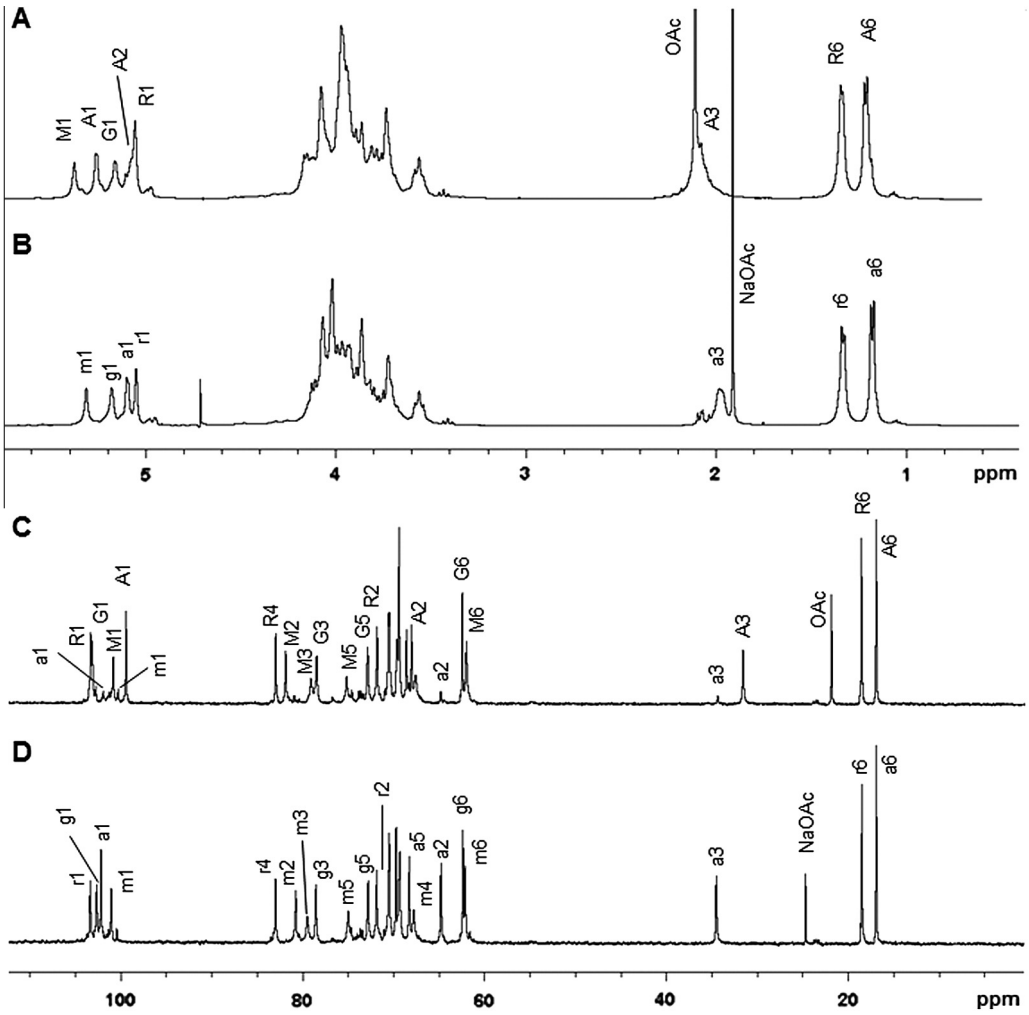

Figure 3. ^{1}H NMR spectra of *S.* Typhimurium strain 2192 OAg with O-acetylation (A) 2192 de-O-acetylated (B) and the corresponding ^{13}C NMR spectra with O-acetylation (C) and de-O-acetylated (D). Some assignments are labelled; the sugar residues are labelled upper case for the O-acetylated repeating unit (A = Abe, G = Gal, M = Man, R = Rha) and lower case for the unacetylated repeating unit.

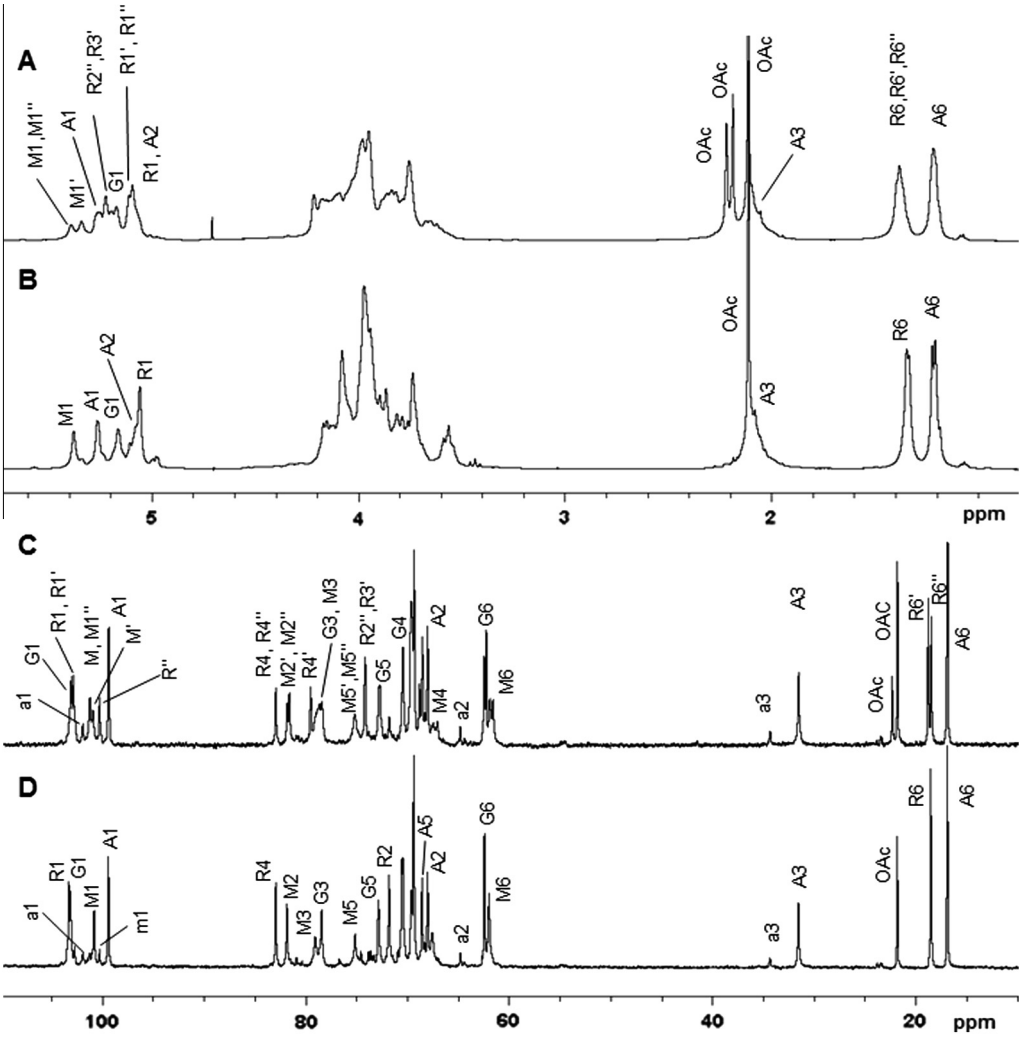

Figure 4. ^{1}H NMR spectra of *S.* Typhimurium strain D23580 (A) and 2192 OAg (B) and the corresponding ^{13}C NMR spectra of strain D23580 (C) and 2192 OAg (D). Some assignments are labelled; the sugar residues are labelled as before with upper case for the Abe2Ac containing repeating unit and the Rha O-acetylation is labelled with dashes (R = Rha, R′ = Rha3Ac, R″ = Rha2Ac, etc.) with lower case for the unacetylated repeating unit.

Table 4
NMR data of *S.* Typhimurium 2192 [de-OAc (upper panel) and native (lower panel)]

Residue	H-1 C-1	H-2 C-2	H-3 C-3	H-4 C-4	H-5 C-5	H6 C-6	*O*-Acetyl Methyl	CO
4)-α-L-Rha*p*-(1→	5.05	4.07	3.97	3.56	3.94	1.33		
(**r**)	103.3	71.8	70.4	82.9	69.3	18.5		
3)-α-D-Gal*p*-(1→	5.18	3.93	3.93	4.06	4.08	~3.72		
(**g**)	102.6	69.3	78.5	70.4	72.7	62.3		
2,3)-α-D-Man*p*-(1→	5.31	4.02	4.02	4.02	3.98	3.86, 3.82		
(**m**)	101.0	80.7	79.5	67.7	74.9	62		
α-D-Abe*p*-(1→	5.09	4.02	1.98	3.87	4.12	1.18		
(**a**)	102.1	64.8	34.5	69.7	68.2	16.9		
4)-α-L-Rha*p*-(1→	5.07	4.09	3.96	3.58	3.94	1.36		
(**R**)	103.3	71.9	70.5	83.0	69.4	18.5		
3)-α-D-Gal*p*-(1→	5.18	3.92	3.97	4.09	4.11	~3.75		
(**G**)	103.1	69.4	78.4	70.5	72.9	62.4		
2,3)-α-D-Man*p*-(1→	5.39	3.99	4.05	4.05	3.98	3.88, 3.83		
(**M**)	100.8	81.8	79.0	67.5	75.1	62.0		
α-D-Abe*p*2OAc-(1→	5.28	5.09	2.09	3.94	4.17	1.23	2.11	
(**A**)	99.4	68.0	31.5	69.6	68.6	16.9	21.1	174.6

The residues of the major de-O-acetylated repeating unit (upper panel) are indicated by lower case and the O-acetylated residues (lower panel) by capitals. Minor peaks due to the presence of low amounts of glucose present are not listed. Deshielded ring carbons (linkage positions) are underlined. The spectra were recorded at 303 K and referenced to added acetone or sodium acetate (after de-O-acetylation).

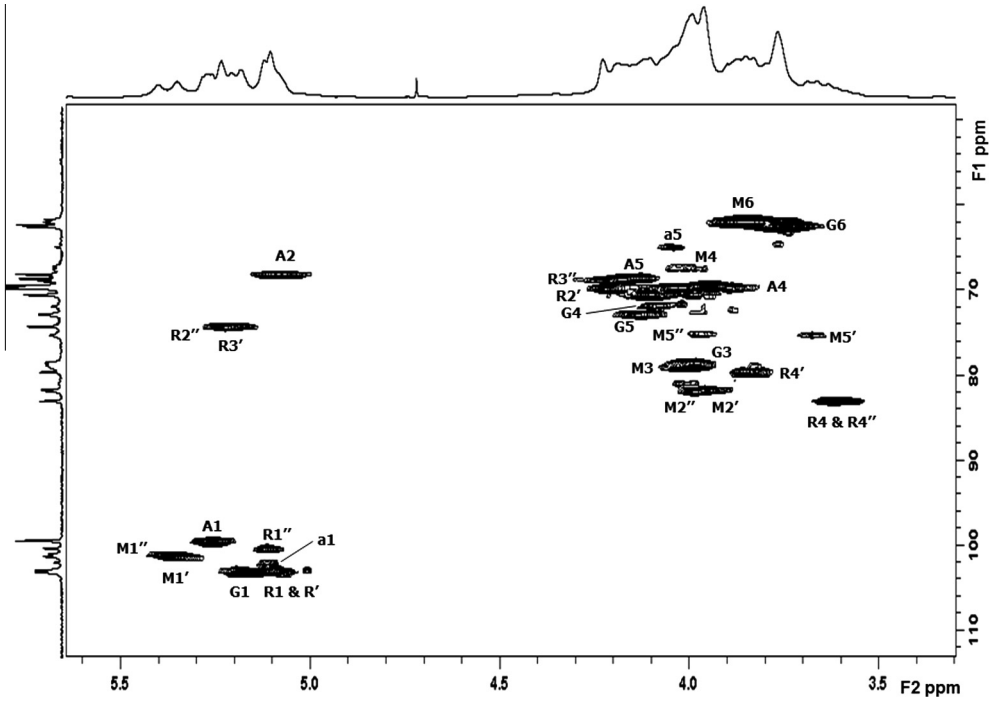

Figure 5. Expansion of the HSQC spectrum of O-polysaccharide from *S.* Typhimurium strain D23580. Major crosspeaks corresponding to the Abe2Ac repeating unit are labelled with the Rha O-acetylation labelled with dashes (R1 = H-1/C-1 of Rha, R′1 = H-1/C-1 of Rha3Ac, R″1 = H-1/C-1 of Rha2Ac, etc.). The key crosspeak at $^{1}H/^{13}C$ 5.09 ppm/68.0 ppm is due to O-acetylation on C-2 of Abe (labelled A2), at 5.21 ppm/74.2 ppm is due to O-acetylation on C-3 of Rha (labelled R3′) and at 5.23 ppm/74.2 ppm is due to O-acetylation on C-2 of Rha (labelled R2″).

signal at 2.13 ppm was assigned to Abe2Ac with a characteristic cross-peak for H-2/C-2 at 5.10/68.1 ppm in the HSQC spectrum (Fig. 5, Table 5). This assignment was supported by the 1D NOESY experiment which showed correlations to H-1 and H-2 of Abe2Ac (Fig. S3A) although these peaks may also be due to correlations with the overlapping H-3 of Abe2Ac at 2.12 ppm. Further proof came from the HMBC experiment (not shown) which contained cross-peaks from the *O*-acetyl methyl group at 2.13 ppm to the carbonyl resonance at 174.6 ppm, which also correlated to H-2 of Abe2Ac at 5.10 ppm. Owing to the complexity of the proton spectrum in the *O*-acetyl region, the amount of O-acetylation on C-2 of Abe was estimated as ~90% from the relative intensities of C-3 signals of Abe2Ac at 31.6 ppm and Abe at 34.5 ppm (Fig. 4C). This is slightly lower than the 95% O-acetylation estimated for strain 2192 (Fig. 4D).

Two additional *O*-acetyl signals were present at 2.23 and 2.19 ppm, although, only a single extra HSQC cross peak was observed (at ~5.22/74.2 ppm) (Fig. 5), compared to strain 2192 (Fig. S2). Detailed analysis by use of COSY, TOCSY (1D and 2D), NOESY (1D and 2D), HSQC-TOCSY and HMBC experiments revealed the presence of multiple Rha spin systems and consequently the cross-peak could be assigned to partially overlapped correlations from Rha2Ac (H-2 at 5.23 ppm) and Rha3Ac (H-3 at 5.21 ppm) to the same carbon at 74.2 ppm. Three H-6 Rha resonances could be discerned which were assigned to H-6 of Rha3Ac (1.41 ppm, C-6 at 18.8 ppm), Rha2Ac (1.38 ppm, C-6 at 18.5 ppm) and Rha (1.35 ppm, C-6 at 18.5 ppm). Use of a series of 1D and 2D experiments elucidated the spin system for Rha3Ac and Rha2Ac as detailed in Supplementary information.

Overlap of the *O*-acetyl signals of O-polysaccharide D23580 with H-3 and core signals in the same region precluded determination of the relative amounts of O-acetylation on C-2 and C-3 of Rha by direct integration. Instead this was estimated from the relative areas of the anomeric protons of Rha2Ac (30%), Rha3Ac (50%), and Rha (20%) in the 1D TOCSY experiment obtained from all three H-6 signals (Supplementary information). This estimation was supported by the equal intensities of the C-6 Rha signals at 18.8 ppm (due to C-6 of Rha3Ac) and 18.5 ppm (due to C-6 of Rha2Ac and Rha) in Figure 4C and is in agreement with the quantification performed by PMAA derivatives (Table 3). The presence of Rha2/3Ac is consistent with the facile migration of *O*-acetyl groups from C-2 to C-3 of Rha described in NMR studies conducted on O-acetylated methyl rhamnosides[33]; however, the possibility that the acetyltransferase involved can modify both positions cannot be excluded. Thus the major repeating unit of *Salmonella* Typhimurium D23580 is defined as [→2)[α-D-Abe*p*2Ac-(1→3)]-α-D-Man*p*-(1→4)-α-L-Rha*p*2/3Ac-(1→3)-α-D-Gal*p*-(1→].

As part of our project to develop a comprehensive conjugate vaccine against invasive NTS disease, we report the full characterization of the O-polysaccharide from 6 different strains of *S.* Typhimurium. The sugar chains of O-polysaccharide were extracted from two lab strains (LT2 and NVGH1792), three animal isolates (1418, 2192 and 2189) and one human isolate (D23580). As reported in Table 1, all purified O-polysaccharides were similar in terms of MM distribution, with two main populations at average MM 80–87 and 28–31 kDa respectively. Only 2192 showed one main peak at average 34.5 kDa (Fig. S1). Sugar analysis by HPAEC-PAD and GLC–MS confirmed the composition of the tetrasaccharide repeating unit as Man, Gal, Rha and Abe. The analysis also showed strain specific variable amounts of glucosylation, ranging from 8% to 84%. The structure of the repeating unit was confirmed by linkage analysis which showed that the terminal glucose present was linked 1→4 and/or 1→6 to Gal, depending on the strain. All the O-polysaccharides were O-acetylated on C-2 Abe although to different extents depending on the strain, while D23580 and NVGH1792 were found to have additional OAc groups on C-2 and C-3 of Rha. The position of the OAc groups was established by GLC–MS and NMR analysis. Finally detailed 1D and 2D NMR studies elucidated the structure of the major repeating unit backbone and the location and extent of the *O*-acetyl groups of

Table 5
NMR data of *S.* Typhimurium (D23580) with Rha, Rha2Ac and Rha3Ac

Residue	H-1 C-1	H-2 C-2	H-3 C-3	H-4 C-4	H-5 C-5	H-6 C-6	*O*-Acetyl Methyl	CO
4)-α-L-Rha*p*-(1→	5.09	4.11	3.99	3.59	3.96	1.35		
(**R**)	102.9	71.7	70.5	83.0	69.4	18.5		
4)-α-L-Rha*p*3Ac-(1→	5.10	4.23	5.21	3.85	4.05	1.41	2.23	
(**R′**)	102.9	~69.7	74.2	79.5	69.4	18.8	22.2	175.0
4)-α-L-Rha*p*2Ac-(1→	5.12	5.23	4.22	3.63	4.04	1.38	2.19	
(**R″**)	100.3	74.2	68.8	83.0	69.4	18.5	21.9	174.6
3)-α-D-Gal*p*-(1→	5.18	3.96	3.99	4.11	4.14	3.76		
(**G**)	103.1	69.4	78.5	70.5	72.7	62.4		
2,3)-α-D-Man*p*-(1→	5.39/5.35	3.99/3.96	3.99	4.03	3.98	3.87, 3.83		
(**M″/M,M′**)	101.0/101.3	81.9/81.7	78.7	67.3	~75.2	61.8		
α-D-Abe*p*2Ac-(1→	5.27	5.10	2.12	3.90	4.19	1.23	2.13	
(**A**)	99.4	68.1	31.6	69.6	68.6	16.9	21.8	174.6

The residues of the major O-acetylated repeating unit are indicated by capitals; minor peaks due to the presence of low amounts of glucose present are not listed. The Rha, Rha3Ac and Rha2Ac spin systems are represented by R, R′ and R″, respectively, and the corresponding spin systems of Man by M, M′ and M″. Deshielded ring carbons (linkage positions) are underlined. The NMR spectra were recorded at 303 K and referenced to the HOD signal.

the O-polysaccharide produced by *S.* Typhimurium strains 2192 and D23580. These assignments will facilitate screening of O-polysaccharide structure and pattern of O-acetylation for LPS from new strains of *S.* Typhimurium.

Due to the structural variability found in this study, future studies will investigate whether these O-polysaccharide structural differences impact on the immunogenicity of corresponding glycoconjugate vaccines. If this is so, then different strains of *S.* Typhimurium will need to be evaluated in order to identify which are optimal as the source of O-polysaccharide for the development of the most promising candidate glycoconjugate vaccines against *S.* Typhimurium.

2. Experimental

2.1. Origin and growth of *S.* Typhimurium strains

The clinical isolate D23580 was obtained from the Malawi–Liverpool–Wellcome Trust Clinical Research Programme, Blantyre, Malawi. D23580 is a typical and representative Malawian invasive NTS isolate belonging to ST313 sequence type and pathovar.[34] 1418, 2189 and 2192 are animal isolates[35,36] and were obtained from University of Calgary. The laboratory strains NVGH1792 and LT2[37] were obtained from the University of Birmingham, UK, and Novartis Master Culture Collection, respectively.

All *S.* Typhimurium bacterial strains were grown in a chemically defined medium, using glycerol as the carbon source. All strains were fermented in a 7 L bioreactor (EZ-Control, Applikon) to OD 35 as previously described.[38,39]

2.2. O-Polysaccharide purification

S. Typhimurium O-polysaccharides were purified as previously described.[38] Briefly, mild acid hydrolysis (2% acetic acid at 100 °C for 3 h) to cleave the acid-labile KDO-lipid A linkage was performed directly on the fermentation culture instead of the isolated LPS. The O-polysaccharide chains linked to the core sugars released into the supernatant, were recovered following centrifugation. Lower MM impurities were removed and the supernatant concentrated by tangential flow filtration (TFF), using a Hydrosart 30 kDa membrane. Protein and nucleic acid impurities were co-precipitated in citrate buffer 20 mM at pH 3. The protein content was further reduced by ion exchange chromatography. Nucleic acids were further removed by precipitation in 18 mM Na_2HPO_4, 24% EtOH and 200 mM $CaCl_2$, pH >4.5. O-Polysaccharide was then recovered in water by a second TFF 30 kDa step.

2.3. O-Polysaccharide size analysis and chemical characterization

Phenol sulfuric acid assay was used for total sugar quantification[40]; micro BCA for protein quantification (using bovine serum albumin as a reference following the manufacturer's instructions [Thermo Scientific]); UV spectroscopy for nucleic acid content (assuming that a nucleic acid concentration of 50 μg/mL gives an OD 260 = 1) and chromogenic kinetic LAL (Limulus Amoebocyte Lysate) for endotoxin level (Charles River Endosafe-PTS instrument). Size-Exclusion High Pressure Liquid Chromatography (HPLC–SEC) with differential refractive index (dRI) detection was used to estimate the molecular size distribution of O-polysaccharide populations.[38] Samples were run on a TSK gel G3000 PWXL column (30 cm × 7.8 mm; particle size 7 μm; cod. 808021) with TSK gel PWXL guard column (4.0 cm × 6.0 mm; particle size 12 μm; cod.808033) (TosohBioscience). The mobile phase was 0.1 M NaCl, 0.1 M NaH_2PO_4, 5% CH_3CN, pH 7.2 at the flow rate of 0.5 mL/min (isocratic method for 30 min). Void and bed volume calibration was performed with λ-DNA (λ-DNA Molecular Weight Marker III 0.12–21.2 Kbp, Roche) and sodium azide (NaN_3, Merck), respectively and dextrans were used as standards. For K_d determination, the following equation was used: $K_d = (T_e - T_0)/(T_t - T_0)$ where: T_e = elution time of the analyte, T_0 = elution time of the biggest fragment of λ-DNA and T_t = elution time of NaN_3.

The sugar monomers constituting the O-polysaccharide repeating unit and *N*-acetyl glucosamine (GlcNAc), a unique sugar of the core region, were quantified by use of HPAEC-PAD.[38] 1D ^{1}H NMR analysis was recorded on all O-polysaccharide samples to confirm identity and purity and to calculate the level of O-acetylation.[38] Addition of NaOD to the sample caused rapid de-O-acetylation (the sample was heated at 37 °C for 20 min to have complete de-O-acetylation) and the degree of O-acetylation was calculated comparing the integrals of acetate and Rha-H6 peaks.

Sugar composition analysis was also performed by GLC, after hydrolysis of the polysaccharides with 2 M TFA at 125 °C for 1 h, and derivatization to alditol acetates.[41] The sugar linkage positions were determined by GLC–MS after per-methylation of the samples,[42] hydrolysis with 2 M TFA at 125 °C for 1 h, followed by reduction and per-acetylation to obtain the partially methylated alditol acetates (PMAA) derivatives. Peak areas were corrected by using the effective carbon response factors[43]; for Abequose the response factor of 6-deoxy hexose were applied. Determination of the absolute configuration of the sugar residues of OAg samples (strains D23580, NVGH1792 and LT2) was performed as previously described.[44]

In order to determine the position of the *O*-acetyl groups, the O-polysaccharides were per-methylated following the method of Prehm,[29] which leaves the *O*-acetyl groups in their native positions. Samples were then treated as above to obtain the PMAA derivatives, which were then analysed by GLC and GLC–MS.

Analytical GLC was performed on a Perkin Elmer Autosystem XL gas chromatograph equipped with a flame ionization detector and a SP2330 capillary column (Supelco, 30 m), using He as carrier gas. The following temperature programs were used: for alditol acetates, 200–245 °C at 4 °C/min; for PMAA, 150–250 °C at 4 °C/min. Separation of the trimethylsilylated (+)-2-butyl glycosides, for determining the absolute configuration of the sugars, was obtained on a HP1 column (Hewlett–Packard, 50 m), using the following temperature program: 50 °C 1 min, 50–130 °C at 45 °C/min, hold 1 min, 130–240 °C at 1 °C/min, hold 20 min. GC–MS analyses were carried out on an Agilent Technologies 7890A gas chromatograph coupled to an Agilent Technologies 5975C VL MSD.

2.4. NMR spectroscopy

Samples (20–40 mg) were lyophilized and exchanged twice with 99.9% deuterium oxide, then dissolved in 600 μL of D_2O and introduced into a 5 mm NMR tube for data acquisition. 1D (^1H and ^{13}C) and 2D, TOCSY, NOESY, HSQC, HMBC and hybrid HSQC-TOCSY NMR spectra were obtained using a Bruker Advance III 400 NMR with an Ultra Shield 400 Plus magnet. The probe temperature was set at 303 K and the 1D and 2D spectra recorded and processed using standard Bruker software (Topspin 2.1). 2D TOCSY experiments were performed using mixing times of 120, 180 ms or 200 ms and the 1D variants using mixing times ranging from 30 to 250 ms. Long mixing times were employed to permit the transfer of magnetization from H6 to H1 of Rha. The HSQC and HMBC experiments were optimized for $J = 145$ and 8 Hz respectively. De-O-acetylation was performed by the addition of 4 μL sodium deuteroxide (NaOD, Sigma Aldrich) to the tube containing the O-polysaccharide sample in D_2O. Spectra were referenced to the HOD signal or to added acetone or sodium acetate (after de-O-acetylation).[45]

Acknowledgements

We thank Francesco Berti of Novartis Vaccines and Diagnostics (Siena) for useful discussion on NMR data, and Luisa Lanzilao and Massimiliano Gavini of Novartis Vaccines Institute for Global Health for their work on O-polysaccharides extraction and purification.

Supplementary data

Supplementary data associated with this article can be found, in the online version, at http://dx.doi.org/10.1016/j.carres.2013.12.003.

References

1. Feasey, N. A.; Dougan, G.; Kingsley, R. A.; Heyderman, R. S.; Gordon, M. A. *Lancet* **2012**, *379*, 2489–2499.
2. Reddy, E. A.; Shaw, A. V.; Crump, J. A. *Lancet Infect. Dis.* **2010**, *10*, 417–432.
3. MacLennan, C. A.; Levine, M. M. *Expert Rev. Anti Infect. Ther.* **2013**, *11*, 443–446.
4. Molyneux, E. M.; Mankhambo, L. A.; Phiri, A.; Graham, S. M.; Forsyth, H.; Phiri, A.; Walsh, A. L.; Wilson, L. K.; Molyneux, M. E. *Ann. Trop Paediatr.* **2009**, *29*, 13–22.
5. MacLennan, C. A.; Gondwe, E. N.; Msefula, C. L.; Kingsley, R. A.; Thomson, N. R.; White, S. A.; Goodall, M.; Pickard, D. J.; Graham, S. M.; Dougan, G.; Hart, C. A.; Molyneux, M. E.; Drayson, M. T. *J. Clin. Invest.* **2008**, *118*, 1553–1562.
6. Feasey, N. A.; Archer, B. N.; Heyderman, R. S.; Sooka, A.; Dennis, B.; Gordon, M. A.; Keddy, K. H. *Emerg. Infect. Dis.* **2010**, *16*, 1448–1451.
7. Mabey, D. C.; Brown, A.; Greenwood, B. M. *J. Infect. Dis.* **1987**, *155*, 1319–1321.
8. Calis, J. C.; Phiri, K. S.; Faragher, E. B.; Brabin, B. J.; Bates, I.; Cuevas, L. E.; de Haan, R. J.; Phiri, A. I.; Malange, P.; Khoka, M.; Hulshof, P. J.; van Lieshout, L.; Beld, M. G.; Teo, Y. Y.; Rockett, K. A.; Richardson, A.; Kwiatkowski, D. P.; Molyneux, M. E.; van Hensbroek, M. B. *N. Engl. J. Med.* **2008**, *358*, 888–899.
9. Bachou, H.; Tylleskar, T.; Kaddu-Mulindwa, D. H.; Tumwine, J. K. *Infect. Dis.* **2006**, *6*, 160.
10. Gilks, C. F.; Brindle, R. J.; Otieno, L. S.; Simani, P. M.; Newnham, R. S.; Bhatt, S. M.; Lule, G. N.; Okelo, G. B.; Watkins, W. M.; Waiyaki, P. G., et al *Lancet* **1990**, *336*, 545–549.
11. Gordon, M. A.; Banda, H. T.; Gondwe, M.; Gordon, S. B.; Boeree, M. J.; Walsh, A. L.; Corkill, J. E.; Hart, C. A.; Gilks, C. F.; Molyneux, M. E. *AIDS* **2002**, *16*, 1633–1641.
12. Agnandji, S. T. et al *N. Engl. J. Med.* **2011**, *365*, 1863–1875.
13. Sigaúque, B.; Roca, A.; Mandomando, I.; Morais, L.; Quintó, L.; Sacarlal, J.; Macete, E.; Nhamposa, T.; Machevo, S.; Aide, P.; Bassat, Q.; Bardají, A.; Nhalungo, D.; Soriano-Gabarró, M.; Flannery, B.; Menendez, C.; Levine, M. M.; Alonso, P. L. *Pediatr. Infect. Dis. J.* **2009**, *28*, 108–113.
14. Gordon, M. A.; Graham, S. M.; Walsh, A. L.; Wilson, L.; Phiri, A.; Molyneux, E.; Zijlstra, E. E.; Heyderman, R. S.; Hart, C. A.; Molyneux, M. E. *Clin. Infect. Dis.* **2008**, *46*, 963–969.
15. Whitfield, C.; Kaniuk, N.; Frirdich, E. *J. Endotoxin Res.* **2003**, *9*, 244–249.
16. Rondini, S.; Lanzilao, L.; Necchi, F.; O'Shaughnessy, C. M.; Micoli, F.; Saul, A.; MacLennan, C. A. *Microb. Pathog.* **2013**, *63*, 19–23.
17. Trebicka, E.; Jacob, S.; Pirzai, W.; Hurley, B. P.; Cherayil, B. J. *Clin. Vaccine Immunol.* **2013**, *20*, 1491–1498.
18. MacLennan, C. A.; Tennant, S. M. *Clin. Vaccine Immunol.* **2013**, *20*, 1487–1490.
19. Watson, D. C.; Robbins, J. B.; Szu, S. C. *Infect. Immun.* **1992**, *60*, 4679–4686.
20. Konadu, E.; Shiloach, J.; Bryla, D. A.; Robbins, J. B.; Szu, S. C. *Infect. Immun.* **1996**, *64*, 2709–2715.
21. Konadu, E. Y.; Lin, F. Y.; Hó, V. A.; Thuy, N. T.; Van Bay, P.; Thanh, T. C.; Khiem, H. B.; Trach, D. D.; Karpas, A. B.; Li, J.; Bryla, D. A.; Robbins, J. B.; Szu, S. C. *Infect. Immun.* **2000**, *68*, 1529–1534.
22. Simon, R.; Tennant, S. M.; Wang, J. Y.; Schmidlein, P. J.; Lees, A.; Ernst, R. K.; Pasetti, M. F.; Galen, J. E.; Levine, M. M. *Infect. Immun.* **2011**, *79*, 4240–4249.
23. Hellerqvist, C. G.; Lindberg, B.; Svensson, S.; Holme, T.; Lindberg, A. A. *Carbohydr. Res.* **1968**, *8*, 43–55.
24. Helander, I. M.; Moran, A. P.; Makela, P. H. *Mol. Microbiol.* **1992**, *6*, 2857–2862.
25. Wollin, R.; Stocker, B. A.; Lindberg, A. A. *J. Bacteriol.* **1987**, *169*, 1003–1009.
26. Hellerqvist, C. G.; Lindberg, B.; Svensson, S.; Holme, T.; Lindberg, A. A. *Carbohydr. Res.* **1969**, *9*, 237–241.
27. Bogomolnaya, L. M.; Santiviago, C. A.; Yang, H. J.; Baumler, A. J.; Andrews-Polymenis, H. L. *Mol. Microbiol.* **2008**, *70*, 1105–1119.
28. Jones, C.; Lemercinier, X. *J. Pharm. Biomed. Anal.* **2002**, *30*, 1233–1247.
29. Prehm, P. *Carbohydr. Res.* **1980**, *78*, 372–374.
30. Jansson, P.; Kenne, L.; Schweda, E. *J. Chem. Soc., Perkin Trans. 1* **1987**, 377–383.
31. Katzenellenbogen, E.; Kocharova, N. A.; Toukach, P. V.; Górska, S.; Bogulska, M.; Gamian, A.; Knirel, Y. A. *Carbohydr. Res.* **2012**, *355*, 56–62.
32. De Castro, C.; Lanzetta, R.; Leone, S.; Parrilli, M.; Molinaro, A. *Carbohydr. Res.* **2013**, *370*, 9–12.
33. Rönnols, J.; Pendrill, R.; Fontana, C.; Hamark, C.; d'Ortoli, T. A.; Engström, O.; Ståhle, J.; Zaccheus, M. V.; Säwén, E.; Hahn, L. E.; Iqbal, S.; Widmalm, G. *Carbohydr. Res.* **2013**, *380C*, 156–166.
34. Kingsley, R. A.; Msefula, C. L.; Thomson, N. R.; Kariuki, S.; Holt, K. E.; Gordon, M. A.; Harris, D.; Clarke, L.; Whitehead, S.; Sangal, V.; Marsh, K.; Achtman, M.; Molyneux, M. E.; Cormican, M.; Parkhill, J.; MacLennan, C. A.; Heyderman, R. S.; Dougan, G. *Genome Res.* **2009**, *19*, 2279–2287.
35. Beltran, P.; Musser, J. M.; Helmuth, R.; Farmer, J. J., 3rd; Frerichs, W. M.; Wachsmuth, I. K.; Ferris, K.; McWhorter, A. C.; Wells, J. G.; Cravioto, A., et al *Proc. Natl. Acad. Sci. U.S.A.* **1988**, *85*, 7753–7757.
36. Beltran, P.; Plock, S. A.; Smith, N. H.; Whittam, T. S.; Old, D. C.; Selander, R. K. *J. Gen. Microbiol.* **1991**, *137*, 601–606.
37. Lilleengen, K. *Acta Pathol. Microbiol. Scand.* **1950**, *27*, 625–640.
38. Micoli, F.; Rondini, S.; Gavini, M.; Pisoni, I.; Lanzilao, L.; Colucci, A. M.; Giannelli, C.; Pippi, F.; Sollai, L.; Pinto, V.; Berti, F.; MacLennan, C. A.; Martin, L. B.; Saul, A. *Anal. Biochem.* **2013**, *434*, 136–145.
39. Rondini, S.; Micoli, F.; Lanzilao, L.; Hale, C.; Saul, A. J.; Martin, L. B. *Clin. Vaccine Immunol.* **2011**, *18*, 460–468.
40. Dubois, M.; Gilles, K. A.; Hamilton, J. K.; Rebers, P. A.; Smith, F. *Anal. Chem.* **1956**, *28*, 350.
41. Albersheim, P.; Nevins, D. J.; English, P. D.; Karr, A. *Carbohydr. Res.* **1967**, *5*, 340–345.
42. Harris, P. J.; Henry, R. J.; Blakeney, A. B.; Stone, B. A. *Carbohydr. Res.* **1984**, *127*, 59–73.
43. David, P. S.; Robert, H. S.; Peter, A. *Carbohydr. Res.* **1975**, *40*, 217–225.
44. Gerwig, G. J.; Kamerling, J. P.; Vliegenthart, J. F. G. *Carbohydr. Res.* **1978**, *62*, 349–357.
45. Gottlieb, H. E.; Kotlyar, V.; Nudelman, A. *J. Org. Chem.* **1997**, *62*, 7512–7515.